INFORMATION TO USERS

This manuscript has been reproduced from the microfilm master. UMI films the text directly from the original or copy submitted. Thus, some thesis and dissertation copies are in typewriter face, while others may be from any type of computer printer.

The quality of this reproduction is dependent upon the quality of the copy submitted. Broken or indistinct print, colored or poor quality illustrations and photographs, print bleedthrough, substandard margins, and improper alignment can adversely affect reproduction.

In the unlikely event that the author did not send UMI a complete manuscript and there are missing pages, these will be noted. Also, if unauthorized copyright material had to be removed, a note will indicate the deletion.

Oversize materials (e.g., maps, drawings, charts) are reproduced by sectioning the original, beginning at the upper left-hand corner and continuing from left to right in equal sections with small overlaps. Each original is also photographed in one exposure and is included in reduced form at the back of the book.

Photographs included in the original manuscript have been reproduced xerographically in this copy. Higher quality 6" x 9" black and white photographic prints are available for any photographs or illustrations appearing in this copy for an additional charge. Contact UMI directly to order.

UMI

A Bell & Howell Information Company
300 North Zeeb Road, Ann Arbor MI 48106-1346 USA
313/761-4700 800/521-0600

Principles of energy and momentum conservation to analyze and model air flow for perforated ventilation ducts

Khaled El Moueddeb

A thesis submitted to the
Faculty of Graduate Studies and Research
In partial fulfilment of the requirement for the degree of
Doctor of Philosophy

Department of Agricultural and Biosystems Engineering
Faculty of Agriculture and Environmental Sciences
McGill University, Montreal

December, 1996

© K. El Moueddeb

National Library of Canada
Bibliothèque nationale du Canada

Acquisitions and Bibliographic Services
Acquisitions et services bibliographiques

395 Wellington Street
Ottawa ON K1A 0N4
Canada

395, rue Wellington
Ottawa ON K1A 0N4
Canada

Your file Votre référence

Our file Notre référence

The author has granted a non-exclusive licence allowing the National Library of Canada to reproduce, loan, distribute or sell copies of this thesis in microform, paper or electronic formats.

L'auteur a accordé une licence non exclusive permettant à la Bibliothèque nationale du Canada de reproduire, prêter, distribuer ou vendre des copies de cette thèse sous la forme de microfiche/film, de reproduction sur papier ou sur format électronique.

The author retains ownership of the copyright in this thesis. Neither the thesis nor substantial extracts from it may be printed or otherwise reproduced without the author's permission.

L'auteur conserve la propriété du droit d'auteur qui protège cette thèse. Ni la thèse ni des extraits substantiels de celle-ci ne doivent être imprimés ou autrement reproduits sans son autorisation.

0-612-29929-5

Canada

Suggested short title:

MODELLING PERFORATED VENTILATION DUCTS

ABSTRACT

Ph.D. Khaled El Moueddeb Ag. & Biosystems Eng.

MODELLING PERFORATED VENTILATION DUCTS

A theoretical model was developed to predict the air distribution pattern and thus to design perforated ventilation ducts equipped with a fan. The analysis of the air distribution pattern of such systems requires accurate measurement procedures. Several experimental methods were tested and compared. Accordingly, the piezometric flush taps and thermo-anemometer were selected to measure respectively the duct air pressure and the outlet air flow.

Based on the equations of energy and momentum conservation, a model was formulated to predict the air flow performance of perforated ventilation ducts and to evaluate the outlet discharge angle and the duct regain coefficients without evaluating frictional losses. The basic assumptions of the model were validated by experimentally proving the equivalence of the friction losses expressed in the 2 cited equations. When compared to experimental results measured from four wooden perforated ventilation ducts with aperture ratios of 0.5, 1.0, 1.5, and 2.0, the model predicted the outlet air flow along the full length of perforated duct operated under turbulent flow conditions with a maximum error of 9%. The regain coefficient and the energy correction factor were equal to one, and the value of the discharge coefficient remained constant at 0.65, along the full length of the perforated duct. The outlet air jet discharge angle varied along the entire duct length, and was not influenced by friction losses for turbulent flow.

Assuming a common effective outlet area, the model was extended to match the performance of the fan and the perforated duct and to determine their balance operating point.

RÉSUMÉ

Un modèle de conception pour conduits perforés de ventilation a été développé pour prédire leur taux de distribution d'air. L'analyse de performance des conduits perforés de ventilation exige une méthodologie expérimentale précise. Suite à un essai, les troues piézométriques et le thermo-anémomètre furent retenus pour mesurer respectivement la pression statique de l'air à l'intérieur de tels conduits et le débit d'air des perforations.

A partir des équations de conservation de l'énergie et de la quantité de mouvement, un modèle fut formulé pour prédire la performance dans les conduits perforés de ventilation et pour évaluer l'angle de décharge des perforations et le coefficient de regain, indépendamment des pertes par friction. L'angle de décharge est considéré dans le calcul du débit net des perforations latérales le long du conduit pour que le coefficient de décharge demeure constant. L'hypothèse principale du modèle a été validée expérimentalement en prouvant l'équivalence des pertes par friction exprimées par les 2 équations citées. Le modèle a été testé avec quatre conduits perforés dont le rapport d'aperture respectif était de 0.5, 1.0, 1.5 et 2.0 et il a prédit le débit d'air des perforations avec un niveau maximum d'erreur de 9% sous écoulement turbulent. Le coefficient de recouvrement et le facteur de correction de l'énergie furent égales à un. le coefficient de décharge fut égal à 0.65 sur la longueur entière du conduit. L'angle de décharge variait sur la longueur totale du conduit perforé, mais n'étant pas influencé par les pertes de friction, sous écoulement turbulent.

Puisque l'ouverture effective de décharge du ventilateur fut trouvée égale à celle des perforations du conduit, le modèle peut relier les caractéristiques du ventilateur à celles du conduit perforé et calculer leur point commun balancé d'opération.

ACKNOWLEDGMENTS

I acknowledge the financial contribution of the Natural Sciences and Engineering Research Council of Canada, Le Ministère de l'agriculture, des Pêcheries et de l'alimentation du Québec and Le Ministère de l'enseignement supérieur de la Tunisie.

The advice and guidance of Dr Suzelle Barrington during the execution of the work and redaction of the thesis are gratefully acknowledged and appreciated. Without her tolerance and understanding, this work would not has come to fruition.

I thank Dr. Barthakur for his constructive suggestions in the development of the model.

I am grateful to my wife for her assistance in the acquisition of the data and particularly her encouragement, and her moral support. I am also very grateful to my father and my mother to their huge sacrifice in helping me to reach this degree.

PREFACE

This thesis is submitted in the form of original papers suitable for journal publications. The thesis format has been approved by the **Faculty of Graduate Studies and Research, McGill University**, and follows the conditions outlined in the **"Guidelines concerning thesis preparation**, section 3, **Traditional and manuscript-based theses"** which are as follows:

"Candidates have the option of including, as part of the thesis, the text of a paper(s) submitted or to be submitted for publication, or the clearly-duplicated text of a published paper(s). These texts must be bound as an integral part of the thesis.

If this option is chosen, **connecting texts that provide logical bridges between the different papers are mandatory**. The thesis must be written in such a way that it is more than a mere collection of manuscripts; in other words, results of a series of papers must be integrated.

The thesis must still conform to all other requirements of the "Guidelines for Thesis Preparation". **The thesis must include**: A Tables of Contents, an abstract in English and French, an introduction which clearly states the rationale and objectives of the study, a comprehensive review of the literature, a final conclusion and summary, and a thorough bibliography or reference list.

Additional material must be provided where appropriate (e.g. in appendices) and in sufficient detail to allow a clear and precise judgement to be made of the importance and originality of the research reported in the thesis.

In the case of manuscripts co-authored by the candidate and others, **the candidate is required to make an explicit statement in the thesis as to who contributed to such work and to what extend.** Supervisors must attest to the accuracy of such statements at the doctoral oral defense. Since the task of the examiners is made more difficult in these cases, it is

in the candidate's interest to make perfectly clear the responsibility of all the authors of the co-authored papers. **Under no circumstances can a co-author of any component of such a thesis serve as an examiner for that thesis.**

N.B. when previously published material is presented in a thesis, **the candidate must obtain official copyright waivers from the copyright holder(s)** and submit these to the Thesis Office with the final deposition.

Although all the work reported here is the responsibility of the candidate, the project was supervised by **Dr S.F. Barrington**, Department of Agricultural and Biosystems Engineering, McGill University, Montreal. The entire research project was conducted at the Macdonald Campus, Saint-Anne de Bellevue.

Dr. S.F. Barrington is co-author in the four manuscripts. Dr. B.G. Newman is co-author in the first manuscript and Dr. N.N Barthkur is co-author in the second and the third manuscripts. The first manuscript was published in the Canadian Agricultural Engineering 38(3): 207-213. The two subsequent manuscripts were accepted for publication after minor revision by the Journal of Agricultural Engineering Research on september 1996. The last manuscript was is to be submitted to the Transactions of the ASAE.

This document examines the modelling of perforated duct used for ventilation and air recirculation. The series of manuscripts is preceded by an introduction and a literature review. The manuscripts are followed by an overall conclusion and the contributions to knowledge.

The thesis is composed of the following chapters:

Chapter one: Introduction. This chapter presents the nature of the problem and justifies the need to accurately model the performance of perforated ventilation ducts. The objectives of the present work were defined and the

experimental hypotheses were presented. Within the limits of the laboratory investigation, the contributions to knowledge were presented.

Chapter Two: Review of the literature

The present state of the art was reviewed and the areas requiring further investigations were highlighted.

Chapter Three: Evaluation of methods to measure the performance of perforated ventilation ducts. Several techniques and devices have been used in the past to measure air pressure inside the duct and air flow at the duct's outlets. The use of accurate measurement methods is a prerequisite for the testing of a design model for perforated ventilation ducts. Through this chapter, measurement methods for duct air flow parameters are presented tested and compared.

Chapter Four: Perforated Ventilation Ducts Part I: A Model for Flow Distribution. To analyze the air distribution patterns from perforated ducts, energy and momentum equations were applied to perforated ventilation ducts. A theoretical solution was developed to model air flow distribution in perforated ventilation ducts based on several hypotheses.

Chapter Five: Perforated Ventilation Ducts: Validation of an Air Distribution Model. The model developed was tested against the air flow performance of 4 wooden perforated ducts equipped with an axial flow fan. The hypotheses supporting the model and the model itself were validated. A value of 0.65 was obtained for the outlet discharge coefficient and of one for the regain coefficient and energy correction factor.

Chapter Six: Design of perforated duct for agricultural ventilation or air recirculation. A complete design method for perforated ventilation ducts is introduced. The mathematical expression to obtain a specific air distribution pattern and a method for the prediction of the balance operating point of the ventilation system are presented.

Chapter Seven: General Conclusion

The general findings are presented and recommendations are made to continue the research work.

Chapter Eight: Contributions to knowledge

The contribution to knowledge are reviewed.

Chapter Nine: References

TABLE OF CONTENTS

LIST OF TABLES

LIST OF FIGURES

1 INTRODUCTION

1.1 General introduction

Heating, ventilation, and air conditioning comprise a major field of engineering. Designing environment control systems for agriculture requires an understanding of the complex interactions between the biological system within the space and the environment provided for that system. The goal of environmental control should be to create a balance favourable for both the biological and physical systems.

In the field of environmental control, it is frequently necessary to distribute air uniformly within buildings. Such distribution is achieved by ventilation systems. Ventilation is a necessary part of any environmental control system used for livestock or plant structures. The purpose of the ventilation system is to provide an exchange of fresh air based on climatic conditions and the environmental requirements of the biological units in the structure. For a rapid mixing of incoming air with air already in the building, high inlet velocities are desirable for both warm and cold weather ventilation. The high velocity creates turbulence and rapid mixing in the vicinity of the jet formed by the incoming air and also induces large scale circulation patterns of air within the ventilated space.

During cold weather and times of limited ventilation rate, inlet air velocity will typically be low. The temperature difference between the jet and the air inside the building is large during cold weather and a low inlet velocity does not promote rapid temperature change within the jet. Thermal buoyancy forces can be sufficiently large for the jet to detach itself from the ceiling, fall to the floor, and cause significant local chilling for the animals or plants located at that point. A recirculation system integrated into that for fresh air distribution, helps to alleviate this problem and promote good air mixing. A system called

"Recirculation-Boosted dual air inlets" (Figure 1.1) is used in Canadian Prairies for very cold winter conditions. The recirculated air intercepts the fresh, cold air entering through the inlet, accelerates it, and provides the momentum to maintain the stability of the air mixing pattern. For more moderate weather conditions, as for the eastern provinces of Canada, a system called "Blended air systems" is used (Figure 1.2). The principle is that room air is recirculated through wooden or plastic ducts, and a variable proportion of fresh air is blended into the recirculated air, to provide fresh air exchange.

For both systems, air recirculation is achieved by means of a ventilation tube or duct with equally spaced outlets along its length. Recirculation ducts are used in the environmental control of livestock and poultry buildings as well as for the conditioning of most agricultural produce.

Air distribution is one of the major design preoccupations for perforated ventilation ducts. The duct must be designed to provide a specific air distribution pattern over its perforated length, such as: 1) uniform air distribution over its perforated length for livestock shelters, or; 2) uniform heat distribution from a gradual heated air distribution for greenhouses. The air distribution pattern can uniform as like as in the case of ventilation of livestock buildings or variable as like as the heating of greenhouses. This pattern can be a function of several inter-related factors such as duct construction material (friction effects), fan capacity against pressure head, outlet size and spacing, duct length and cross-sectional area and as well as air density and viscosity. All other variables involved in the performance of air duct can be expressed, in mathematical models as a combination of these factors.

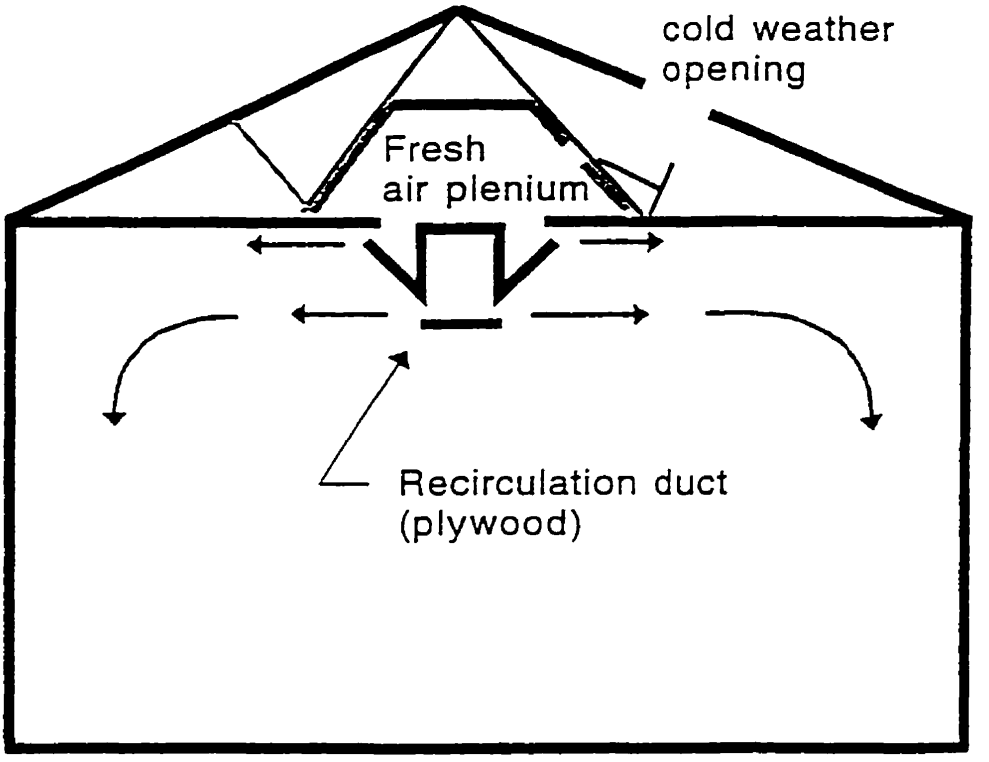

Figure 1.1 Recirculation-boosted dual air inlets

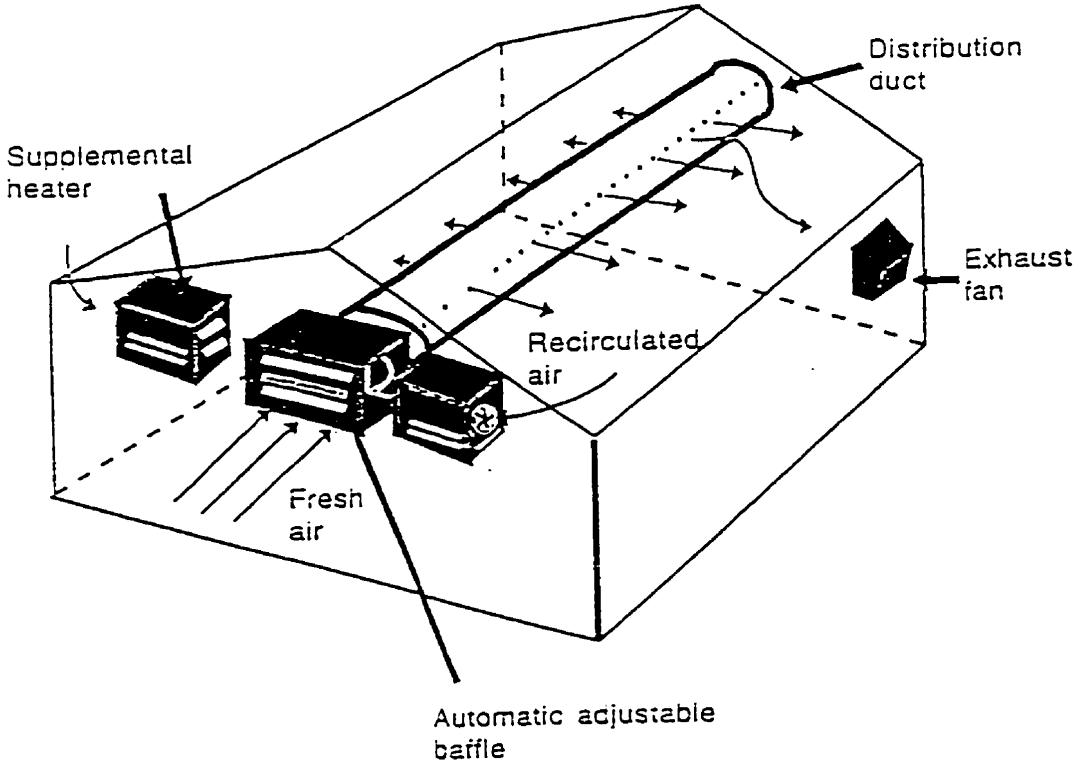

Figure 1.2 Blended air systems

With recent developments in the science of ventilating air spaces, ventilation and recirculation duct design must be improved. Past designs for perforated ventilation ducts have been based on experience more than on scientific data. Accurate design of duct ventilation systems offers many performance and economic advantages. If the airflow characteristics of a perforated duct can be determined, a more accurate prediction of the fan and duct balance point can be achieved by matching the duct performance curve with that of the fan. Being able to predict the operating point allows for the selection of a fan with adequate airflow and minimal horsepower, thereby reducing operating costs. The operating point corresponds to the common performance point of the fan and the duct air flow capacity. With an accurate mathematical model, duct parameters such as the outlet area can be varied and optimized for specific needs.

In chapter 2, it will be demonstrated that the design methods which have been used in the past, diverge in basic assumptions as well as in the application of fluid mechanic theories. Often, the hypotheses used for such design are poorly stated and have not been proved. In order to develop an accurate approach to the design of ventilation ducts, precise mathematical models must be introduced. These must be initiated from a complete fluid mechanic analysis. This analysis can be condensed through the testing of hypotheses and elimination or simplification of terms.

1.2 Objectives

The main objective is to establish design criteria and tools for the design of perforated ventilation ducts. To ensure proper room ventilation, the ducts are expected to distribute a defined volume of air at a specified balanced (uniform) or unbalanced (non uniform) rate along the length of the duct.

The main objective will be met by considering several sub-objectives:

- verification of the best method to measure duct static air pressure and outlet air flow;
- evaluation of basic fluid mechanic equations when applied to operating perforated ducts;
- evaluation of air discharge angle;
- evaluation of the static regain coefficient;
- verification of energy losses along the perforated duct;
- development of an expression for the outlet air discharge coefficient based on duct characteristics and operating conditions;
- verification of friction energy losses for the air travelling inside the perforated duct;
- formulation of a standard basis of interpretation and definition of terms;
-recommendation of standard practices for the monitoring of duct air flow distribution;
- recommendation of standard practices for the prediction of the fan and duct balance operating point.

1.3 Hypotheses

The following hypotheses will be tested:

1- The total head losses of the air inside the duct result from friction losses;

2- The discharge angle for the air jet leaving the outlets can be calculated from a longitudinal average velocity of the air inside the duct and the potential air outlet velocity;

3- The variation of the outlet air flow along the duct is mainly influenced by the variation of the discharge angle of the outlet air jet.

1.4 Scope

The study and modelling of the perforated ventilation ducts was based on laboratory investigation. The data collected pertained to the duct static air pressure and air velocity, as well as the outlet air jet angle and velocity. The study was limited to a wooden ventilation duct fed by an axial fan. The experimental duct was built of a wooden frame made of 39 mm by 39 mm members covered with 6 mm thick presswood panelling. The duct offered an inside cross-sectional area of 0.17 m^2 (597 mm by 295 mm minus four time 39 mm x 39 mm). Its side panels were removable as to change the size of the outlets. The rectangular outlets were present in pairs, one on each side of the duct, at a spacing of 610 mm. The experiments were carried out using, successively, four aperture ratios (0.5, 1, 1.5 and 2.0) and one length of ducts.

2 LITERATURE REVIEW

Air distribution performance of mechanically fed manifolds and perforated ducts have been investigated ever since the late 1800's (Howland[1]). It was only in the early 1950's that agricultural engineers took interest in applying these systems to improve ventilation of their structures (Carpenter[2]).

Air velocity at the outlets has become an important factor in the design of ventilation systems which will provide a specific air displacement at the floor or within the living space of the animal (Ogilvie et al.[3]). The perforated duct must therefore be designed to give specific outlet air velocity distributions. This parameter can vary along the perforated duct. Ducts with small cross-section areas, are preferred in practical situations, which tends to create unbalanced air flow from a nonuniform static air pressure and velocity over the length of the duct. The static air pressure variation results from two phenomena: friction losses characterized by the friction effect of the fluid moving along the walls of the duct causing a decrease of air pressure in the direction of the flow; and; the reduction of fluid momentum in the duct as fluid is discharged at the outlets leading to an increase of air pressure in the duct across each outlet. The amount of air discharged at any outlet in a duct is dependent on its discharge coefficient and its static air pressure differential (Bailey[4]). If both of these quantities remain constant along the distributor, then uniform discharge will result and the system is considered balanced. Conditions of balanced air flow simplify the analysis of the flow performance of ventilation ducts. As opposed to balanced flow conditions, unbalanced conditions produce a non linear gradient over the length of duct and the solution therefore becomes more complicated.

2.1 Models developed to predict air distribution from perforated ducts

In order to develop a mathematical model for the analysis of air distribution patterns from ducts, several analyses have been carried out in the past, each by different researchers. In general, a one-dimensional model is used to consider the flow of air along a duct with uniform cross-section and with openings of equal area and spacing. The conditions are assumed to be incompressible and viscous effects are presumed negligible.

The mathematical description of air flow from ventilation ducts was attempted as early as the 1950's by Koestel and Young[5]. They used tapered ducts to eliminate static regain and to improve duct air distribution. They also developed a model that accurately predicted the angle of the air jet emitted from the long slot of the tapered conduit. This model assumed that the regain in pressure was equal to the loss in duct velocity.

Shove and Hukill[6] developed an equation, similar to that of Koestel and Young[5], but introduced friction losses. The rate of change of the static pressure regain along the duct was equated to the change in velocity pressure head multiplied by a constant called regain coefficient, less the friction head. The regain coefficient was found to range between 1.5 to 1.7 for a perforated duct used for the ventilation of grain masses. No experimental testing of this model was carried out.

Davis et al.[7] used the equations developed by Shove and Hukill[6] to formulate a computer model predicting the air flow distribution from perforated corrugated metal ducts. The outlet discharge coefficient of 0.61 was used and assumed to vary over the length of the duct by a multiple of the static head divided by the total air pressure head. The model predicted air flow performances within an error level of 25%

for aperture ratios of 1.3 and less. Davis et al.[7] manifested the need for future research on discharge coefficients to better define them for ducts with helical corrugations.

In his investigation of the flow in a 1.22 m manifold with open and closed end, Horlock[8] assumed that the fluid leaves the slots with a longitudinal velocity equal to that of the upstream velocity inside the duct. From the application of Bernoulli's equation along the discharging streamlines, the discharge velocity normal to the outlet was found to be related to the duct static air pressure. No loss of total air pressure was considered at the outlet. Along the manifold, the air-wall friction and the discharge coefficient were assumed constant. The air-wall friction coefficient was equated to the value corresponding to the entry Reynolds number and the discharge coefficient was equated to 0.61. The momentum differential equation was solved along the length of the duct in terms of the ratio of duct air velocity to the normal outlet air jet velocity.

Allen[9] used Bernoulli's equation and considered friction losses for tapered duct. To account for the fact that less than 100% of the velocity head was converted to static head, he introduced a regain coefficient, Cr, as defined earlier by Ashley et al.[10].

For a pipe with equally spaced openings and fed by a centrifugal fan, Bailey[4] used a theoretical analysis to describe the variation of duct static air pressure by considering friction effect between holes using Colebrook[11] equation and the static regain at the outlet level. Like Bailey[4], Pastula et al.[12], considered that the theoretical normal discharge air velocity is derived from the excess static air pressure in the duct. The discharge coefficient was plotted as a function of the air velocity head ratio using empirical parameters and was found to have a maximum value of 0.63. The coefficient of static regain over the length of the duct was also defined by an equation involving empirical

parameters determined by an iterative computer program. The model required as input parameters, values for the static and dynamic air pressures at the duct entrance, air temperature as well as the physical dimension of the duct and its perforations.

Saunders and Albright[13] used a mathematical series applied by iteration from one outlet to the next, to compute the air distribution performance under several conditions. Air pressure differentials were assumed to result solely from friction losses and reduction in average duct air velocity head. The value for the discharge coefficient was changed from 0.786 to 0.72 for duct diameters of 0.31m and 0.76m respectively. Despite this adjustment in the value of the discharge coefficient, the predicted flow distribution profile deviated from that measured by as much as 10%. They concluded that the largest factor which affects the accuracy of the prediction model was the value of the discharge coefficient.

A mathematical equation was developed by Barrington and MacKinnon[14] to express the average air velocity of a wooden ventilation duct under any flow condition. The average air velocity along the duct was found to be related to the static air pressure and discharge coefficient measured at the back of the duct and the average inlet velocity. Even if the mathematical equation reproduced the duct flow conditions with an acceptable accuracy, the use of the average air velocity concept along the duct requires the translation of the duct end parameters to the fan position.

The ventilation duct models developed have used a variety of equations and hypotheses. Among others, several authors have considered friction losses while others assume these negligible. In some models the Bernouill's equation was assumed to apply, in others the momentum equation was assumed to apply. To analyze air distribution from ventilation ducts, a thorough analysis of fundamental equations will be carried out in an attempt to develop a consistent but complete

performance model.

2.2 The measurement of air pressure inside perforated ventilation ducts

Several techniques and devices have been used to measure air pressure along the ventilation ducts. Bailey[4] as well as Saunders and Albright[13] have used the wall taps while Carpenter[2] as well as Brundrett and Vermes[15] have used the pitot tube to measure static air pressure. The pitot tube can be used to detect both the static and the dynamic air pressure. The wall tap is used to detect only the static air pressure and it offers the advantage of avoiding eventual error stemming from pitot tube misalignment. But to avoid the difficulties of attaching the piezometric taps to thin tube walls, such as those of polyethylene, static air pressures can be obtained from a pitot tube inserted inside the duct. These two methods of pressure detection, wall tap and pitot tube inside the duct, require evaluation and comparison.

2.3 The measurement of air velocity and angle at the duct outlets

Similarly, several methods have been used to measure air flow and discharge angle at the duct outlets. In several instances, discharge angle is not considered (Carpenter[2]; Saunders and Albright[13]) despite the fact that it is an important factor when calculating the net flow equal to the air velocity perpendicular to the outlet area times this area. When the vane anemometer is used, its relatively large size limits to one reading the measurement of the outlet air jet velocity and discharge angle. Such application does not accurately measure the variation in air jet angle and velocity over the face of the outlet. Koestel and Tuve[16] have shown that the angle of discharge varies along a duct containing a long slot. A more accurate method of measuring the discharge

angle variation and velocity along each hole is therefore necessary for slotted outlets.

2.4 References

[1] **Howland W E** Design of perforated pipe for uniformity of discharge. Proceeding 3rd Midwestern Conference on Fluid Mechanics 1953, 687-701.

[2] **Carpenter G A** The design of permeable ducts and their application to the ventilation of livestock building. Journal of Agricultural Engineering Research 1972, 17:219-230.

[3] **Ogilvie J R; Barber E M; Randall J M** Floor air speeds and inlet design in swine ventilation systems. Transactions of the ASAE 1990, 33(1): 255-259.

[4] **Bailey G J** Fluid flow in perforated pipes. Journal Mechanical Engineering Science. 1975, 17(6): 338-347.

[5] **Koestel A; Young C** The control of air stream from a long slot. Transactions of the ASHVE 1951, 12: 407-418.

[6] **Shove G C; Hukill W V** Predicting pressure gradients in perforated grain ventilation ducts. Transactions of the ASAE 1963, 6(2): 115-116,122

[7] **Davis D C; Romberger J S; Pettibone C A; Andales S C; Yeh H J** Mathematical model for air flow from perforated circular ducts with annular corrugations. Transactions of the ASAE 1980, 19(4): 661-666

[8] **Horlock J H** An investigation of the flow in manifolds with open and closed ends. Technical Notes. Journal of the Royal

Aeronautic Society 1956, November 749-753.

[9] **Allen D** Air flow distribution from tapered ducts. paper 74-6514. ASAE 1974, St. Joseph, Michigan, USA.

[10] **Ashley C M; Gilman S F; Church R A; Syracuse N Y** Branch fitting performance at high velocity. Transactions of the ASHRAE 1956, 56: 279-294

[11] **Colebrook C F** Turbulent flow in pipes with particular reference to the transition region between smooth and rough pipe laws. Journal of the Institution of Civil Engineers 1938, 4: 133-156.

[12] **Pastula R; Feddes J J R, Leonard J J** Discharge coefficients for openings in metal or plywood walls of recirculation ducts. Canadian Agricultural Engineering 1992, 34(4):359-363

[13] **Saunders D D; Albright L D** Airflow from perforated polyethylene tubes. Transactions of the ASAE 1984, 23(6): 1144-1149.

[14] **Barrington S F; MacKinnon I R** Air distribution from rectangular wooden ventilation ducts. Transactions of the ASAE 1990, 33(3):944-948.

[15] **Brundrett E; Vermes P T** Evaluation of tube diameter and fan induced swirl in polyethylene ventilation tubes. Transaction of the ASAE 1987, 30(4): 1131-1138.

[16] **Koestel A; Tuve G L** The discharge of air from a long slot. Transactions of ASHVE 1948, 54: 87-100.

3 EVALUATION OF METHODS TO MEASURE THE PERFORMANCE OF PERFORATED VENTILATION DUCTS

3.1 Introduction

Perforated ventilation or recirculating ducts are used in the environmental control of livestock and poultry buildings as well as for the conditioning of agricultural produce. These systems are preferred for the heating and cooling of air spaces because of their efficiency in blending fresh air into the structure space with minimum drafts (Randall and Battams[1], Leonard and McQuitty[2]).

The air distribution pattern of these perforated ducts is complicated by the inter-relation of several factors such as construction material and friction effects, fan capacity against pressure head, outlet size and spacing, and perforated duct length and cross-sectional area. Recent developments in the science of ventilation require the improvement of the design of perforated ducts to predict, for example, air velocity at the outlets since this affects air velocity at the floor of the ventilated room and, hence the level of comfort of the animals housed (Ogilvie et al.[3]). This design problem can be solved with exact fluid mechanics models refined through the testing of hypotheses and the elimination or simplification of terms. Consequently, fluid mechanics parameters of experimental, perforated ventilation ducts must be measured accurately.

To measure static air pressure inside ducts (Table 3.1), Bailey[4] and Saunders and Albright[5] used piezometric wall taps, while Carpenter[6] and Brundrett and Vermes[7] used the pitot-static tubes. The pitot-static tube can detect both the static and the total air pressure while the wall tap can only detect static air pressure. The wall tap avoids errors stemming from the misalignment of the pitot-static tube but its attachment to thin flexible walls, such as those of polyethylene, can be difficult. With such perforated ducts,

static air pressure is best obtained with a static tube inserted inside the perforated duct. For non-perforated pipes with a smooth inside surface, these two devices are known to measure the same static air pressure at any cross section (Streeter and Wylie[10]) whereas, they have not been compared for perforated ventilation ducts with equally spaced outlets.

Similarly, several methods have been used to measure air velocity and discharge angle, at the outlets of perforated ventilation ducts. Often, the discharge angle is not considered (Carpenter[6]; Saunders and Albright[5]) but the true flow across an area is the product of the area and the velocity component perpendicular to that area. This is of importance since the outlet air jet angle varies along the length of perforated ducts (Koestel and Tuve[11]).

The work described here had three objectives. The first was to compare static air pressure readings using the static tube and piezometric taps in order to establish which method is most appropriate for perforated ventilation ducts. The second was to adapt and test an instrument to simultaneously measure both the outlet air jet angle and velocity. The third was to find an accurate method of measuring outlet air flow. Thus, a grid method was applied in two ways; one across the inside section of the duct, upstream and downstream from each outlet, and; another outside the duct across the outlet area. As described by Burgess et al.[12], the grid method requires that the rectangular flow area be divided into equal areas and that measurement be taken at the centre of these equal areas and parallel to the flow.

Table 3.1 Perforated duct parameter measurement

Author	Duct	Parameter	Measurement methods	
			Equipment	Method
Bailey[4]	Perforated polyethylene duct	Discharge angle	Vane anemometer+ protractor	in arc above the outlet
		Discharge velocity	Static tube	6-point log-linear method
		Static pressure	Piezometric opening	Flush tap
Carpenter[6]	Perforated polyethylene duct	Discharge velocity	Vane anemometer	No angle measurement
		Static pressure	Static tube	Centre of cross-section
Barrington and MacKinnon[8]	Perforated wooden duct	Outlet velocity	Compuflow thermo-anemometer	Traverse method
		Static pressure	Piezometric opening	Outstanding tap
Saunders and Albright[5]	Perforated polyethylene duct	Outlet velocity	Pitot tube	At centre of outlet
		Static pressure	Piezometric opening	Flush tap
Brundrett and Vermes[7]	Perforated polyethylene duct	Outlet velocity & angle	Pitot tube	Protractor+ yarn tellate
		Static pressure	Static tube	Centre of cross-section
Pastula et al.[9]	Perforated wooden or metal duct	Outlet velocity	Hotwire anemometer	No angle measurement
		Static pressure	Piezometric opening	flush tap

3.2 Materials and methods

3.2.1 Measurement of perforated duct static air pressure

To measure duct air static pressure, the static tube and the piezometric taps were compared using a wooden perforated duct built of frame members, 39 mm by 39 mm, covered with 6 mm thick presswood panelling (Figure 3.1). The duct offered an inside net cross-sectional area of 0.17 m^2 (597 mm by 295 mm less 4 times 39 mm x 39 mm) and was perforated on both sides, at every 610 mm over a length of 8.5 m, by 14 pairs of rectangular outlets, (125 mm by 25 mm) located at the mid height of the side panels. The first pair of outlets was 440 mm from the closed end of the duct. The duct sections were sealed using caulking compound. The 450 mm axial duct fan (ACME EJF 18F-V 18". ACME Eng. & Man. Corp. Muskogie, Oklahoma 74401) had a 0.25 kW motor running at 1600 rpm and an air straightener (Figure 3.2). A 1800 mm long tapered section was used to fit the fan onto the perforated duct and to reduce swirling at the first outlets (Figure 3.1). The straight section of 4900 mm between the tapered and the perforated sections and appearing in figure 3.1 was added after the pressure measurement test, for the method described in Section 3.2.2.

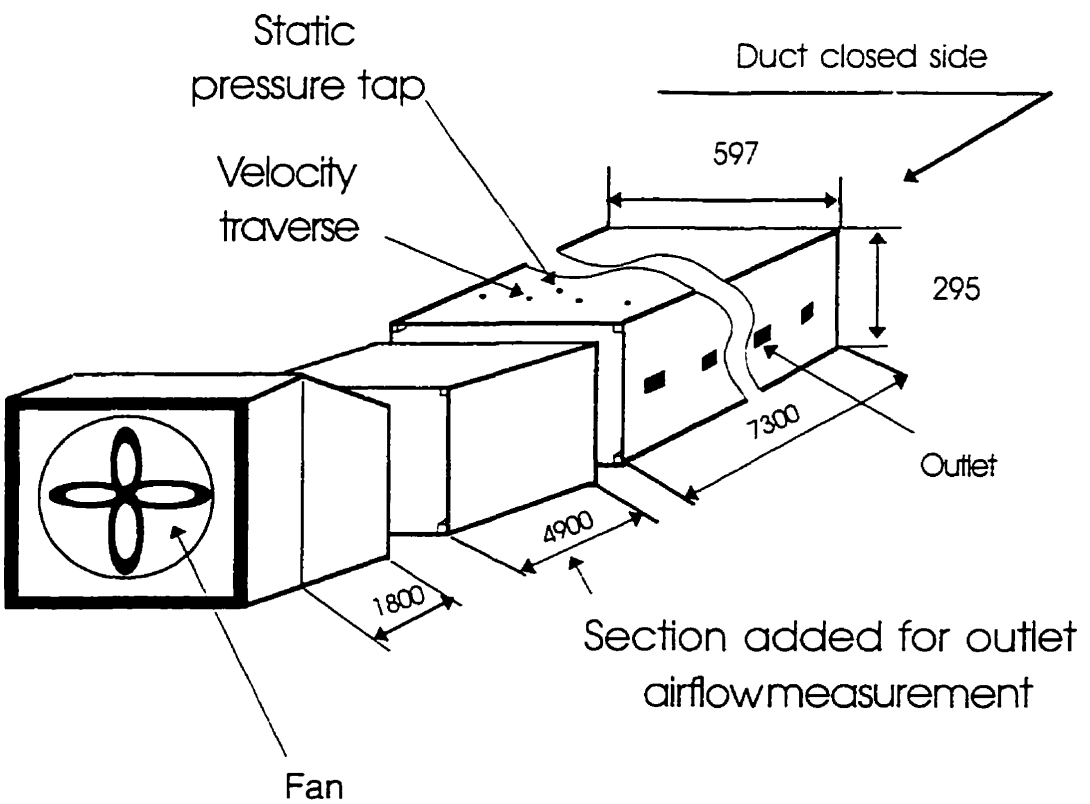

Figure 3.1 A three dimensional view of the ventilation duct
The dimensions are in mm

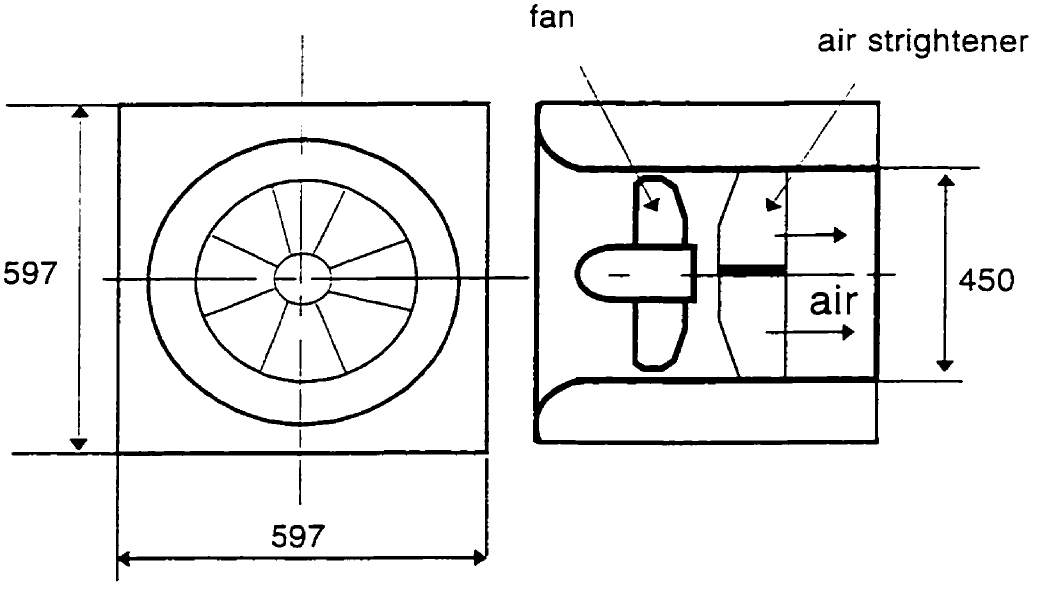

Figure 3.2 The frame of the fan inside the duct
The dimensions are in mm

A vertical micro-manometer (MICROTECTOR® GAGE, DWYER INSTRUMENTS, INC. Michigan City, Indiana 46360, U.S.A) with an accuracy of ±0.062 Pa, was used in both instances to read static air pressure. To insert the static tube or the wall piezometric taps (3 mm in inner diameter), small holes (8 mm in diameter) were drilled along the centre line of the top panel of the perforated duct, half way between each two pairs of outlets, for a total of twelve such holes. For both instruments, static air pressure measurements were repeated seven times before moving to the next hole. All measurements were taken under the same room air (pressure and temperature) and fan setting.

Using the static tube, perforated duct static air pressure was measured at depths of 50, 100, 150, 250 and 290 mm from the top panel, at the 12 locations along the length of the perforated duct. At the same 12 locations, the measurements were repeated using three methods, a piezometric tap inserted either flush or outstanding into the top panel and a static tube inserted at the centre of the cross-section of the perforated duct. The instruments were connected to the micro-manometer. For both tests, Duncan's New Multiple Range Test, at a 95% confidence level, and a completely randomized design (Steel and Torrie[13]) were used to identify any significant difference in pressure measurement, at each of the 12 locations. For the first and second experiments, the treatments were depth from the top panel and static air measurement instrument, respectively and the reading was static air pressure.

3.2.2 Measurement of outlet air flow

Outlet air flow is obtained from the product of a flow area surface and the velocity component perpendicular to this area:

$$q_o = (A_o/n) * \Sigma_1^n \, V_{oi} * \sin(\alpha_i) \quad \ldots\ldots\ldots\ldots \quad (1)$$

where :

q_o: air flow from one outlet, m^3/s

A_o: outlet area, m^2

n: number of grid areas over the air flow cross section

V_{oi}: i^{th} grid area air outlet velocity, m/s

α_i: i^{th} grid area air outlet angle, º

Inside the perforated duct, outlet flow can be obtained from the difference in duct flow upstream and downstream from the outlet (figure 3.3):

$$q_o = A/n * \Sigma_1^n V_{iu} - A/n * \Sigma_1^n V_{id} \quad \ldots\ldots\ldots\ldots \quad (2)$$

A: perforated duct cross sectional area, m^2

V_{iu}: air velocity inside the perforated duct upstream from the i^{th} outlet and summed from the grid measurements, m/s

V_{id}: air velocity inside the perforated duct downstream from the i^{th} outlet and summed from the grid measurement, m/s

A 7.3 m wooden perforated duct structure (Figure 3.1, Table 3.2) was built of interchangeable side panels with 12 pairs of outlets spaced at 610 mm, located at mid height and giving aperture ratios ($\Sigma A_o/A$) of 0.5, 1.0, 1.5 and 2.0. An unperforated section of 4.9 m was installed between the tapered fan transition sections and the perforated duct sections to reduce air swirling at the outlets nearest to the fan end.

Using the grid method (Burgess et al.[12]), outlet air flow was initially determined from the difference in air flow across the inside section of the duct, upstream and downstream from each pairs of outlets (equation 2). The duct cross-sectional area was divided into 16 equal sections (Burgess et al.[12]) and, for each section, the average air velocity was computed from 10 consecutively repeated measurements taken with an ALNOR compuflow thermo-anemometer (model 8500D-II,

Alnor Instrument Company, Niles, Illimois, 60648) with an accuracy of 0.05 m/s or ±3% of the indicated reading over a range from 0.1 to 15 m/s.

Outlet air flow was then determined by applying the grid method to the outlet flows, outside the perforated duct. To simultaneously measure the outlet air jet discharge angle and velocity, a three-tube-pitot instrument was used (Figure 3.4). Fixed on a mechanism allowing its rotation about a vertical axis facing the outlet, this instrument accounted for its orientation by means of a horizontal needle moving over a fixed protractor. By being connected to the one port of a micro-manometer where the left port is left open to atmospheric pressure, the central tube of the three-tube-pitot instrument measured a relative pressure which can be converted to air velocity using Bernoulli's principle. The two exterior tubes of the instrument were connected to opposite ports of an identical micro-manometer and thus measured the outlet air direction when they registered the same dynamic pressure, as the instrument was being slowly rotated about its vertical axis. This three-tube-pitot instrument was calibrated inside the low speed wind tunnel of the Mechanical Engineering Research Laboratory of McGill University and gave a pitot correction factor (real velocity/pitot tube velocity) of 0.992 over a range of 5 to 16 m/s. It repeatedly measured air jet angles with an error of $\pm$ 2.5°. However, two persons were required to manipulate the instrument and to read the micrometers.

The three-tube-pitot instrument was used to obtain the total outlet flow, at the outlet surface. Three repeated measurements of the angle and velocity, perpendicular to the air flow surface (equation 1), were performed using a grid with 16 subsections to measure the air contraction. The three-tube-pitot instrument was held at 10 mm from the duct wall to measure air flow properties at the vena contracta (Esmay and Dixon[14]). The individual outlet flow measurements

were also summed up to give an equivalent air flow inside the perforated duct, starting from the farthest end away from the fan :

$$Q_{13} = V_{13}*A = 0$$

$$Q_{12} = V_{12}*A = 0 + [((2*A_o/n))*\Sigma_1^n V_{oi}*\sin(\alpha_1)]_{12}^{**}$$

$$Q_{11} = V_{11}*A = V_{12}*A + [((2*A_o/n))*\Sigma_1^n V_{oi}*\sin(\alpha_1)]_{11}^{**}$$

.....

.....

$$Q_1 = V_1*A = V_2*A + [((2*A_o/n))*\Sigma_1^n V_{oi}*\sin(\alpha_1)]_1^{**} \quad . . \quad (3)$$

** 12^{th}, 11^{th},....and 1st pairs of outlets

where:

V_{13}: perforated duct air velocity downstream from the 12^{th} pair of outlets, m/s

V_{12}: perforated duct air velocity upstream from the 12^{th} pair of outlets, m/s.

Accordingly, the air flow across the internal section of the perforated duct was compared to that summed from the flow measured outside the duct at the outlet.

3.3 Results and discussion

3.3.1 Measurement of static air pressure

For the static tube readings taken at different depths inside the perforated ducts, Duncan's Multiple Range Test (Table 3.3) showed difference only for the first five locations away from the fan end (95% confidence level). Air swirling explains this observed variation in static air pressure over depth, for a length from the fan end of 3.66 m or 9 times the perforated duct's hydraulic diameter. Swirling pertains to the rotational movement given to an air stream as it is propelled forward by an axial fan. Brundrett and Vermes[7] also observed air swirling inside perforated ducts over a similar distance. Thereafter and for the outlet flow measurement, a 4.9 m, non-perforated duct section was added to the 1.8 m tapered section just downstream from the fan.

Table 3.2 Characteristics of the experimental perforated ducts used for outlet air flow measurement

Duct	Outlet size mm*mm	Aperture ratio*
1	145* 25	0.5
2	145* 50	1.0
3	145* 75	1.5
4	145*100	2.0

* The aperture ratio equals $\Sigma A_o/A$.

Note: The experimental duct used to test static pressure instruments had 14 pairs of outlets while the 4 experimental ducts used to test outlet flow measurement techniques had 12 pairs of outlets.

All ducts had section of 7.3 m perforated by 12 outlets spaced at 610 mm.

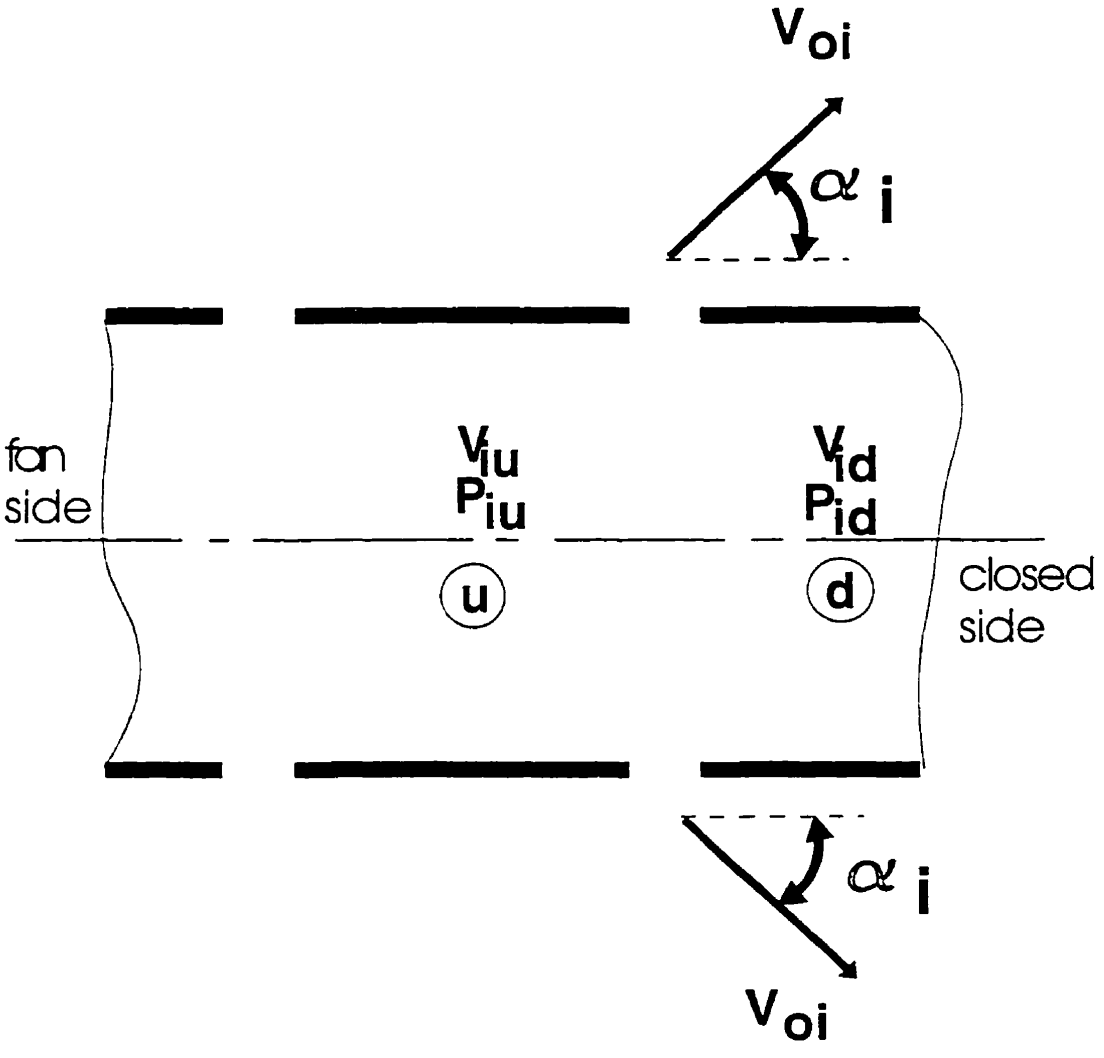

Figure 3.3 The outlet air jet angle

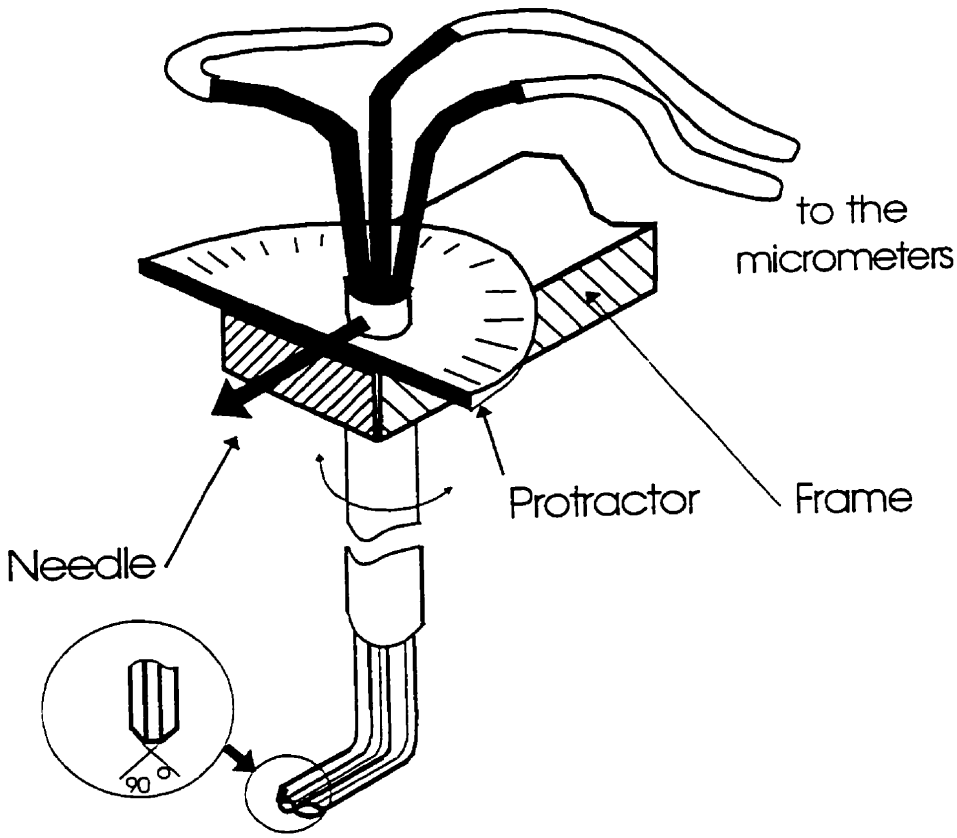

Figure 3.4 The three-tube-pitot instrument facing away from the duct

Duncan's Multiple Range Test (95% confidence level) indicated that static air pressures measured with the static tube and the piezometric flush taps were significantly different for the first 4.2 m of perforated duct length downstream from the fan end (Table 3.4). This 1.1 to 4.5% variation in static air pressure readings (Table 3.5) between instruments, was caused by air swirling over a distance equivalent to 9 times the duct hydraulic diameters (Table 3.3). Compared to the static tube and piezometric opening with flush taps, the outstanding taps had more pressure variation. With these taps, significant differences in static pressure were detected for the first section of 4.2 m and at 0.6 and 1.3 m from the closed end of the perforated duct (Table 3.4). Moreover, with the air swirling over the section of 4.2 m, the outstanding taps had higher pressure error level (table 3.5).

For experimental accuracy and to prevent air swirling, in addition to the air straightener, a non perforated duct of length equal to 10 times its hydraulic diameter should be inserted, between the perforated section and the fan. Also, the outstanding taps should be avoided for static pressure measurements because of their possible reading error resulting from their misalignment during installation. Furthermore, the effect of misalignment seemed to have been amplified with the air swirling.

3.3.2 Outlet Air Flow

The three-tube-pitot instrument proved to be very sensitive to outlet air jet discharge angle and velocity. For the smallest angles measured (35°), a 3% coefficient of variation was obtained from the three consecutive readings. Nevertheless, the grid method applied at the outlet surface, to estimate outlet air flow, proved inaccurate when compared to the air flow measurement inside the perforated duct (Table 3.6).

Generally, the sum of the outlet flow exceeded that measured inside the duct by 3 to 28% for aperture ratios ($\Sigma A_o/A$) of 0.5 to 2 respectively. Further observations indicated that the outlet air jet contraction could not be accurately detected by the grid method. The air jet leaving each outlet contracts because of its longitudinal velocity component and unless its vena contracta can be accurately measured, the outlet air flow area will appear greater than it actually is. In the present case, a non detected contraction of 2.5 mm around the edge of an outlet measuring 145 mm by 25 mm created a 25% error while being too narrow to be measured by a set of three pitot tubes, each 3 mm in diameter, held at 10 mm from the perforated duct wall. Therefore, outlet air flow can be more accurately measured from the difference in air velocity over the perforated duct's inside cross section, upstream and downstream from the outlet.

Table 3.3 Duncan's Multiple Range Test for static tube measurements.

Measurement point number	Measurement distance from duct end (m)	Distance of the pitot tube from the top panel of the perforated duct (mm): 50	100	150	200	250	290
		Duncan's analysis with measurement means (Pa)					
1	8.5	49.2 **B**	49.2 **B**	49.5 **AB**	49.8 **A**	49.2 **B**	48.6 **C**
2	8.0	50.5 **A**	50.1 **AB**	50.0 **B**	50.0 **B**	49.6 **B**	49.6 **B**
3	6.8	50.9 **C**	51.0 **C**	51.2 **BC**	51.6 **A**	51.7 **A**	51.4 **AB**
4	6.1	50.9 **BC**	50.9 **C**	51.1 **ABC**	51.4 **AB**	51.5 **A**	51.3 **AB**
5	5.5	51.7 **BC**	51.5 **C**	51.8 **AB**	51.8 **AB**	52.0 **A**	52.0 **A**
6	4.3	53.2 **A**	52.8 **A**	52.9 **A**	52.9 **A**	53.2 **A**	52.9 **A**
7	3.7	52.7 **A**	52.9 **A**	52.9 **A**	53.1 **A**	53.0 **A**	53.0 **A**
8	3.1	53.3 **A**	53.1 **A**	53.3 **A**	53.3 **A**	53.1 **A**	53.1 **A**
9	1.9	56.1 **A**	56.2 **A**	56.3 **A**	56.3 **A**	56.3 **A**	56.0 **A**
10	1.3	56.6 **A**	56.6 **A**	56.3 **A**	56.4 **A**	56.3 **A**	56.2 **A**
11	0.6	55.8 **A**	55.9 **A**	55.7 **A**	55.8 **A**	55.9 **A**	55.8 **A**
12	0.1	55.1 **A**	55.0 **A**	55.1 **A**	54.9 **A**	54.8 **A**	55.0 **A**

Note: for each measurement distance, means with the same letter are not significantly different; A, B and C stand for the highest, intermediate and lowest values respectively.

Table 3.4 Duncan's Multiple range Test to compare static tube and piezometer taps readings

Measurement point number	distance from duct end (m)	Measurement instruments: Piezometric openings flush tap — Duncan's analysis with measurement means (Pa)	Piezometric openings outstanding tap	static tube
1	8.5	48.3 **A**	44.9 **B**	48.3 **A**
2	8.0	48.7 **B**	47.3 **C**	50.6 **A**
3	6.8	50.5 **B**	50.2 **B**	52.9 **A**
4	6.1	53.4 **B**	52.9 **B**	54.0 **A**
5	5.5	54.0 **C**	54.5 **A**	54.8 **A**
6	4.3	55.7 **B**	56.5 **A**	56.5 **A**
7	3.7	58.1 **A**	58.2 **A**	58.2 **A**
8	3.1	58.7 **A**	58.7 **A**	58.7 **A**
9	1.9	59.9 **A**	60.0 **A**	59.9 **A**
10	1.3	60.5 **B**	60.9 **A**	60.6 **AB**
11	0.6	60.9 **AB**	61.1 **A**	60.9 **B**
12	0.1	60.5 **A**	60.5 **A**	60.6 **A**

Notes:

1 -for each measurement distance, means with the same letter are not significantly different; A, B and C stand for the highest, intermediate and lowest values respectively.

2 -The pressure values reported in Table 3.4 are higher than those of Table 3.3, because both experiments were conducted on different day.

Table 3.5 Numerical comparison of piezometric tap and static tube

Measurement		flush taps	outstanding taps	Static tube
point number	distance* from duct end (m)	P_m Pa (error)**	P_m Pa (error)**	P_{ms} Pa
1	8.5	48.3 (0.0%)	44.9 (7.0%)	48.3
2	8.0	48.7 (3.7%)	47.3 (6.5%)	50.6
3	6.8	50.5 (4.5%)	50.2 (5.1%)	52.9
4	6.1	53.4 (1.1%)	52.9 (2.0%)	54.0
5	5.5	54.0 (1.4%)	54.5 (0.5%)	54.8
6	4.3	55.7 (1.4%)	56.5 (0.0%)	56.5
7	3.7	58.1 (0.1%)	58.2 (0.0%)	58.2
8	3.1	58.7 (0.0%)	58.7 (0.0%)	58.7
9	1.9	59.9 (0.0%)	60.0 (0.1%)	59.9
10	1.3	60.6 (0.1%)	60.9 (0.5%)	60.6
11	0.6	60.9 (0.0%)	61.1 (0.3%)	60.9
12	0.1	60.5 (0.1%)	60.5 (0.0%)	60.6

Note :
P_{ms}: average static pressure obtained from a static tube, Pa;
P_m: average static pressure obtained from a wall tap, Pa, for a duct aperture ratio of 0.5;
* from the closed end of the perforated duct;
** error = $100^* (P_m - P_{ms})/P_{ms}$.

Table 3.6: Error due to air jet contraction at outlets

Aperture ratio	Measured velocity* m/s	Calculated velocity** m/s	Error %
0.5	4.63	4.78	3.24
1	7.22	8.54	18.28
1.5	8.08	9.96	23.27
2	8.44	10.77	27.61

* inside the perforated duct, upstream from the perforated section;
** from the sum of the outlet air flows.

3.4 Conclusion

To measure static air pressure inside perforated ventilation ducts, both static tube and piezometric flush taps can be used as they give similar readings. Nevertheless, air swirling inside the perforated duct, close to the fan end, must be eliminated by inserting a non perforated section of length equal to 10 times the duct's hydraulic diameter, between the fan and the perforated section. This is in agreement with ANSI/AHRAE[15] recommendations. The static tube is better suited to polyethylene perforated ducts because of the flexible lining while the piezometric flush taps are preferred for wooden perforated ducts. The outstanding taps have to be avoided because of the error which can result from misalignment.

The three-tube-pitot instrument was sensitive enough to accurately measure air jet angle and velocity at the outlet surface and demonstrated that both parameters vary over the length of the perforated duct. But, the instrument was too large to measure the air jet contraction area, which led to errors of 3 % to 28 % in reading outlet air flow for aperture ratios of 0.5 to 2.0, respectively. A larger error was obtained with larger outlet openings because the same number of grid subsections was used for all four outlet sizes. Therefore, accurate outlet and duct air flow are difficult to obtain from measurements at the orifice, outside the duct, even if the discharge angle is taken into consideration. Rather, outlet air flow is more easily and accurately measured using the grid method over the duct inside cross-sectional area.

3.5 Acknowledgement

The authors acknowledge the financial contribution of the Natural Sciences and Engineering Research Council of Canada, the Tunisian government and Le Ministère de l'Agriculture, des

Pêcheries et de l'Alimentation du Québec.

3.6 References

[1] **Randall J M; V A Battams** Stability criteria for airflow patterns in livestock buildings. Journal of Agricultural Engineering Research 1979, 24: 361-374.

[2] **Leonard J J; McQuitty J B** Archimedes number criteria for the control of cold ventilation air jets. Canadian Agricultural Engineering 1986, 28(2): 117-123.

[3] **Ogilvie J R; Barber M E; Randall J M** Floor air speeds and inlet design in swine ventilation systems. Transactions of the ASAE 1990, 33(1): 255-259.

[4] **Bailey G J** Fluid flow in perforated pipes. Journal of Mechanical Engineering Science. 1975, 17(6): 338-347.

[5] **Saunders D D; Albright L D** Airflow from perforated polyethylene tubes. Transactions of the ASAE 1984, 23(6): 1144-1149.

[6] **Carpenter G A** The design of permeable ducts and their application to the ventilation of livestock building. Journal of Agricultural Engineering Research 1972, 17: 219-230.

[7] **Brundrett E; Vermes P T** Evaluation of tube diameter and fan induced swirl in polyethylene ventilation tubes. Transactions of the ASAE 1987, 30(4): 1131-1138.

[8] **Barrington S F; MacKinnon I R** Air distribution from rectangular wooden ventilation ducts. Transactions of the ASAE 1990, 33(3): 944-948.

[9] **Pastula R; Feddes J J R; Leonard J J** Discharge coefficients for openings in metal or plywood walls of recirculation ducts. Canadian Agricultural Engineering 1992, 34(4):359-363.

[10] **Streeter V L; Wylie E B** Fluid mechanics. First SImetric edition 1981. McGraw-Hill Ryerson Limited.

[11] **Koestel A; Tuve G L** The discharge of air from a long slot. Transactions of the ASHVE 1948, 54: 87-100.

[12] **Burgess W A; Ellenbecker M J; Treitman R D** Ventilation for control of the work environment 1989. A Wiley-Interscience publication.

[13] **Steel R D; Torrie J H** Principles and procedures of statistics 1980. A biometrical approach. Second edition. McGraw-Hill Book Company.

[14] **Esmay, M L; Dixon J E** Environmental control for agricultural buildings. The AVI Publishing Company, Inc., 1986, Westport, Connecticut, U.S.A. page 84-88

[15] **ANSI/ASHRAE** Laboratory methods of testing fans for rating. ANSI/ASHRAE Standard 51-1985. AMCA, Inc. and ASHRAE, Inc.

CONNECTING TEXT

Having established accurate methods for the measurement of the air flow parameters of perforated ventilation ducts, the second objective was undertaken and basic fluid mechanic equations where applied to model the air flow distribution of perforated ventilation duct. The validation of this model will follow the upcoming manuscript.

4 PERFORATED VENTILATION DUCTS PART I: A MODEL FOR FLOW DISTRIBUTION

4.1 Introduction

Perforated ducts are used widely for the air-conditioning of public, industrial, and agricultural buildings. These ducts are preferred for heating and cooling spaces because of their efficient and uniform distribution of the entire air volume. However, the quality of air conditioning is directly dependent upon the proper design of the perforated ventilation ducts. Ogilvie et al.[1] reported that the outlet velocity of an air jet sets the velocity at the floor and within the ventilated space. Moreover, the air distribution pattern of perforated ducts is a complex function of several inter-related factors such as duct construction material, fan capacity and performance, perforation geometry, size and spacing, duct length, and internal cross-sectional area.

The regain coefficient is an additional problem to consider when modelling duct air flow distribution. This coefficient was introduced by McNown[2] who reported that the mechanical energy of the air mass upstream from an outlet can be greater than from that of downstream. Bajura and Jones[3] attributed this phenomenon to the air stream re-arrangement between the boundary layer and the main stream as the outlet is traversed, where by the fluid of low kinetic energy is discharged into the lateral outlet with higher kinetic energy fluid remaining in the header. Ashley et al.[4] defined the regain coefficient as the ratio of the static pressure rise to the decrease in velocity pressure based upon the mean air stream velocity over the cross-sectional area of the duct.

Air distribution in ducts has been analyzed and modelled by Koestel and Young[5], Horlock[6], Haerter[7], Bailey[8], Saunders and Albright[9], and Newman[10]. The design methods diverged in basic assumptions and in the application of fluid mechanic

principles. Some authors have considered frictional losses while others have assumed these to be negligible. In general, Bernoulli's equation has been applied along the length of the duct but adjustments for frictional losses were introduced only in few cases. The momentum equation was often used instead of the energy equation.

A model is therefore needed to clarify and simplify the air flow characteristics in ducts. The fundamental equations of fluid mechanics and thermodynamics should form the basis of the model and its simplification is desirable only if experimental results so warrant. Thus, the objective of this paper is to develop a consistent and complete air distribution model for perforated ventilation ducts from the basic principles of thermodynamics and fluid mechanics of a newtonian fluid.

4.2 Application of the fundamental equations

The first law of thermodynamics applied to the control volume sketched in Figure 4.1 can be written in the average rate form as,

$$dE/dt = (\delta Q/dt) - (\delta W_f/dt) \quad \ldots\ldots\ldots\ldots\ldots \quad (1)$$

where $\delta W_f/dt$ = traction work done on the control volume surfaces by flowing fluids. The absence of electrical and magnetic forces, and shafts in the control volume produced no other work and no work transferred at the control surface to the surroundings by direct contact between non-fluid elements. The traction work is given by,

$$\delta W_f/dt = \iint_{cs} PV \, dA = \iint_{cs} [PV(\rho V \, dA)], \quad \rho V = 1 \quad \ldots \quad (2)$$

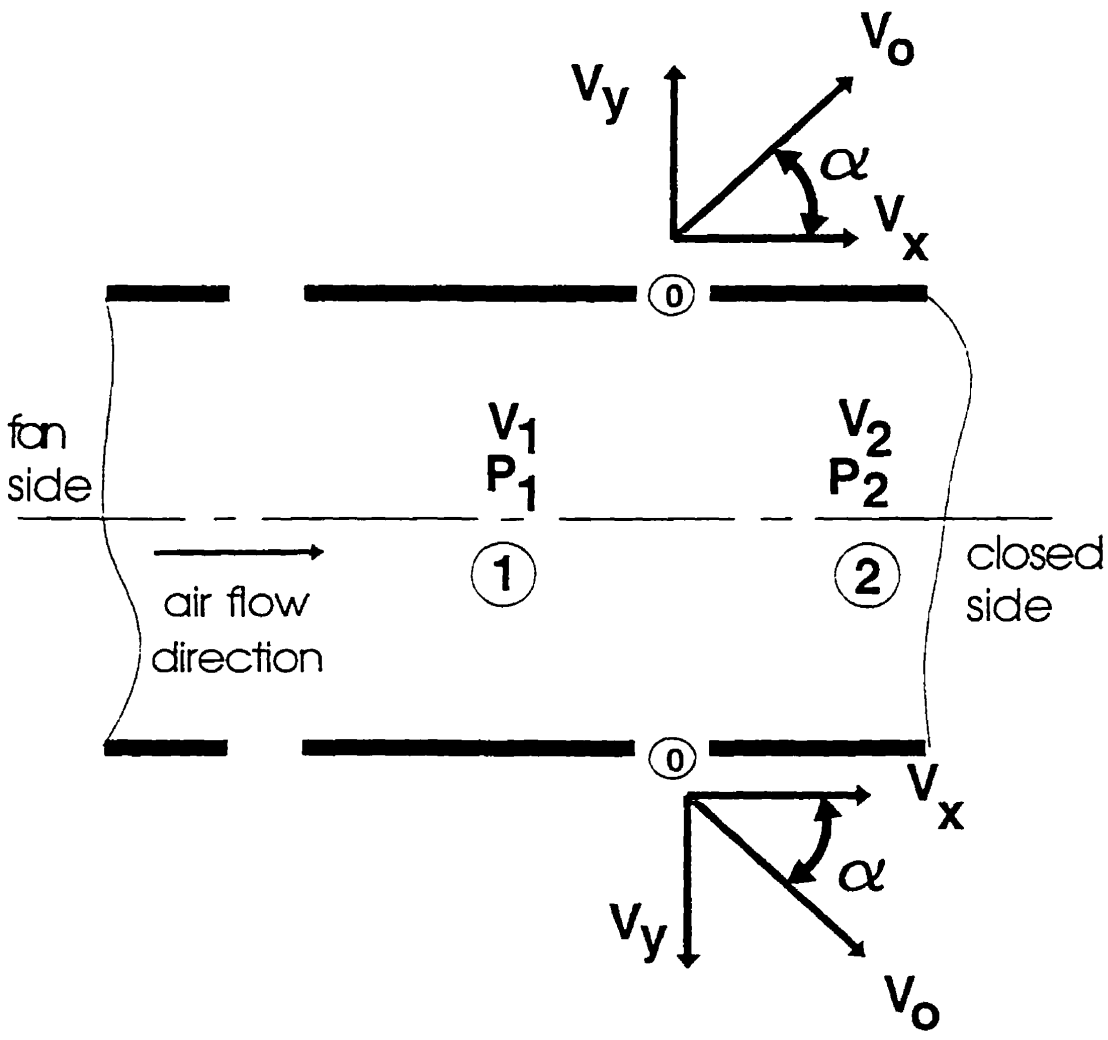

Figure 4.1 One dimensional model flow inside a module of the duct

For a specific control volume, consisting of air flowing down the length of a duct past an outlet, dE/dt can be defined from the Reynolds transport equation as,

$$dE/dt = \iint_{cs}[e(\rho V\ dA)] + \partial/\partial t \iiint_{cv}[e(\rho dv)] \quad . . . . \quad (3)$$

Substituting equation (3) into (1), and assuming a steady-state flow, we get, $\delta Q/dt - \delta W_f/dt = \iint_{cs}[(\frac{1}{2}V^2+gz+u)\rho V\ dA]$. (4) Using equation (2), equation (4) can be reformulated as,

$$\delta Q/dt = \iint_{cs}[(\frac{1}{2}V^2+gz+u+PV)\rho V\ dA] \quad . . . . . \quad (5)$$

4.2.1 Energy equation for the control volume

The control volume (Figure 4.1) has an upstream inflow and a downstream outflow of an air mass over an area A and two outlets leading to losses in air mass, each over an area A_o. Since the changes in flow properties are negligible, they can be assumed constant over the duct length and considering one dimensional flow, the cross-sectional air velocities V_i, elevation z_i, internal energy u_i, and pressure P_i, can also be considered constant. Thus, the energy equation (3) applied to our control volume can be expanded into equation (6).

$$\begin{aligned}\delta Q/dt = &-(\tfrac{1}{2}V_1^2+gz_1+u_1+P_1/\rho_1) \iint_{A1}[\rho_1 V_1\ dA_1] \\ &+ (\tfrac{1}{2}V_2^2+gz_2+u_2+P_2/\rho_2) \iint_{A2}[\rho_2 V_2\ dA_2] \\ &+ 2(\tfrac{1}{2}V_o^2+gz_o+u_o+P_o/\rho_o) \iint_{Ao}[\rho_o V_o\ dA_o] \quad . . . . . \quad (6)\end{aligned}$$

since, $z_0=z_1=z_2$, as provided by the position of the lateral outlets of the ventilation duct. The terms "gz_i" can be eliminated as, for gases, they are negligible compared with other terms in equation (6).

The rate of mass flow upstream and downstream from the

control volume and through the outlets are defined, respectively, for each flow cross-section as,

$$\iint_{A1}[\rho_1 V_1\ dA_1] = \rho_1 V_1\ A = dm_1/dt \quad \ldots\ldots\ldots \quad (7)$$

$$\iint_{A2}[\rho_2 V_2\ dA_2] = \rho_2 V_2\ A = dm_2/dt \quad \ldots\ldots\ldots \quad (8)$$

$$\iint_{Ao}[\rho_o V_o\ dA_o] = \rho_o V_o\ A_o\ C_d\ \sin(\alpha) = dm_o/dt \quad \ldots \quad (9)$$

The conditions of continuity apply to the control volume and since the air flow is assumed incompressible and inviscid, ρ is assumed constant and the temperature change is too small for an equation of state to make any significant contribution to the flow along the duct. The equation of continuity is simplified to,

$$V_1\ A = V_2\ A + 2\ V_o\ A_o\ C_d\ \sin(\alpha) \quad \ldots\ldots\ldots \quad (10)$$

The energy equation can be written as,

$$[\tfrac{1}{2}V_1^2 + u_1 + P_1/\rho]\ dm_1/dt + \delta Q/dt = [\tfrac{1}{2}V_2^2 + u_2 + P_2/\rho]\ dm_2/dt + [\tfrac{1}{2}V_o^2 + u_o + P_o/\rho]\ dm_o/dt \quad \ldots\ldots\ldots \quad (11)$$

The assumptions implicit in equation (11) do not exclude skin friction because it includes internal and mechanical energy. In our case, the loss of mechanical energy by the skin friction is assumed to account strictly for the gain of internal energy and the heat transfer from the flow to the outside. Equation (11) can be transformed by grouping the friction losses and by defining mass flow in terms of only dm_1 and dm_0. The term $(\tfrac{1}{2}V_2^2 + u_2 + P_2/\rho)\,(dm_o/dt)$ - $(\tfrac{1}{2}V_2^2 + u_2 + P_2/\rho)\,(dm_o/dt)$ is added to the right-hand-side of equation (11) and all components are multiplied by (dt/dm_1), yielding equation (12).

$$[\tfrac{1}{2}V_1^2 + u_1 + P_1/\rho] = [\tfrac{1}{2}V_2^2 + u_2 + P_2/\rho](dm_2/dm_1) - \delta Q/dm_1 + (\tfrac{1}{2}V_2^2 + u_2 + P_2/\rho)(dm_o/dm_1) - (\tfrac{1}{2}V_2^2 + u_2 + P_2/\rho)(dm_o/dm_1) + [\tfrac{1}{2}V_o^2 + u_o + P_o/\rho](dm_o/dm_1) \quad \ldots\ldots (12)$$

Rearranging terms and applying the continuity condition,

$$(dm_2/dm_1 + dm_0/dm_1) = dm_1/dm_1 = 1$$

equation (12) becomes equation (13) after expressing all pressures relative to the atmospheric pressure P_o,

$$[\tfrac{1}{2}V_1^2 + P_1/\rho] = [\tfrac{1}{2}V_2^2 + P_2/\rho] + [-u_1 + u_2 - \delta Q/dm_1] + [\tfrac{1}{2}V_o^2 - \tfrac{1}{2}V_2^2/2 - P_2/\rho + u_o - u_2](dm_o/dm_1)] \quad \ldots (13)$$

The friction losses (F_L) for a perforated duct can be represented by,

$$F_L = [-u_1 + u_2] + [u_o - u_2](dm_o/dm_1) - \delta Q/dm_1 \quad \ldots\ldots (14)$$

Equation (13) can therefore be reduced to equation (15) after solving for the pressure differential upstream and downstream from the outlet.

$$P_1 - P_2 = \rho\,[\tfrac{1}{2}V_2^2 - \tfrac{1}{2}V_1^2] + \rho\,F_L + \rho\,[\tfrac{1}{2}V_o^2 - \tfrac{1}{2}V_2^2 - P_2/\rho]\,(dm_o/dm_1)] \quad \ldots\ldots\ldots (15)$$

Equation (15) holds true when the air inside a perforated duct flows as one streamline and $\tfrac{1}{2}V_o^2$ represents the total specific energy at the outlet. Bernoulli's equation (16) defines the potential outlet air jet velocity if there were no friction losses at the outlet level.

$$V_o = \sqrt{(2\ g\ H)} \quad \ldots\ldots\ldots\ldots\ldots\ldots\ldots (16)$$

4.2.2 Outlet air jet velocity and discharge coefficient

The air flow through the outlets reduces the average air velocity inside the duct from V_1 to V_2. Therefore, dm_o/dt is a direct function of the duct cross-sectional area, A, and can be expressed in terms of the outlet area corrected by a discharge coefficient, C_d as,

$$dm_o/dt = \rho\ (V_1-V_2)\ A\ = 2\ \rho\ (V_o\ sin(\alpha))\ C_d\ A_o \quad . . \quad (17)$$

The discharge coefficient corrects for the friction losses and the contraction which occurs as the air exits the outlet. Thus, C_d is a product of two other coefficients as in equation (18).

$$C_d = C_v\ C_c \quad . . . . . \quad (18)$$

The contraction coefficient, C_c, represents the air jet contraction as it leaves the outlet because the air is flowing axially with respect to the opening and has to turn at an angle to exit. The maximum outlet contraction occurs at the vena contracta where the streamlines are parallel through the air jet and the pressure is atmospheric (Streeter and Benjamin[11]). The ratio of the jet area at the vena contracta to that of the orifice is the contraction coefficient, C_c. The velocity coefficient C_v is the ratio of the actual average velocity, V_a, to the potential velocity, V_o. The actual discharge, q_a, at the orifice is the product of the actual velocity and the area of the jet at the vena contracta. C_d can be computed directly as the ratio of q_a to the product of the component of V_o normal to the discharge area as shown in equation (19).

$$q_a = C_d\ A_o\ V_o\ sin(\alpha) = C_c\ A_o\ V_a\ sin(\alpha) \quad . . . . . \quad (19)$$

Newman[10], Davis[12], and McNown and Hsu[13] used a modified

discharge coefficient = $C_d \sin(\alpha)$. Under such conditions, C_d varies along the length of the duct in parallel with the sine of the discharge angle (Figure 4.2). This variation in discharge angle was also observed by Koestel and Young[5].

4.2.3 Momentum equation for the control volume

The momentum equation for the control volume (Figure 4.1) shows a relationship between pressure and velocity as given in equation (20).

$$P_1-P_2 = \rho\ [V_2^2-V_1^2] + \rho\ [V_1-V_2]\ V_o \cos(\alpha) + P_f. \quad \ldots\ (20)$$

where P_f is the static pressure losses due to the skin friction of air flow.

The static pressure differential between upstream and downstream from the outlet is given by equations (15) and (20). It is assumed that the thermodynamic friction losses converted to the pressure losses in the energy equation are equivalent to the pressure friction losses in the momentum equation. Thus, equations (15) and (20) can be combined to eliminate the friction term and to redefine P_2 in terms of the outlet discharge angle and average velocities as,

$$P_2 = \rho\ [V_1\ (\tfrac{1}{2}(V_1+V_2)-V_o \cos(\alpha)) + \tfrac{1}{2}(V_o^2-V_2^2)] \quad \ldots\ (21)$$

However, the concept of a regain coefficient must be introduced to account for the less than perfect uni-streamline flow.

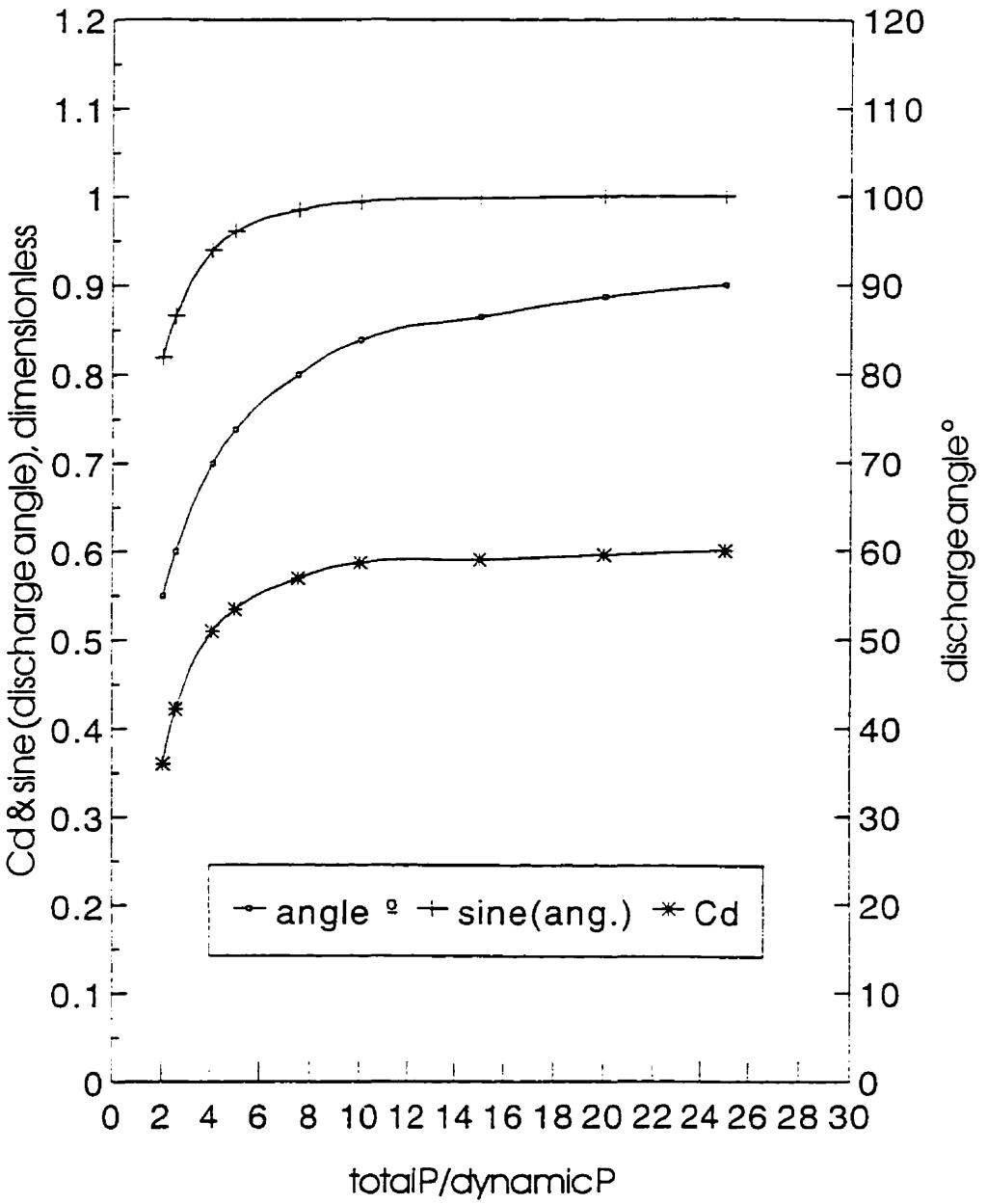

Figure 4.2 Outlet dDischarge coefficient and angle along the duct as a function of total and dynamic pressures ratio (Newman, 1989)

4.3 The regain coefficient

The regain coefficient concept originated from the fact that, as compared to upstream from the outlet, more specific mechanical energy may be available downstream. It can lead to an outlet air jet with a lower mechanical energy than upstream from the outlet, because the outlet air jet comes mainly from the boundary layer. The kinetic energy of the fluid flowing onward inside the duct may be higher than calculated from the average upstream velocity. Asheley et al.[4] developed charts for the prediction of the regain coefficient and found its value to range from 49.75 to 447.8 Pa when both V_1 and V_2 vary from 5 to 29.5 m/s. The regain coefficient chart was obtained by measuring the pressure differential between upstream and downstream from a single outlet in a smooth pipe and by adding the measured values for friction losses. Haerter[7] suggested that the regain coefficient for pipes with pairs of diametrically opposite holes be increased by 15%, compared with single outlets. In his model for flow distribution in manifolds, Bajura[14] used a regain coefficient of 0.94 for dividing flows. Bailey[8] developed a model to predict the coefficient of the static regain by measuring the static pressure along a perforated pipe and estimated the friction losses (Colebrook[15]) from equation (22).

$$C_r = 0.78 + [0.284 + 0.098 \log (d/D)] \log [V_1/(V_1-V_2)] \quad (22)$$

An energy correction factor must also be applied to the mean velocity, V, to account for the non-uniform profile in air velocity over the duct's cross section. This factor can be determined either in terms of the kinetic energy or the momentum and is about two for laminar and 1.01 to 1.10 for turbulent flow (Streeter[16]). Equations (20) and (21) contain the average velocity over the duct's cross-sectional area based on an energy correction factor of unity. The importance

of the energy correction factor in the model depends upon how well the equations reproduce the real static pressure and discharge angle.

4.3.1 The regain coefficient from the energy equation

Equation (15) can be modified to define P_1-P_2 in terms of the regain coefficient in combination with equation (17) and can be written as,

$$P_2-P_1 + \rho F_L = \tfrac{1}{2}\rho [V_1^2-V_2^2] C_r \quad \ldots\ldots\ldots\ldots (23)$$

where $C_r = [1 - [2/((V_1+V_2) V_1)][\tfrac{1}{2}(V_o^2-V_2^2) - P_2/\rho]]$

If $[\tfrac{1}{2}(V_o^2-V_2^2) - P_2/\rho] = 0$, $\tfrac{1}{2}V_o^2 = \tfrac{1}{2}V_2^2 + P_2/\rho$, and $C_r = 1$

If $[\tfrac{1}{2}(V_o^2-V_2^2) - P_2/\rho] > 0$, $\tfrac{1}{2}V_o^2 > \tfrac{1}{2}V_2^2 + P_2/\rho$, and $C_r < 1$

If $[\tfrac{1}{2}(V_o^2-V_2^2) - P_2/\rho] < 0$, $\tfrac{1}{2}V_o^2 < \tfrac{1}{2}V_2^2 + P_2/\rho$, and $C_r > 1$

The energy correction factor can be introduced into equation (23) so that equation (24) may accurately estimate the duct static pressure.

$$[P_1/\rho - P_2/\rho] = [K_{e2}\ \tfrac{1}{2}V_2^2 - K_{e1}\ \tfrac{1}{2}V_1^2] + F_L + [\tfrac{1}{2}V_o^2 - K_{e2}\ \tfrac{1}{2}V_2^2 - P_2/\rho](dm_o/dm_1)] \quad \ldots (24)$$

The outlet velocity, V_o in equation (24) requires no energy correction factor as it represents the potential outlet energy. Equation (24) can be simplified by assuming $K_{e1} = K_{e2}$, and these quantities are a direct function of friction (Streeter[16]) which in turn is a function of Reynold's number. Thus, equation (24) becomes,

$$P_2-P_1 + \rho F_L = \tfrac{1}{2}\rho [V_1^2-V_2^2][K_{e1} - (2/((V_1+V_2) V_1))(\tfrac{1}{2}(V_o^2-K_{e2} V_2^2) - P_2/\rho)] \quad (25)$$

and

$$C_r = K_{e1} - [2/((V_1+V_2) V_1)][\tfrac{1}{2}(V_o^2-K_{e2} V_2^2) - P_2/\rho] \quad (26)$$

The conditions for the verification of C_r are then:

If $\tfrac{1}{2}V_o^2 = K_{e2}\ \tfrac{1}{2}V_2^2 + P_2/\rho$, then $C_r = K_{e1}$

If $\tfrac{1}{2}V_o^2 > K_{e2}\ \tfrac{1}{2}V_2^2 + P_2/\rho$, then $C_r < K_{e1}$

If $\tfrac{1}{2}V_o^2 < K_{e2}\ \tfrac{1}{2}V_2^2 + P_2/\rho$, then $C_r > K_{e1}$

The principle of conservation of mechanical energy suggests that $C_r \approx 1$. It is highly unlikely that $C_r < K_{e1}$ as it requires that the outlet air jet contain more specific energy than the air stream inside the duct, downstream from the outlet. The outlet air jet originates from the boundary layer of the duct air stream where the kinetic energy is lower than the average because of skin friction. Thus, more specific kinetic energy is carried downstream for conversion to static pressure which implies that $\tfrac{1}{2}V_o^2$ cannot be higher than $[K_{e2}\ \tfrac{1}{2}V_2^2 + P_2/\rho]$ and $C_r \geq k_{e1}$.

For the purpose of discussions, the regain coefficient can be simplified as follows:

$$C_r = K_{e1} - [2/((V_1+V_2)V_1)] [\tfrac{1}{2}(V_o^2 -V_2^2) - P_2/\rho -(K_{e2}-1)\tfrac{1}{2}V_2^2] \quad (27)$$

If the outlet air velocity V_o is calculated from the duct average air velocity and if friction losses between points o and 2 are neglected, $[\tfrac{1}{2}V_o^2 - \tfrac{1}{2}V_2^2 - P_2/\rho] \approx 0$, and C_r becomes,

$$C_r = K_{e1} + [(K_{e2}-1)/((V_1+V_2)V_1)]\ V_2^2) \quad (28)$$

The range of C_r is between 1.03 and 1.11, which is slightly higher than the energy correction factor, when calculated from

the above equation under conditions of turbulent flow (Re $4.5x10^3$ to $1.5x10^6$) and for K_e ranging from 1.02 to 1.1 (Streeter[16]) and for V_2/V_1 between 0.45 and 0.98 (Figure 4.3). Thus, C_r is highly depended on the velocity profile over the cross-section of the duct which is described by K_e. Without introducing a significant error, C_r can therefore be considered equal to the energy correction factor.

4.3.2 The regain coefficient from the momentum equation

C_r can also be calculated from the momentum equation corrected for the non-uniform air velocity profile over the cross-sectional area of the duct. C_r, as defined by Haerter[7], can be obtained from the momentum equation and written as,

$$C_r = [2 - [V_o \cos(\alpha) / (\tfrac{1}{2}(V_1+V_2))]] \quad \ldots\ldots\ldots \quad (29)$$

If $V_o \cos(\alpha) = \tfrac{1}{2}(V_1+V_2) = V$, then $C_r = 1$
If $V_o \cos(\alpha) < \tfrac{1}{2}(V_1+V_2) = V$, then $C_r > 1$
If $V_o \cos(\alpha) > \tfrac{1}{2}(V_1+V_2) = V$, then $C_r < 1$

The introduction of a momentum correction factor yields the relationship:

$$C_r = [2 K_{m1} - (2(K_{m1}-K_{m2})V_2^2)/(V_2^2-V_1^2) - [V_o \cos(\alpha) / (\tfrac{1}{2}(V_1+V_2))]] \quad \ldots\ldots\ldots \quad (29)$$

showing $C_r \geq 1$. Since the momentum correction factor depends upon the friction coefficient (Streeter[16]), the term $[K_{m1}-K_{m2}]$ becomes insignificant and,

$$C_r = [2K_{m1} - [V_o \cos(\alpha) / (\tfrac{1}{2}(V_1+V_2))]] \quad \ldots\ldots\ldots \quad (30)$$

Thus,
If $V_o \cos(\alpha) = \tfrac{1}{2}(V_1+V_2) = V$, then $C_r = 2K_{m1} - 1$

If $V_o \cos(\alpha) < \frac{1}{2}(V_1+V_2) = V$, then $C_r > 2K_{m1} - 1$
If $V_o \cos(\alpha) > \frac{1}{2}(V_1+V_2) = V$, then $C_r < 2K_{m1} - 1$

K_{m1} can be assumed close to one for the present application, and the term $V_o \cos(\alpha)$ cannot be higher than $V = \frac{1}{2}(V_1+V_2)$. Thus, $C_r \geq 1$, and if $C_r = [2K_{m1} - 1]$, then the outlet velocity component along the manifold equals the corresponding manifold average velocity. But if the outlet fluid comes exclusively from the neighbourhood of the boundary layer, the outlet velocity component along the manifold will be lower which implies a higher C_r and a higher specific mechanical energy downstream from the outlet.

4.4 Conclusions

The air flow within a perforated ventilation duct with an internal static pressure and a discharge angle at the outlet air jet was modelled by using both the energy and momentum equations, instead of just the momentum equation as has been done in the past. The model allowed determination of the flow parameters without the need for the evaluation of the friction losses. Expressions for the friction losses were derived independently from energy and momentum equations and their equivalence remained to be experimentally verified. A discharge angle was included for the calculation of outlet air flow, which implied a constant discharge coefficient over the length of the duct. The regain coefficient was estimated from both the energy and the momentum equations with the conclusion that it is equal to or slightly greater than the energy correction factor, and more specifically, for turbulent flow, $C_r \approx 1$ (Re 4.5×10^3 to 1.5×10^6).

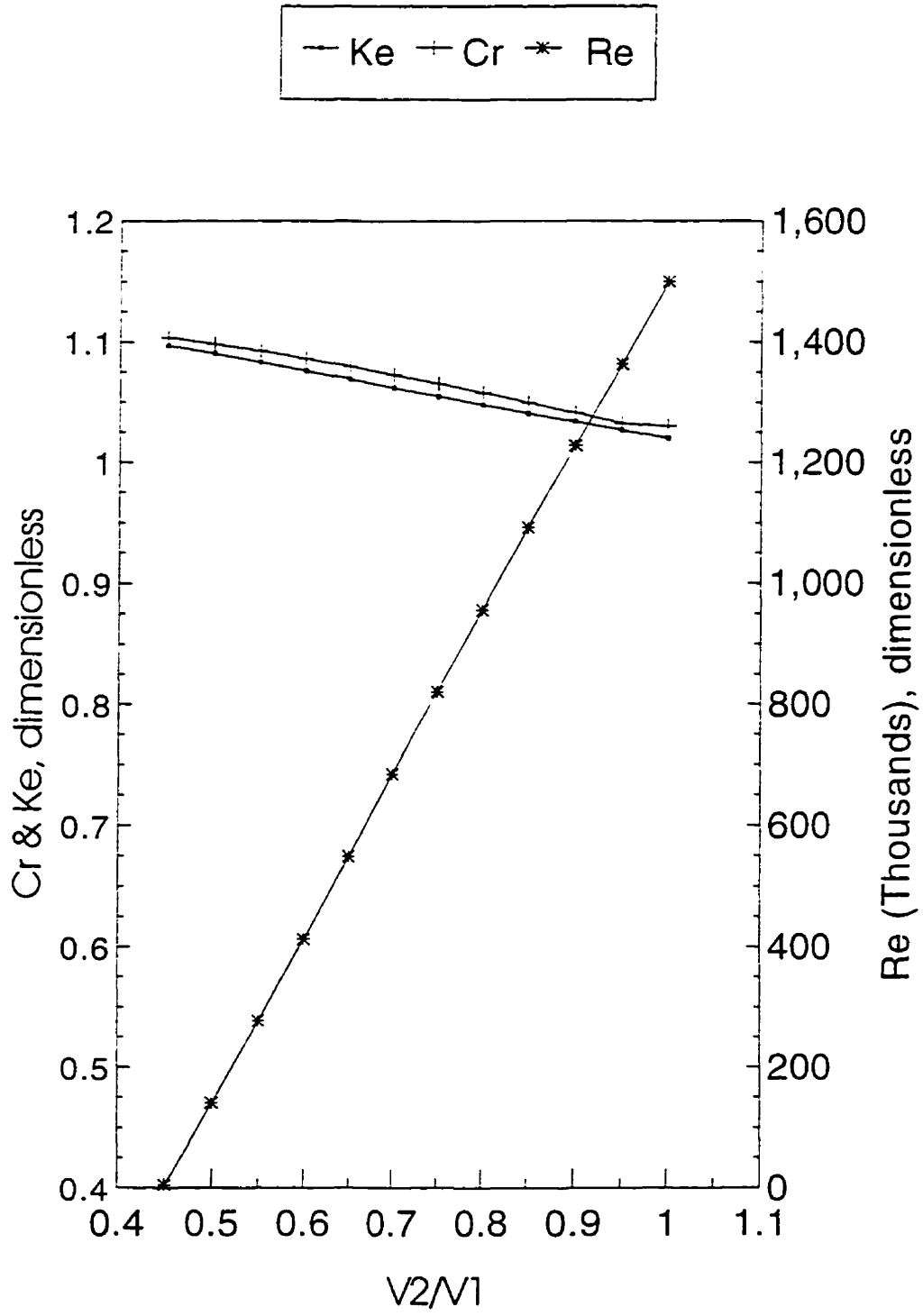

Figure 4.3 Theoretical regain coefficient

Table 4.1 Notation

A_o	outlet area, m^2
A	duct cross-sectional area, m^2
B	force distribution on the control volume from the surrounding (not requiring direct control)
C_d	discharge coefficient at each outlet, dimensionless
C_c	contraction coefficient at each outlet, dimensionless
C_v	velocity coefficient at each outlet, dimensionless
C_r	regain coefficient in the duct at each outlet, dimensionless
d	equivalent diameter of an outlet, m;
D	equivalent diameter of the duct distributing the air, m
dm_i/dt	mass air flow near the outlet, kg s^{-1}
dE/dt	rate of change of energy of a system, J s^{-1}
$\delta Q/dt$	rate of heat added to the system, J s^{-1}
$\delta W/dt$	fluid work, J s^{-1}
dv	volume of fluid that has crossed area δA of the control surface, m^3
E	stored energy in the control volume, J kg^{-1}
e	specific energy, $[V^2/2+gz+u]$, J kg^{-1}
F_L	friction losses, $[u^2-u^1- dQ/dt]$, J kg^{-1}
g	gravity constant, 9.806 m s^{-2}
h	air specific enthalpy at the outlet, J kg^{-1}
H	duct total head, m
K_{ei}	kinetic energy correction coefficient at position i, dimensionless

Table 4.1 Notation (follow)

K_{mi}	momentum energy correction coefficient at position i, dimensionless
P	static pressure, Pa
P_i:	static pressure at position i, Pa
q_a:	measured outlet flow, $m^3\ s^{-1}$
q_{ot}:	calculated outlet flow, $m^3\ s^{-1}$
t	time, s
u_i	specific air internal energy, $J\ kg^{-1}$
V	air velocity, $m\ s^{-1}$
V_a	actual outlet velocity, $m\ s^{-1}$
V_o	potential outlet velocity, $[2gH]^{1/2}$, $m\ s^{-1}$
V_i:	air velocity at position i, $m\ s^{-1}$
V_x:	axial air discharge velocity, $m\ s^{-1}$
V_y:	normal air discharge velocity, $m\ s^{-1}$
$V^2/2$	specific kinetic energy, $J\ kg^{-1}$
z_i	elevation at position i, m
α	discharge angle, degree
ρ	air density, $kg\ m^{-3}$
v	specific air volume, m^3kg^{-1}
$\int_{cs}$	integration over the control volume

Subscripts :

0	outlet
1	upstream from the outlet
2	downstream from the outlet

4.5 Acknowledgement

The authors acknowledge the financial contribution of the Natural Sciences and Engineering Research Council of Canada, Le Ministère de l'Agriculture, des Pêcheries et de l'Alimentation du Québec and the Tunisian government.

4.6 References

[1] **Ogilvie J; Barber E; Randall J M** Floor air speeds and inlet design in swine ventilation systems. Transactions of the ASAE 1990, 33(1): 255-259.

[2] **McNown J S** Mechanics of manifold flow. Transactions ASCE 1954, 119: 1103-1142.

[3] **Bajura R A; Jones E H** Flow Distribution Manifold. Transactions of the ASME 1976, 98: 654-665.

[4] **Ashley C M; Gilman S F; Church R A; Syracuse N Y** Branch fitting performance at high velocity. Transactions of the ASHRAE 1956, 56: 279-294

[5] **Koestel A; Young C Y** The control of air streams from a long slot. Transactions of the ASHRAE 1951, 51: 407-418.

[6] **Horlock J H** An Investigation of the flow of manifolds with open and closed ends. Journal of the Royal Aeronautical Society 1956, 60: 749-753.

[7] **Haerter A A** Flow distribution and pressure change along slotted or branched ducts. Transactions of the ASHRAE 1963, 69: 124-137.

[8] **Bailey B J** Fluid flow in perforated pipes. Journal of Mechanical Engineering Science 1975, 17 338-347.

[9] **Saunders D D; Albright L D** Airflow from perforated polyethylene tubes. Transactions of the ASAE 1984, 27(04): 1144-1149.

[10] **Newman B G** A hodographic solution for flow leaving a manifold through a slit. Canadian Aeronautics and Space Journal 1989, 35: 205-210.

[11] **Streeter V L; Benjamin E W** Fluid mechanics. First SI metric edition 1981. MacGraw-Hill Ryerson limited, 342-344.

[12] **Davis D C; Romberger J S; Andales S C; Yeh H J** Mathematical model for air flow from perforated ducts with annular corrugations. Transactions of the ASAE 1980, 23(3) 661-666

[13] **McNown J S; Hsu E Y** Application of conformal mapping to divided flow. Proc. Mid-western Conference on Fluid Dynamics 1951, 143-155.

[14] **Bajura R A** A model for flow distribution in manifolds. ASME Journal of Engineering for Power 1971, 93: 7-12.

[15] **Colebrook C F** Turbulent flow in pipes with particular reference to the transition region between smooth and rough pipe laws. Journal of the Institution of Civil Engineers 1938-39, 4: 133-156.

[16] **Streeter V L** The kinetic energy and momentum correction factors for pipes and open channels of great width. Civil Engineering 1942, 12(04): 212-213.

CONNECTING TEXT

Applying principles of fluid mechanics to perforated ventilation ducts, a mathematical model was developed to predict their pattern of air flow distribution. To validate the model and its basic hypotheses and assumptions, air flow distribution patterns were obtained from four experimental ducts. The measured parameters were compared to those predicted by the model.

5 PERFORATED VENTILATION DUCTS. PART II: VALIDATION OF AN AIR DISTRIBUTION MODEL

5.1 Introduction

The air distribution pattern in a perforated ventilation duct has generally been modelled by applying Bernoulli's equation, the first law of thermodynamics, and the principle of momentum conservation. Since this approach assumes that all streamlines have the same air velocity, two correction factors should be considered. The air velocity profile over the duct cross-section is not constant and a velocity head correction factor is required to compute the kinetic energy and the momentum of the air moving inside the duct. Since there is an uncertainty in establishing a precise streamline leaving the outlet, a correction factor is needed to account for the correct downstream energy available. Bajura and Jones[1], and Soucek and Zelnick[2] have used a regain coefficient to account for the less than perfect axial discharge of lateral momentum at the outlet.

A simplified, one-dimensional model was developed by El Moueddeb et al.[3], using the fundamental equations of thermodynamics and fluid mechanics for an incompressible and inviscid fluid. The model was based on equation (1) which related the expected pressure downstream from a single or a pair of outlets to the duct average air velocity and to the outlet air jet discharge angle and velocity, and a regain coefficient of equation (2).

$$P_2 = \rho\ [V_1\ ((1/2)\ (V_1+V_2) - V_o\ \cos(\alpha)) + (V_o^2 - V_2^2)/2)] \quad . . \quad (1)$$

$$C_r = K_{e1} - [2/((V_1+V_2)\ V_1)]\ [(V_o^2 - K_{e2}\ V_2^2)/2 - P_2/\rho] \quad . . \quad (2)$$

where the outlet velocity, V_o, defined by the total duct air energy head, does not require an energy correction factor as it represents the potential outlet energy.

The hypotheses upon which the model was built were: (a) the energy and momentum correction factor are almost one for conditions of turbulent flow inside the perforated duct, and (b) the friction losses expressed by the momentum equation are equivalent to those expressed by the thermodynamic energy equation where the gain in internal energy and the heat transfer to the outside were mainly due to skin friction. The second hypothesis was used to combine the kinetic energy and the momentum equations to derive equation (1), which related the ventilation parameters upstream and downstream from the outlet without a friction term. Based on the conservation of mechanical energy over the average cross-sectional area of the duct, the model can also demonstrate that the regain coefficient is almost one, and so are the energy and momentum correction factors.

The objective of this paper was to validate the above hypotheses of the model represented primarily by equation (1). The model validation can be accomplished by measuring the evolution of the pressure (P_1) and (P_2), the outlet discharge angle (α) and velocity (V) along the length of the duct. This will simultaneously verify whether the regain coefficient and the energy correction factors assumed unit values. The outlet air jet discharge coefficient can then be determined using equation (3) of the model,

$$q_a = C_d A_{on} V_o = C_d A_o V_o \sin(\alpha) \quad . . . . . \quad (3)$$

where V_o is the potential outlet air jet velocity and α will be measured from an experimental duct at each outlet. The friction losses along the length of the duct can be verified using the principles of conservation of kinetic energy and momentum.

5.2 Methodology

5.2.1 The experimental duct

The study was limited to a wooden perforated ventilation duct fed by an axial fan and built of a frame of wooden members measuring 39 mm by 39 mm and covered with 6 mm thick presswood panelling (Figure 5.1). The perforated duct offered an inside cross-sectional area of 0.17 m^2 [597 mm x 295 mm) - 4(39 mm x 39 mm]. Its side panels had rectangular pairs of outlets, one on each side panel, 12 in number, and spaced at every 0.61 m. By replacing the side panels of the perforated duct, the experiment was repeated, successively, for four aperture ratios of 0.5, 1, 1.5 and 2.0 (Table 5.1) while keeping the perforated length constant.

The experimental duct was equipped with a 0.450 m diameter ACME axial fan with a 0.25 kW motor operating at 1600 rpm. To reduce air swirling at the outlets, an air straightener, a 1.8 m long tapered section and a 4.9 m non-perforated section were fitted between the fan and the 7.3 m perforated duct. The non-perforated section of 4.9 m had a length equivalent to more than ten times the hydraulic diameter of the perforated duct.

5.2.2 The monitoring equipment

The air static pressure was read using a vertical Dwyer micrometer (MICROTECTOR® GAGE by DWYER INSTRUMENTS, INC.) with an accuracy of ± 0.062 Pa. Through the top panel of the duct and to receive the wall piezometric taps, one small hole was perforated half way between each two pairs of outlets and upstream from the perforated section, for a total of 13 holes. A plastic tube 3 mm in diameter was used to link the piezometric taps to the micrometer and to read static air pressures against that of the atmosphere. At each of the 13 locations, static air pressure readings were repeated three times and averaged.

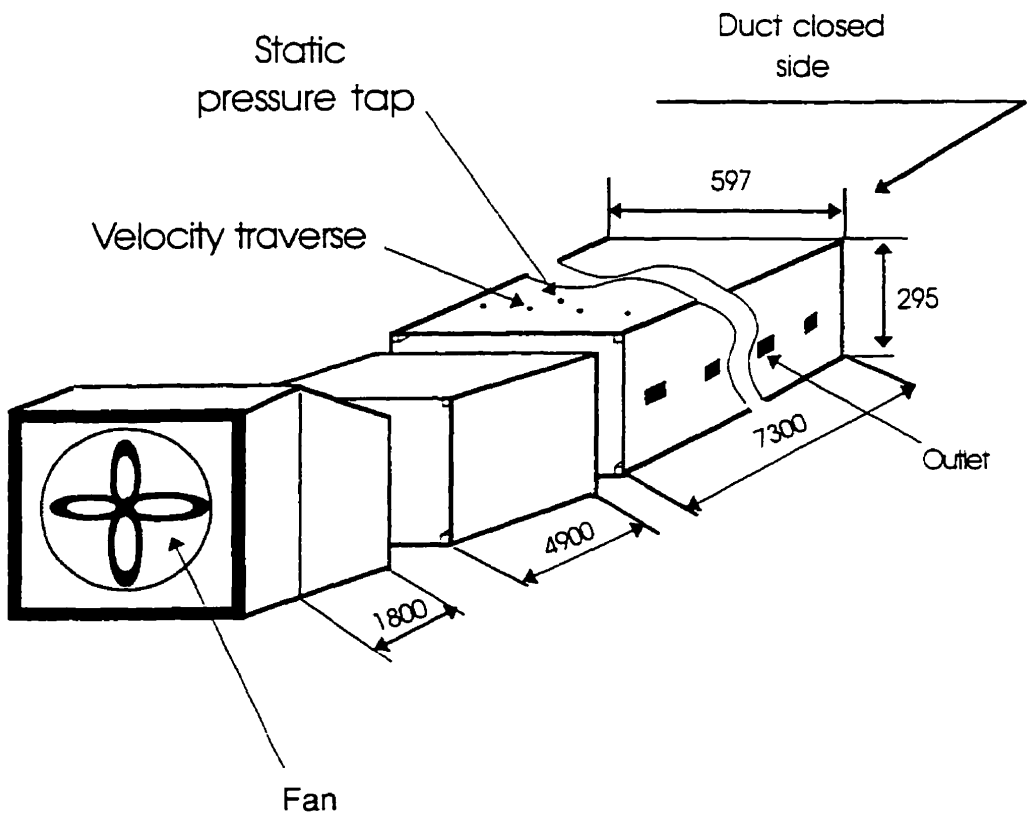

Figure 5.1 The experimental duct.
The dimensions are in mm

According to El Moueddeb et al.[4], a three-port-pitot instrument is recommended to measure the outlet air jet discharge angle and velocity (Figure 5.2). Air leaves the outlets at an angle α (discharge angle) with respect to the wooden side of the duct and must be accurately measured in order to calculate the true axial lateral air jet momentum.

The three-port-pitot instrument was built of three pitot tubes, 3 mm inside diameter, soldered together. The central tube was used to measure the dynamic pressure of the outlet air jet by connecting to the right port of a micrometer while the left port was left open to the atmosphere. Thus, the average outlet air jet velocity was indirectly measured by converting the measured dynamic pressure to velocity using Bernoulli's equation. The two exterior tubes were used to measure the air jet angle by connecting to the opposite port of a second micrometer and by aligning the instrument with the jet angle when zero pressure was recorded. With respect to the duct side panel, the instrument angle of rotation was indicated using a horizontal needle moving over a fixed protractor. The instrument was moved using a grid pattern over the outlet surface to obtain an average value for the air jet discharge angle and velocity.

The three-tube-pitot instrument was calibrated inside the low speed wind tunnel of the Mechanical Engineering Research Laboratory, McGill University, and showed a pitot correction factor as 0.992. During the experiment, the accuracy of the air jet angle measurements was found to be $\pm$ 2.5° for conditions of low air swirling (El Moueddeb et al.[4]).

Table 5.1 Description of the experimental duct

Duct	Outlet size mmxmm	Aperture ratio
1	145x 25	0.5
2	145x 50	1.0
3	145x 75	1.5
4	145x100	2.0

Note : The perforated duct measured 7.3m in length and in all cases, 12 pairs of outlets were used at a spacing of 610 mm.

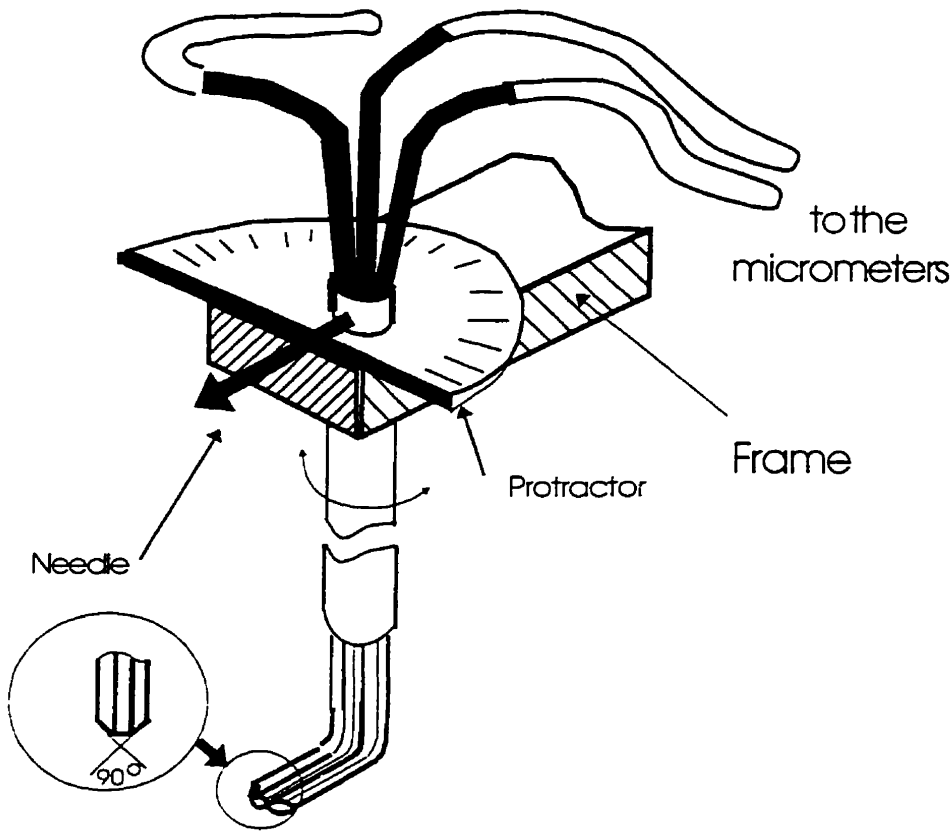

Figure 5.2 The three-port-pitot instrument facing away from the duct outlet. Used to measure outlet air jet discharge angle and velocity.

According to El Moueddeb et al.[4], the outlet air flow could not be obtained with the grid method applied at the outlet surface because the contraction effect was too small to be measured accurately. A small contraction of 2.5 mm on the perimeter of an outlet measuring 2.5 mm by 100 mm cannot be detected by a set of three, 3 mm pitot tubes which produced an error of 24%. Thus, the outlet air flow was determined by measuring the air flow inside the duct, over its cross-section and by calculating the difference in air flow between each outlet. For this purpose, the grid method was applied across the duct's inside cross-section, upstream and downstream from each pair of outlets. Air velocity was measured using an ALNOR compuflow thermo-anemometer with an accuracy of ± 3% of the indicated reading or 0.05 m/s over a range of 0.1 to 15 m/s. For each duct cross-section measured, ten consecutive readings were taken over 16 equal rectangular areas and averaged. The air temperature was measured using the ALNOR thermo-anemometer (thermo-couple sensor) with an accuracy of ± 1º C.

5.2.3 Data accuracy

The maximum uncertainties were 0.8% in static pressure, 3% in mean axial velocity, ±1º C in air temperature, ±2.5º in air discharge angle, 1.2 percent in duct cross-section, 4% in the air outlet area, and 0.1% in the atmospheric pressure at 95% confidence level. As the air density and the average outlet air jet velocity were calculated from measured parameter [$\rho=P/RT$ and $V_o=\sqrt{(2*(P/\rho+V^2/2)}$], their maximum uncertainties were 4 and 5%, respectively. The maximum corresponding uncertainty was 10.3% for the discharge coefficient, 10% in the regain coefficient for a $Re \geq 10^5$, and 10% or ± 2 Pa in the calculated static pressure. The calculated cosine of the discharge air angle had a maximum uncertainty of 6%. The levels of uncertainty were measured and

computed according to ANSI/ASME[5] and Kline[6].

5.2.4 Verification of the model

The model was verified by monitoring the parameters in the experimental duct and by comparing the measured static air pressure and outlet air flow data with those predicted from the equations. The characteristic duct parameters, such as the regain coefficient, the outlet air jet discharge coefficient, and angle were calculated. The variation in static air pressure upstream and downstream from the outlet was also calculated using equation (1) with measured duct average air velocity, the outlet air jet discharge angle, and potential velocity V_o. V_o accounted for energy friction losses occurring at the outlet level as it was calculated from the measured duct total head using Bernoulli's equation.

The calculated static air pressure values were compared with those measured using the experimental duct. After the validation of equation (1), it was used along with the equation derived from the principle of energy conservation to calculate the friction losses along the length of the duct. The outlet air jet discharge angle observed over the length of the duct was compared to that derived from the total energy head and velocity of the air inside the duct. Thus, the effect of friction losses on the discharge angle could be determined. The regain coefficient was calculated using equation (2) by comparing the outlet potential velocity to that averaged upstream and downstream from the outlet.

The outlet air jet contraction coefficient was observed by considering the air inside the duct that must contract to exit at an angle. Therefore, it maintained an axial velocity component that reduced the jet area. The outlet cross-section where the contraction is maximum is called the vena contracta. At this point, the streamlines are parallel throughout the jet and the pressure is atmospheric (Streeter and Benjamin[7]). The

ratio of the actual velocity, V_a, to the ideal potential velocity given by the Bernoulli's equation, is called velocity coefficient C_v which represents the friction loss at the orifice. The actual discharge, q_a, from the orifice is the product of the actual velocity at the vena contracta, V_a, and the area of the jet. The ratio of the jet area at the vena contracta to the area of the orifice normal to the jet is the contraction coefficient C_c, and the discharge coefficient $C_d = C_v\ C_c$. The flow at the outlets was calculated from the air jet velocity normal to the area of the orifice using equation (3).

5.3 Results and Discussion

5.3.1 The evolution of pressure along the duct

When compared with that measured, the static pressure along the length of the duct was predicted with a maximum error of 10% (Figure 5.3). This is equal to or less than the combined experimental error associated with the measurement of the duct average air velocity, static pressure and of physical characteristics for all four aperture ratios of 0.5, 1.0, 1.5 and 2.0. When the aperture ratio was 2.0, a deviation occurred for the first three outlets, located close to the fan end. This could be due to air swirling which created some difficulty in accurately measuring the outlet discharge angle. The number of outlets affected by air swirling increased from none to three for the aperture ratios of 0.5 to 2.0, respectively.

Thus, the good agreement between the measured and the calculated static air pressures confirmed our assumptions that the air flowing in the duct was incompressible with negligible viscous effects. Also, the friction loss expressions obtained independently from momentum and energy equations are equivalent. The energy and momentum correction factors are almost one for the turbulent flow inside the perforated duct.

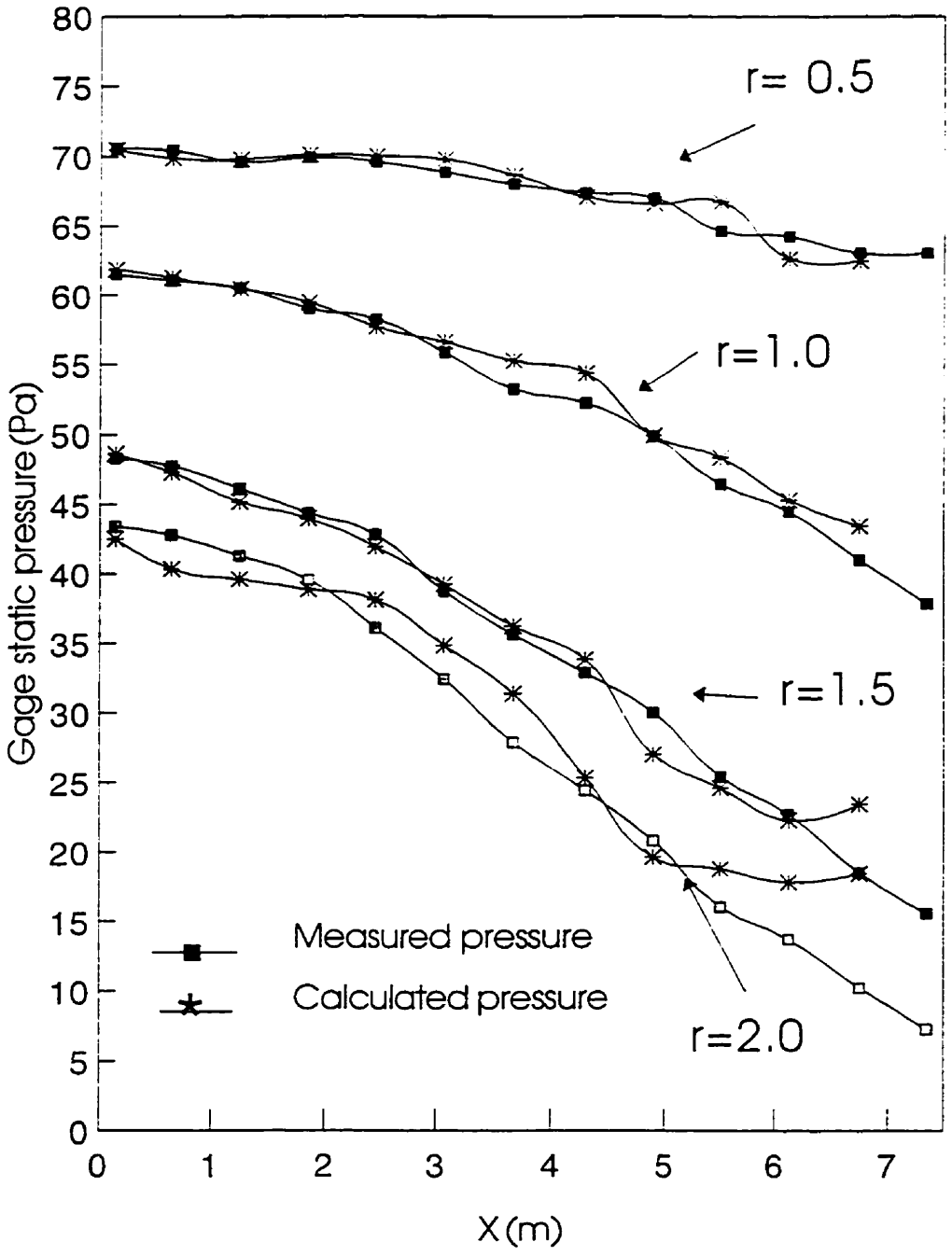

Figure 5.3 Static air pressure along the length of the perforated duct, where X is measured from the closed end of the duct.

The calculation of the friction losses over the length of the perforated duct from equation (4) followed the validation of equation (1) (El Moueddeb et al.[3]).

$$P_1 - P_2 = \rho\,[V_2^2/2 - V_1^2/2] + \rho\,F_L + \rho\,[V_o^2/2 - V_2^2/2 - P_2/\rho]\,(dm_o/dm_1)] \quad \ldots\ldots \quad (4)$$

The friction losses were calculated by inserting into equation (4) the static air pressure value for $P_{1,equ.1}$ (upstream from the outlet) obtained from equation (1), obtaining a value for $P_{2,equ.4}$ with equation (4) leaving F_L = 0 and comparing this $P_{2,equ.4}$ to the $P_{2,equ.1}$ (downstream from the outlet) obtained from equation (1). Thus, $F_L = (P_{2,equ.4} - P_{2,equ.1})$. The cumulative effect of static friction losses (Figure 5.4) was the increased discrepancy between the two static air pressures, starting from the fan side where X = 7.4 m and going towards the closed end where X = 0. The combination of equation (1) and (4) therefore defined static air pressure losses between outlets $\rho\,F_L$.

5.3.2 Outlet air jet discharge angle

The outlet air jet discharge angle varied over the length of the duct (Figure 5.5). Koestel and Tuve[8], Carpenter[9], Bailey[10] and Newman[11] also found the outlet air jet discharge angle to vary along both slotted and perforated ducts. The evolution of the discharge angle, measured in the laboratory with the three-pitot-tube instrument, was compared with that calculated from equation (1) (Figure 5.5). The outlet air jet discharge angle was also calculated based on the principle of conservation of mechanical energy, using the duct average air velocity and the effect of friction losses as in equation (5).

$$\cos(\alpha) = (V_1 + V_2)/(2\,V_o) \quad \ldots\ldots\ldots\ldots \quad (5)$$

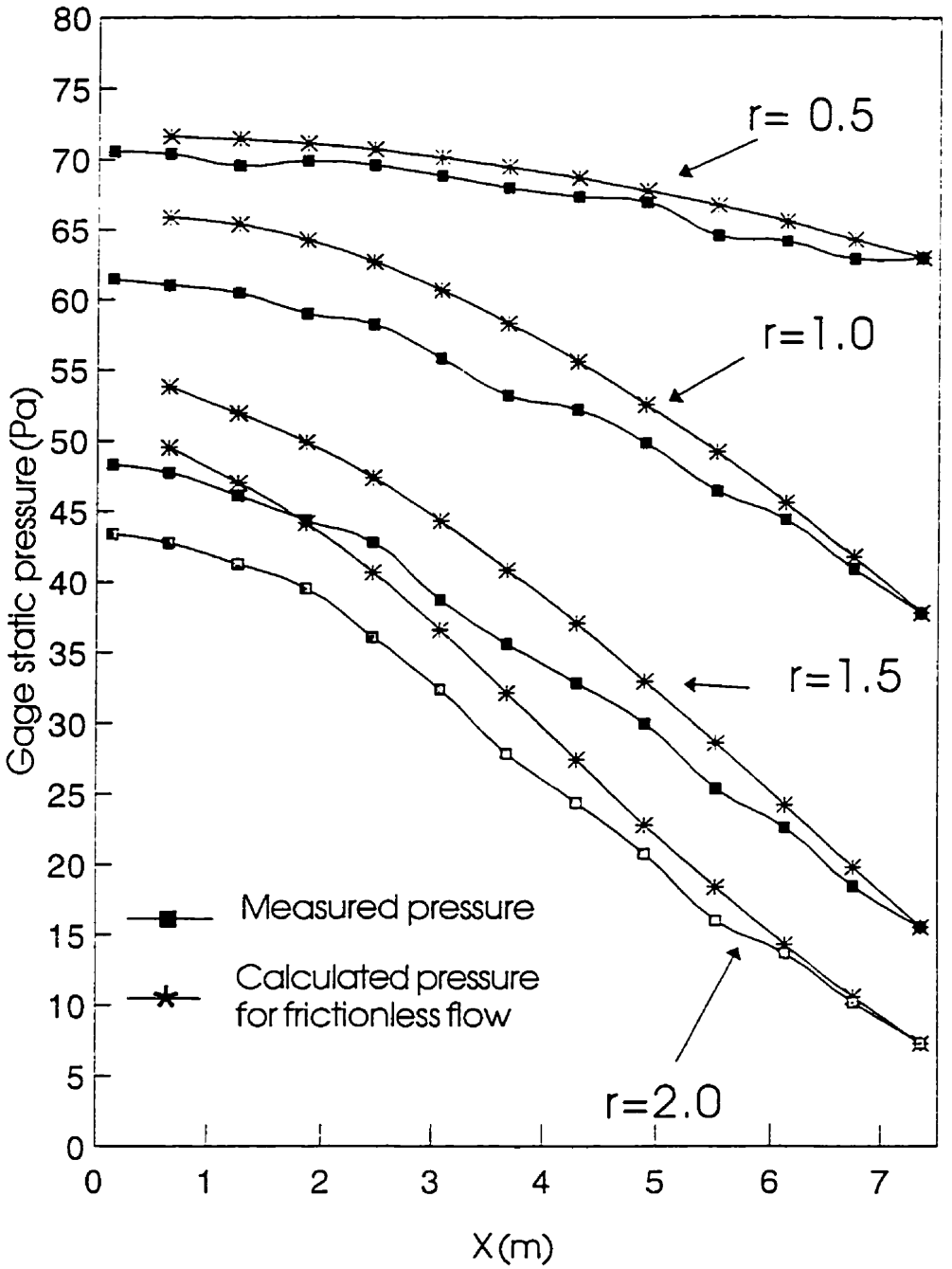

Figure 5.4 Friction losses measured from the discrepancy between measured and calculated static air pressure values along the length of the perforated duct, where X is measured from the closed end of the duct.

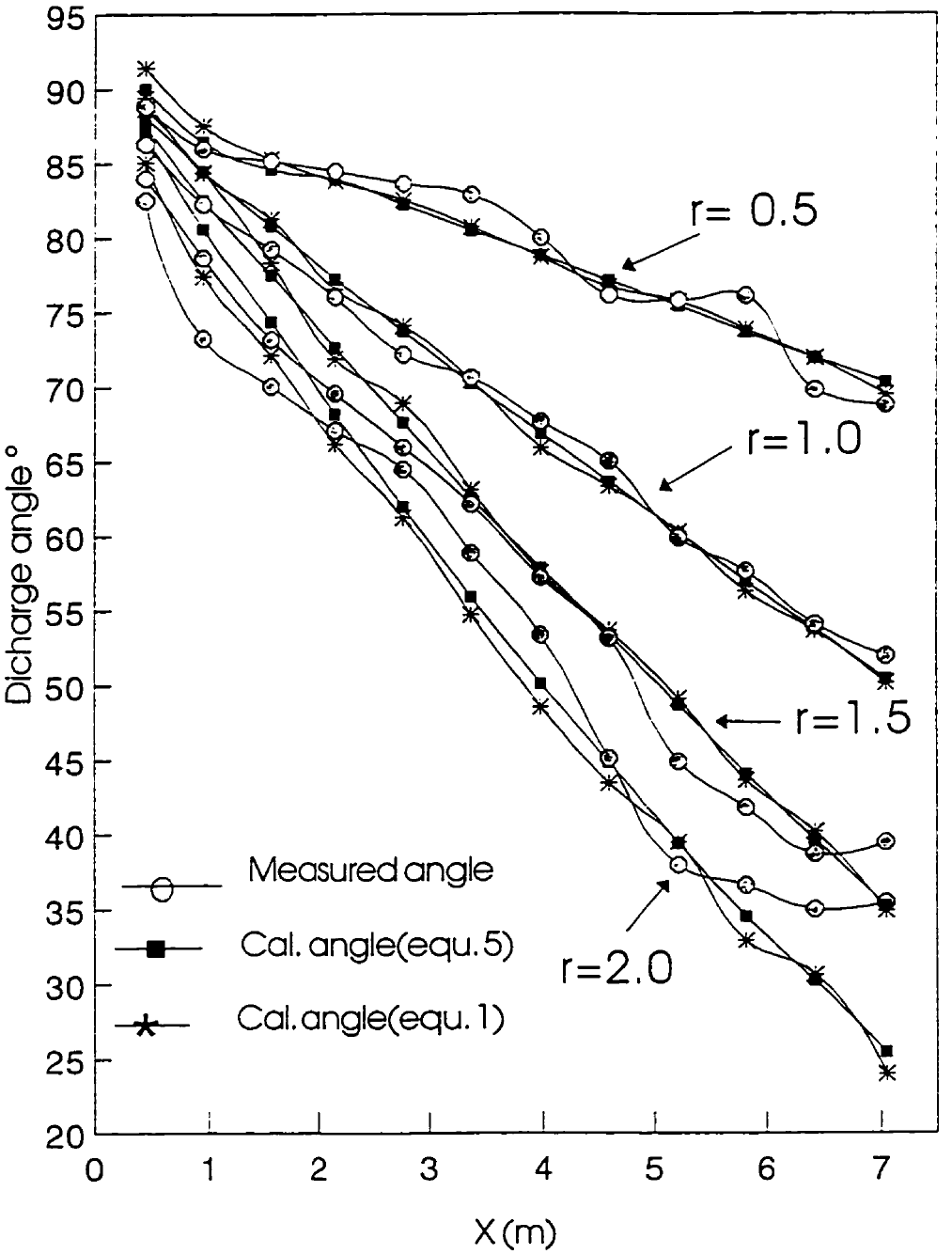

Figure 5.5 Outlet air jet discharge angle along the length of the perforated duct, where X is measured from the closed end of the duct.

Since the outlet air jet discharge angle was directly related to the ratio of $((V_1 + V_2)/2)$ and V_o, the effect of friction losses were studied by comparing the calculated outlet air jet discharge angles from equations (1) and (5) to those measured (Figure 5.5).

The frictional losses on the discharge angle can therefore be assumed negligible for turbulent flow because both the calculated and measured values for α were similar. Also, V_o can be calculated from the total air energy head inside the duct and equation (5) can be used to determine the discharge angle.

5.3.3 The Regain Coefficient

The regain coefficient was calculated from equation (2) using the velocities measured inside the duct. The coefficient was also calculated from the momentum equation of Haerter[12]. For the four aperture ratios, the calculated regain coefficients, using these equations were both found to be equal to or to be very close to one (Figure 5.6). The deviation observed near the closed end $(X = 0)$ of the duct resulted from the high experimental error associated with the measurement of air velocities using the Alnor anemometer where, for example, a velocity of 0.3 m/s has an error of 0.05 m/s (17%), and from the high uncertainty resulting from the equation (2) for low Re.

The value of one for the regain coefficient also implied a value of one for the energy correction factor (El Mouedden et al.[3]). Based on an energy correction factor of one, the validity of equation (1) again held true and it accurately predicted static air pressure for turbulent flow observed with all four aperture ratios of 0.5 to 2.0, where Re varied, respectively, from 95000 to 8000 and 205000 to 23000 (Figure 5.7). This also implies that there is no need to include an energy correction factor in equation 1 because its value is

one. This observation is in agreement with Streeter[13], where the energy correction factor is said to be approximately one for high turbulent flow.

The unit value for the regain coefficient is a more reliable evaluation compared with the values obtained by previous researchers because equation (2) is independent of friction losses. Asheley et al.[14] and Jackson[15] found the regain coefficient to vary as a function of $[V_1/V_2]$ for a single outlet in a smooth pipe. Bailey[10] also found the regain coefficient to vary with distance for a perforated duct over its entire length. But in all these cases, the regain coefficient was determined by calculating the frictional losses, according to Colebrook[16], and from the measured static air pressure evolution along the length of a perforated pipe.

5.3.4 Discharge coefficient

For the entire length of the experimental duct with aperture ratios of 0.5, 1 and 1.5, C_d remained at a constant value of 0.65 with a maximum uncertainty of 10.3% as shown in the section of data accuracy (Figure 5.8). This value is equal to the C_d of a simple orifice with an outlet fluid jet normal to its area McQuiston and Parker[17] . For an aperture ratio of 2.0, the variation of C_d for the first three outlets of the duct from the fan end was attributed to errors in measuring discharge angle because of residue at air swirling effect and of the very low ratio of static to total pressure, as the fan capacity was exceeded. According to ASHRAE[18], an axial fan operated at low static air pressures has a poor efficiency and a minimum static air pressure is required for its efficient operation. Thus, C_d of a perforated ventilation duct can be expected to be constant over the length of the system, if the fan is operated under a normal static air pressure range.

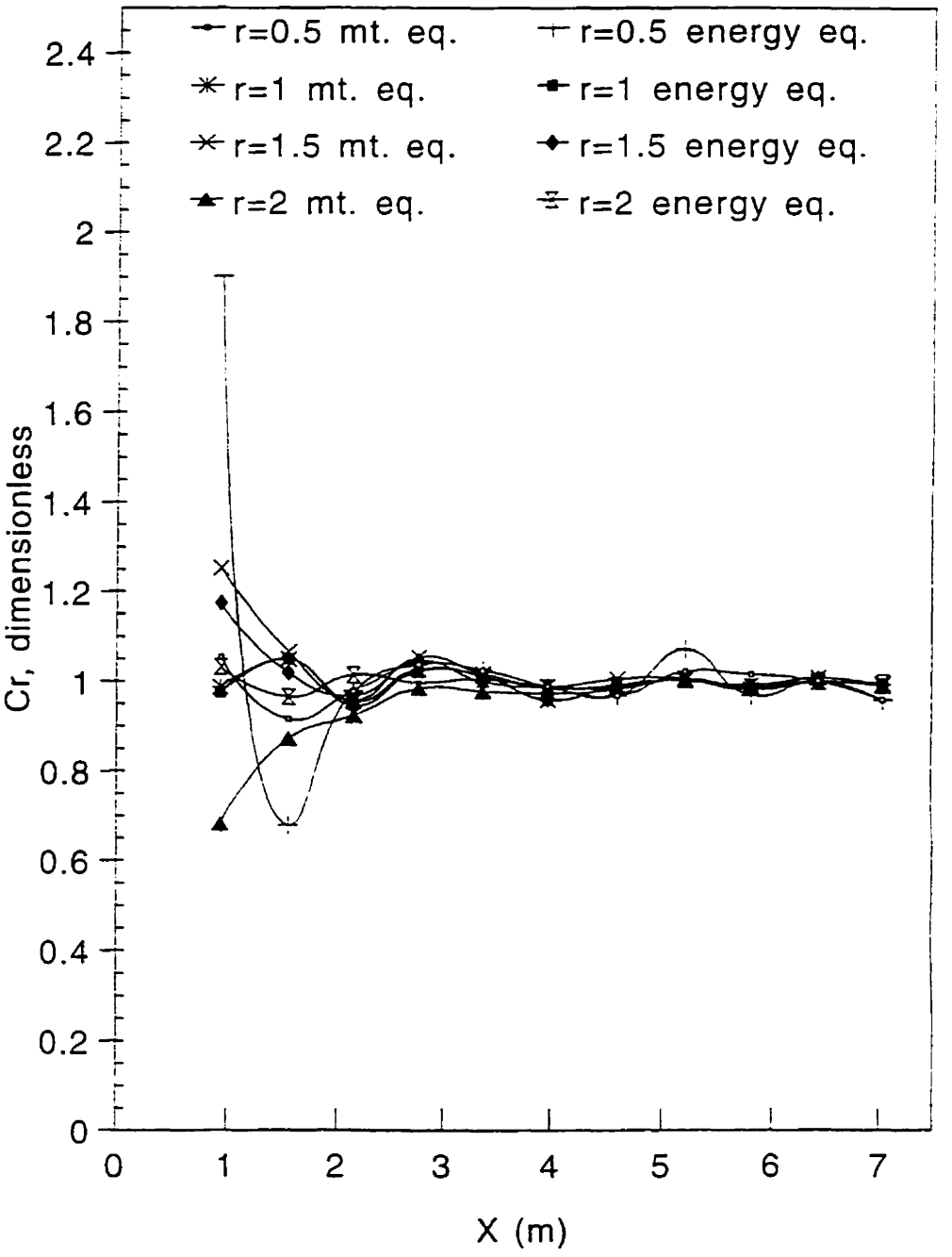

Figure 5.6 The regain coefficient along the length of the perforated duct, where X is measured from the closed end of the duct.

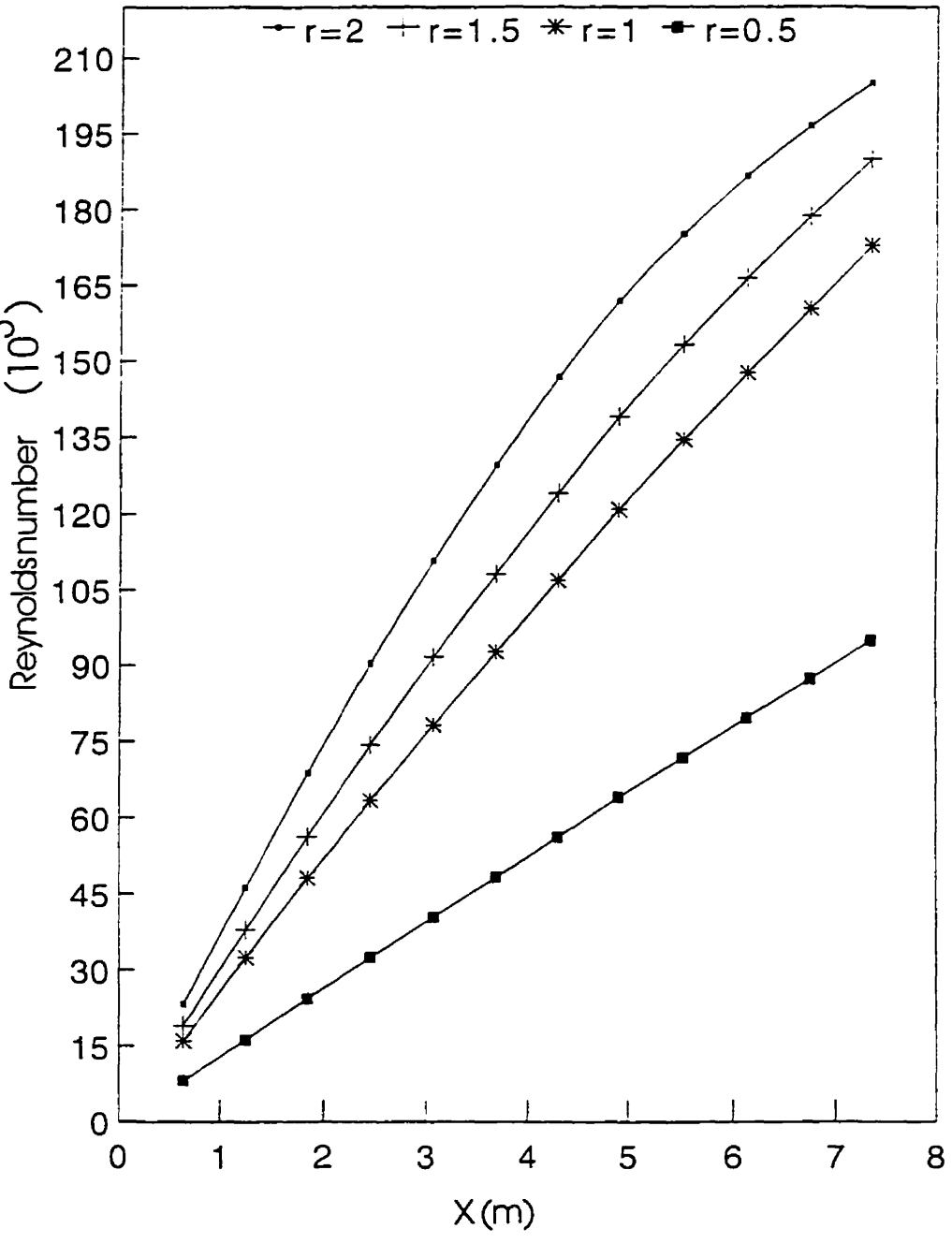

Figure 5.7 The Reynolds number for the four experimental perforated duct with respective aperture ratios of 0.5, 1.0, 1.5 and 2.0, where X is measured from the closed end of the duct.

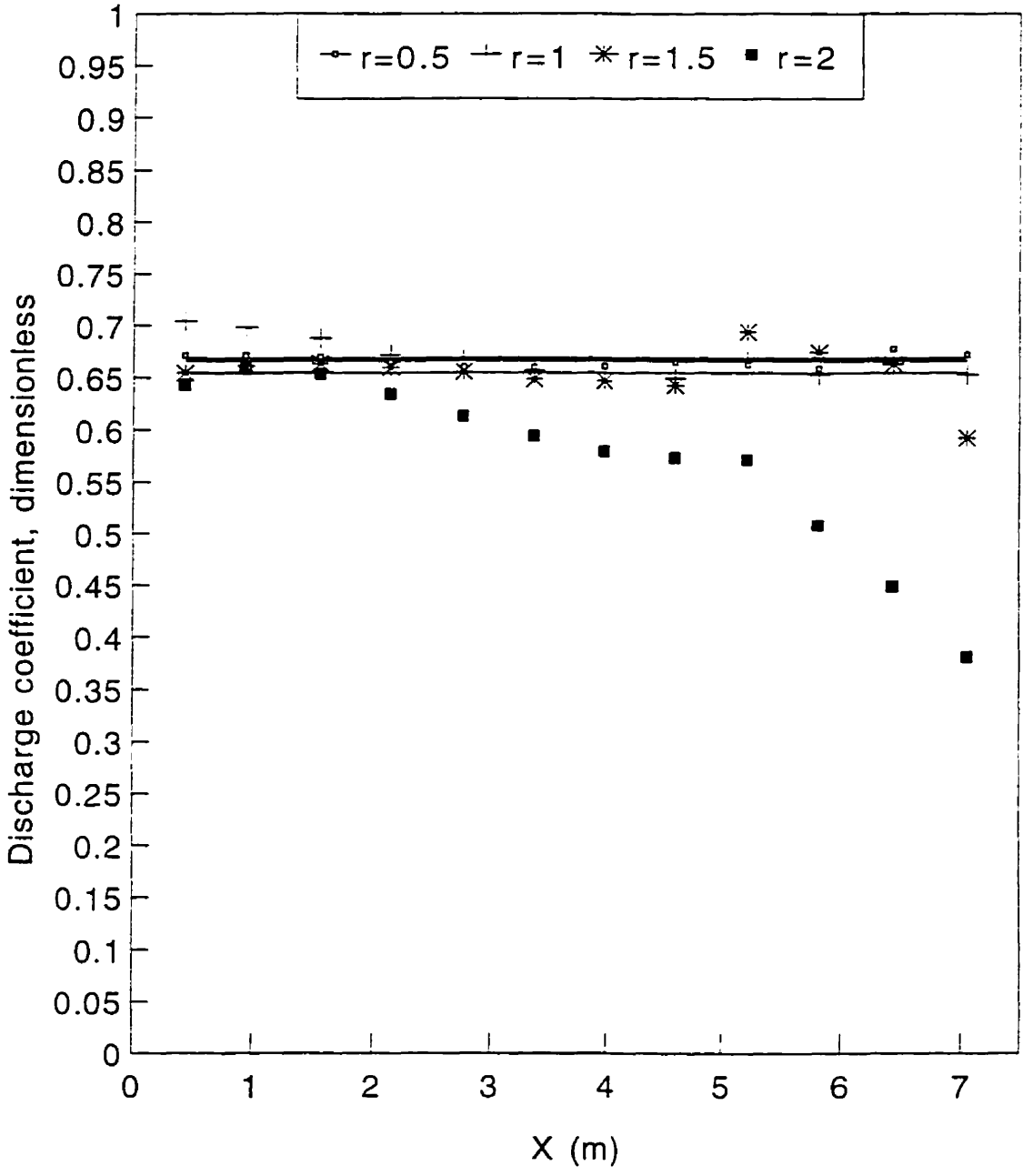

Figure 5.8 The discharge coefficient of the outlets along the length of the perforated duct, where X is measured from the closed end of the duct.

5.4 Conclusions

The mathematical model for air flow distribution pattern in a perforated duct was validated by measuring the flow performance in four experimental ducts. The basic assumptions of the model were upheld. The skin friction loss calculated from the momentum equation was the same as the energy equation provided. Thus, the energy equation can be used to evaluate the regain coefficient without considering the friction losses. The regain coefficient and the energy correction factor were almost one for turbulent flow. The discharge coefficient was constant and approximately 0.65, along the full length of the perforated duct. The frictional losses occurred along the length of the duct but had no significant effect on the discharge angle. The discharge angle can be calculated from the duct average air velocity and the potential outlet air jet velocity, V_o. Future research should concentrate on fan performance in perforated ducts.

5.5 Acknowledgement

The authors acknowledge the financial contribution of the Natural Sciences and Engineering Research Council of Canada, the Tunisian government and Le Ministère de l'Agriculture, des Pêcheries et de l'Alimentation du Québec.

Table 5.2: Notation

A_{on}: outlet normal to the air jet, m^2
A_o: one outlet area, m^2
A: duct cross-section, m^2
C_d: discharge coefficient at the outlet, dimensionless
C_c: contraction coefficient at the outlet, dimensionless
C_v: velocity coefficient at the outlet, dimensionless
C_r: regain coefficient in the duct at the outlet, dimensionless
F_L: friction losses, J kg^{-1}
g: gravity constant, 9.806 m s^{-2}
P_i: air static pressure at a position i, Pa
q_a: measured outlet air flow, m^3 s^{-1}
u_i: specific air internal energy at a position i, J kg^{-1}
V_a: actual average air outlet velocity, m s^{-1}
V_o: potential air outlet velocity, m s^{-1}
V_i: duct average air velocity at a position i, m s^{-1}
V_x: axial air discharge velocity, m s^{-1}
V_y: normal air discharge velocity, m s^{-1}
α: discharge angle, degree
ρ: air density, kg m^{-3}
v: specific air volume, m^3kg^{-1}
r: aperture ratio: $\sum A_o/A$, dimensionless
i: =0, 1, 2
0: outlet
1: upstream from the outlet
2: downstream from the outlet

5.6 References

[1] **Bajura R A; Jones E H** Flow distribution manifold. Transactions of the ASME 1976, 98: 654-665.

[2] **Soucek E; Zelnick E W** Lock manifold experiments. Transactions of ASCE, 1945, 1357-1400.

[3] **El Moueddeb K; Barrington S F; Barthakur N** Perforated ventilation ducts. Part I. A model for flow distribution. Journal of Agricultural Engineering Research. In Press.

[4] **El Moueddeb K; Barrington S F; Newman B.G** Evaluation of methods to measure the performance of ventilation ducts. Submitted to Canadian Agricultural Engineering 1996, 38(3): 207-213.

[5] **ANSI/ASME** Measurement Uncertainty. ANSI/ASME PTC 19.1-1985 Part 1 1986. The American Society of Mechanical Engineers, 345 East 47th Street New York, N.Y. 10017.

[6] **Kline S J** The purposes of uncertainty analysis. Journal of Fluids Engineering 1985, 107: 153-160

[7] **Streeter V L; E Benjamin W** Fluid mechanics 1981. First SI metric edition. MacGraw-Hill Ryerson limited, 342-344.

[8] **Koestel A; Tuve G L** The discharge of air from a long slot. Transaction of Amercan Society of Heating and Ventilating Engineers 1948, 54; 87-100.

[9] **Carpenter G A** The design of permeable ducts and their application to the ventilation of livestock building. Journal of Agricultural Engineering Research 1972, 17: 219-230.

[10] **Bailey B J** Fluid flow in perforated pipes. Journal of Mechanical Engineering Science 1975, 17: 338-347.

[11] **Newman B G** A Hodographic solution for flow leaving a manifold through a slit. Canadian Aeronautics and Space Journal 1989, 35: 205-210.

[12] **Haerter A A** Flow distribution and pressure change along slotted or branched ducts. Transactions of the ASHRAE 1963, 69: 124-137.

[13] **Streeter V L** The kinetic energy and momentum correction factors for pipes and open channels of great width. Civil Engineering 1942, 12(04): 212-213.

[14] **Ashley C M; Gilman S F; Church R A; Syracuse N Y** Branch fitting performance at high velocity. Transactions of the ASHRAE 1956, 56: 279-294

[15] **Jackson K R** Branched losses in high velocity duct systems. Journal Institution Heating and Ventilating Engineers 1969, 4: 208-214.

[16] **Colebrook C F** Turbulent flow in pipes with particular reference to the transition region between smooth and rough pipe laws. Journal of the Institution of Civil Engineers 1938, 4: 133-156.

[17] **McQuiston F C; Parker J D** Heating, ventilating and air conditioning analysis and design 1988. Third edition. Jhon Wiley and Sons, 344-347.

[18] **ASHRAE** 1993. Equipment Handbook, 1993 Chapter 18. Atlanta, Georgia.

CONNECTING TEXT

The two previous chapters developed and validated a design model for perforated ventilation ducts. This last chapter provides a design method to calculate outlet area or spacing to obtain the required air flow distribution. Finally, this last chapter tests an hypothesis which incorporates the fan characteristics into the design model. Thus, this last chapter finalizes the conception of the design model and provides the basis for the calculation of the balance operating point, given a specific fan and duct.

6 DESIGN OF PERFORATED DUCTS FOR AGRICULTURAL VENTILATION

6.1 Introduction

Uniform air distribution is a prerequisite for the heating, ventilation, and air conditioning of all air spaces. Agricultural requirements are stringent as the productivity of the biological component within the air space is directly related to the quality of its surroundings. Perforated ventilation ducts have often been used to help improve fresh air distribution. But, their air distribution pattern is a complex function of several inter-related factors such as duct construction material and air friction effects, fan capacity against air pressure head, outlet size and spacing and duct length and cross-sectional area.

A theoretical model introduced by El Moueddeb et al.[1], describing the air distribution pattern of perforated ventilation ducts, combined both the equations of momentum and energy conservation to eliminate the measurement or the estimation of friction losses. The hypotheses supporting the model proved to be valid and the following were demonstrated:

1) under conditions of turbulent air flow, the regain coefficient between the duct's outlets is equal to one;
2) when the outlet air flow is described by means of a discharge angle and a discharge coefficient, the discharge coefficient is constant along the full length of the perforated ventilation duct and is equal to 0.65;
3) the discharge angle is defined from the ratio of the duct average air velocity and the potential outlet air velocity.

The proposed model requires the input of the static and dynamic air pressure at the entrance of the perforated duct which are defined by the physical characteristics of the fans and the perforated ventilation duct. These air pressures are called the system's balance operating point and their accurate

prediction requires the matching of the duct's air performance curve with that of the fan. Accurately predicting this balance operating point results in the selection of a fan with adequate airflow and optimal horsepower, for reduced operating costs. A complete theoretical model for perforated ventilation ducts must be able to optimize the selection of the fan and duct characteristics to obtain a balanced operating point for a specific air distribution pattern.

The two objectives of this work are to develop a perforated ventilation duct design method based on the model developed by El Moueddeb et al.[1] and to finalize its application by introducing a method of calculating the balance operating point based on the characteristics of the fan and the perforated duct. For the first objective aims at validating the model of El Moueddeb et al.[1], by comparing the actual air flow distribution pattern of perforated duct to that predicted. The second objective will be achieved by testing the hypothesis that the fan's effective delivery area is equal to the effective outlet area. Effective area implies area times its discharge coefficient. As a result, fan characteristics will be included in the theoretical model if their air flow performance curve can be described as a function of their static air pressure differential and their effective delivery area. Based on such a performance curve, the fan characteristics can be included in the iterative process of the theoretical model and the system's balance operating point can be calculated.

6.2 Literature review

The air distribution performance of mechanically fed manifolds and perforated ducts has been investigated ever since the late 1800's (Howland[2]). It was only in the early 1950's that agricultural engineers took interest in applying these system to improve the ventilation of their structures

(Carpenter[3]).

Air velocity at the outlets of perforated ventilation ducts has become an important design factor because it predicts the air velocity at the floor of the living space of the animals (Ogilvie et al.[4]). Smaller ducts are preferred to limit their space requirements and the ceiling height but they tend to create situations of unbalanced air flow as their nonuniform static air pressure and velocity give more flow at the closed end.

The static air pressure variation inside a perforated ventilation duct results from two phenomena: the first is associated with the friction of the fluid along the walls, which causes a decrease in air pressure in the direction of flow; the second is associated with the reduction of fluid momentum in the duct with discharge at the outlets and results in an increase in static air pressure in the direction of flow (Bailey[5]).

6.2.1 Models predicting air distribution from perforated ventilation ducts

Several theoretical models have been developed to predict the distribution patterns of perforated ventilation ducts. Davis et al.[6] formulated a computer model predicting the air flow distribution from perforated corrugated metal ducts. A constant outlet discharge coefficient of 0.61 was used and was assumed to vary over the length of the duct by a multiple of the static air pressure head divided by the total air pressure head. Bernoulli's equation was used to calculate the outlet air jet velocity. The model predicted air flow performances within an error of 25% for aperture ratios of 1.3 and less. Further research on discharge coefficients was recommended to improve the air distribution modelling.

For a pipe with equally spaced openings and fed by a centrifugal fan, Bailey[6] theoretically analyzed and described

the variation of the static air pressure of perforated ducts by considering friction effects between holes and the static regain between outlets. The theoretical discharge velocity normal to the outlet was presumed derived from the excess static air pressure in the pipe. The discharge coefficient was plotted as a function of the ratio of duct's air dynamic pressure to the duct's total air pressure head ($[\frac{1}{2}V^2]/[P/rho+\frac{1}{2}V^2]$) using empirical parameters. For the outlet at the closed end, the discharge coefficient had a maximum value of 0.63. A coefficient of static regain was also defined as a function of duct length by means of empirical parameters determined by an iterative computer program. The input parameters of the model were the static and dynamic air pressures at the duct entrance, the air temperature and the physical dimensions of the duct and its outlets.

To compute the air distribution performance of perforated ventilation ducts under several air flow conditions, Saunders and Albright[7] used a mathematical series applied by iteration from one outlet to the next. Air pressure differentials were assumed to result solely from friction losses and the reduction in average air duct velocity. The discharge coefficient was assumed constant over the length of the perforated duct but was found to vary with duct size. Despite the fact that the discharge coefficient was adjusted with the duct size, the predicted flow distribution profile deviated from the real one by 10%. The most important factor affecting model accuracy was presumed to be the discharge coefficient.

Because of the lack of accurate models to predict the air distribution pattern of perforated ducts, such systems are approximated before hand and adjusted on site by trial and error. The present work develops a method to improve the accuracy of predicting the cited balance operating point.

6.3 Duct design parameters

The model of El Moueddeb et al.[1] calculates the outlet air discharge velocity, V_o, from the total specific energy of the air inside the duct using the Bernoulli's equation (1):

$$V_o=\sqrt{2\,(\tfrac{1}{2}V_1^2 + P_1/\rho)} \quad \ldots\ldots\ldots\ldots\ldots\ldots \quad (1)$$

where:

V_1: duct average air velocity upstream from the outlet, m s^{-1}

P_1: duct static air pressure upstream from the outlet, Pa

ρ: air density, kg m^{-3}

The discharge air jet angle, α, is calculated as:

$$Cos(\alpha)=\tfrac{1}{2}(V_1+V_2)/(V_o) \quad \ldots\ldots\ldots\ldots\ldots\ldots \quad (2)$$

where :

V_1 and V_2: duct average air velocity upstream and downstream from the outlet respectively, m s^{-1}

The outlet discharge coefficient was found equal to 0.65, which defines the outlet air flow, q_o, for an outlet of area, A_o:

$$q_o = 0.65*A_o*V_o*sin(\alpha) \quad \ldots\ldots\ldots\ldots\ldots\ldots \quad (3)$$

The total air pressure losses along the length of the duct are assumed to result solely from friction losses and the friction coefficient, f, is calculated using the Swamee and Jain[8] equation :

$$f= 0.25/(log[(e/3.78*D) + (5.74/R_{ey}^{0.9})])^2 \quad \ldots\ldots \quad (4)$$

valid for the ranges:

$$5*10^3 \leq R_{ey} \leq 10^8$$

$$10^{-6} \leq (e/D) \leq 10^{-2}$$

where:

e: a measure of duct roughness, mm

D: duct hydraulic diameter, mm

R_{ey}: Reynolds number, dimensionless

To calculate the air flow performance of the perforated ventilation duct, a mathematical series is applied by

iteration from one outlet to the next to compute the outlet air discharge. As initial input, a value is assumed for the dynamic and static air pressures for the outlet at the fan end. Since for the first iteration, only the value of the air velocity upstream from the outlets is available, the discharge angles is calculated from:

$$Cos(\alpha) = (V_1)/V_o \quad \ldots\ldots\ldots\ldots\ldots\ldots \quad (5)$$

Using values provided by the first iteration, equation (2) is used to compute the discharge angle for the following iterations. The iteration is continued by adjusting the discharge angles and the outlet flow for all the outlets, until the calculated air flow at the duct's closed end is close to zero. Then, the corresponding air distribution performance of the perforated duct had been predicted.

6.3.1 Duct design for a specific air distribution

The perforated duct can give a specific air distribution pattern along its full length if the area or the spacing of the outlets is varied accordingly. The air distribution can be defined as:

$$q_{ox} = a * x \quad \ldots\ldots\ldots\ldots\ldots\ldots \quad (6)$$

where:

a is the coefficient defining the air distribution pattern along the length of the ventilation duct, $m^2.s^{-1}$.

x is the abscise coordinate along the length of the perforated section of the duct, m

q_{ox} is the outlet air flow at the abscise x, $m^3\ s^{-1}$.

For example, the area of the outlet at a distance x, A_{ox} along the perforated duct and corresponding to the desired air distribution is defined by the equations (7a) and (7b) as follows:

$$A_{ox} = q_{ox}/(C_d * V_o * \sin(\alpha)) \quad \ldots\ldots\ldots\ldots\ldots\ldots \quad (7a)$$

$$= (V_{1x} - V_{2x}) * A_x/(C_d * V_o * \sin(\alpha)) \quad \ldots\ldots\ldots\ldots \quad (7b)$$

where:

A_x: duct cross-section area at the abscise x, m^2

A_{ox}: outlet area at the abscise x, m^2

C_d: discharge coefficient, dimensionless

For an uniform air distribution along the perforated section, the parameter a is defined as:

$$a = (Q/n)\ x \quad \ldots\ldots\ldots\ldots\ldots\ldots\ldots\ldots\ldots \quad (8)$$

where:

Q: total duct air flow $m^3\ s^{-1}$.

n: number of outlets

6.3.2 Duct fan balanced operating point

For the perforated ventilation duct, the resistance to flow depends upon the individual components of the system, the duct and the fan, and is due to friction losses and delivery areas. Accordingly, the following hypothesis will be tested: the summation of the effective duct outlet areas $(\Sigma A_{io} \sin(\alpha)\ C_{id})$ is equal to the fan's effective delivery area $(A_f\ C_{df})$ perpendicular to its discharge air velocity. This hypothesis is founded on the basis that the discharge coefficient, C_d, is a multiple of the outlet contraction coefficient, C_c, with the velocity coefficient, C_v, which is practically equal to one for both the effective duct outlets and the fan delivery area.

If this hypothesis proves valid, the fan characteristics required to calculate the balance operating point of a perforated ventilation duct are its air flow performance curve as a function of its static air pressure differential and its effective delivery area. So far, fans have been rated solely based on their static air pressure differential. Also, this hypothesis provides a common parameter to establish the balance operating point between the fan and the duct based on

the fan's effective delivery area and the static air pressure upstream from the outlet, at the fan end.

6.4 Methodology

The methodology consists of a first experiment designed to validate the duct design method by predicting the air distribution performance of three wooden ventilation ducts and a second experiment designed to validate the hypothesis that the fan effective delivery area is equal to the duct's total and effective outlet area. The second experiment was done using a duct with either one pair of side outlets (lateral outlet) or one outlet at the closed end (frontal outlet- Figure 6.1).

6.4.1 Monitoring instruments

The static air pressure inside the duct was read using a vertical Dwyer micrometer (MICROTECTOR® GAGE by DWYER INSTRUMENTS, INC.) with an accuracy of ± 0.062 Pa, connected to wall piezometric taps installed at the point of measurement. To validate the duct design method, the taps were installed before the first and at equal distance between each two pairs of outlets. Thus, the static air pressure was measured at 13 locations over the length of the perforated section of the duct. For the duct with a single pair of outlet or an outlet at its closed end, the piezometric tap was installed at 1.00 m from the closed end. All static air pressure measurements were repeated 5 times.

To measure the duct's average air velocity, the grid method (Burgess[9]) was applied over 16 equal rectangular areas distributed over the duct's inside cross section. The velocity at the centre of each rectangular section was measured with an ALNOR compuflow thermo-anemometer with an accuracy of 0.05 m/s or ±3% of the indicated reading over the range of 0.1 to 15 m/s. Ten consecutive readings were

averaged for each of the grid's 16 rectangular areas. The air temperature was measured using the ALNOR thermo-anemometer (thermo-couple sensor) with an accuracy of ± 1º C.

The outlet air leaves the duct at an angle (α) with respect to the side of the duct and this discharge angle must be measured to calculate the true outlet air flow. Thus, a three-pitot tube instrument was used (El Moueddeb et al.[10]) to detect the outlet air jet angle with an accuracy of ± 2.5 º. All discharge angle measurements were repeated 3 times.

6.4.2 Experimental ducts

Both experiments used a wooden ventilation ducts fed by a 450 mm diameter ACME variable speed axial fan with a 0.25 Kw motor operating at 1600 rpm at full speed. The fan was equipped with an air straightener, a 1800 mm long tapered section to fit it onto the experimental duct. The duct's wooden frame was made of 39 mm by 39 mm members covered with 6 mm thick presswood panelling and it offered an inside cross-sectional area of 0.17 m^2 ([597 mm x 295 mm] - 4[39 mm x 39 mm]). Its side panels were removable as to change the size and type of outlets.

For the first experiment, a 4.9 m unperforated section was used between the tapered section and the 7.3 m perforated duct, to reduce air swirling close to the fan and to improve the accuracy of the experimental measurements. For the second experiment, a 2.4 m duct was connected to the tapered section and it was perforated either by a pair of lateral outlets at 100 mm from the closed end or a frontal outlet in its closed end. According to ACMA[11], the length of this unperforated section suffices in establishing a uniform velocity profile. AMCA[11] recommends a length of 2.5 times the hydraulic diameter for an air flow of 1.1 $m^3.s^{-1}$ or less, plus one hydraulic diameter for each additional 0.472 $m^3.s^{-1}$.

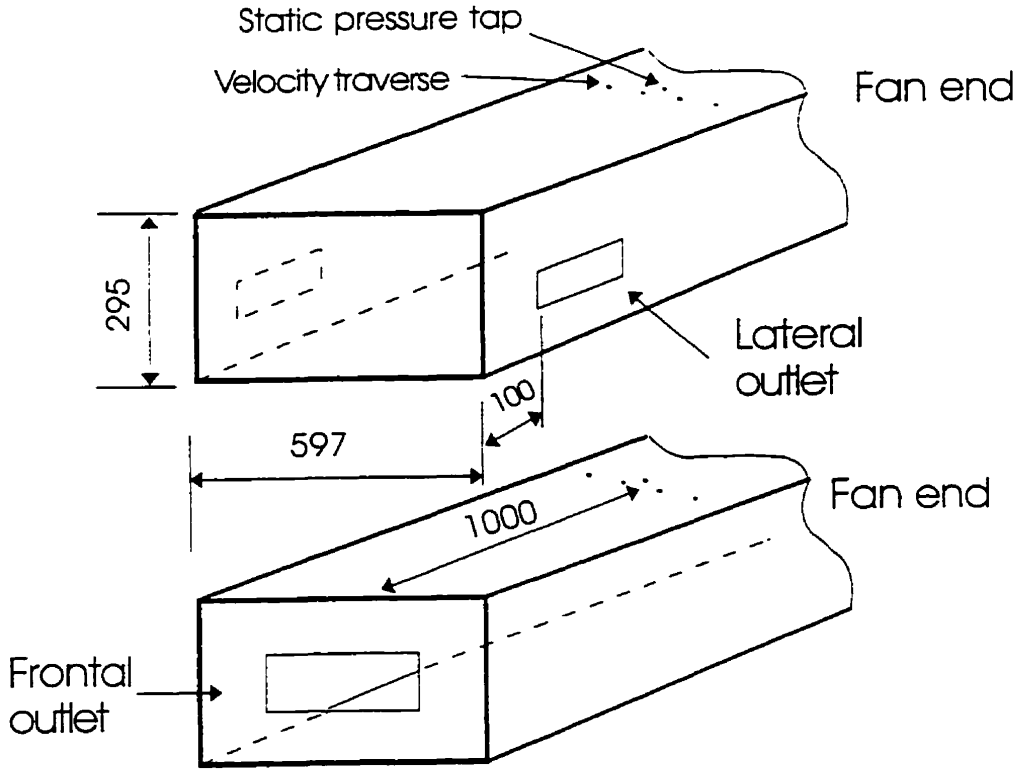

Figure 6.1 Lateral and frontal outlets for the determination of the balance operating point. The dimensions are in mm

6.4.3 Validation of the design method

For the validation of the design method, the side panels of the 7.3m perforated section were changed in turn to test three aperture ratios of 0.5, 1 and 1.5 (Table 6.1). In all three cases, 12 pairs of rectangular outlets were present one on each side of the duct at a spacing of 0.61m.

The duct's inside air velocity, the static air pressure and the outlet air flow were measured at each pair of outlets. These parameters were compared with those calculated theoretically and the model error was computed from the percentage of error between the measured and predicted values.

6.4.4 Testing the hypothesis for the balance operating point

The hypothesis was tested by comparing the duct's air flow performance using a pair of lateral outlets as opposed to a frontal outlet (Figure 6.1). This perpendicular outlet represents the fan's delivery area.

A wooden duct, 2.4 m in length, was connected to the previously cited fan and tapered section. The type and size of outlet was changed by interchanging the duct panelling.

At 1.00 m upstream from the closed end of the duct, the average duct air velocity and static air pressure were measured for 18 combinations of opening size, opening type and fan operating speed. The three sizes of openings used for the frontal outlet were 0.0544 m^2 (230 mm x 236 mm), 0.0833 m^2 (230 mm x 362 mm) and 0.1105 m^2 (230 mm x 480 mm) for an effective aperture ratios of 0.32, 0.49 and 0.65, assuming a discharge coefficient, C_{df}, of one. For the lateral outlets, their area gave an effective aperture ratio of 0.325 (200 mm x 425 mm), 0.49 (200 mm x 640 mm) and 0.650 (200 mm x 850 mm), based on the known discharge coefficient, C_d, of 0.65 and assuming that the effect of the discharge angle is negligible.

Table 6.1 Description of the experimental duct

Duct	Outlet size mmxmm	Aperture ratio
1	145x 25	0.5
2	145x 50	1.0
3	145x 75	1.5

* The aperture ratio equals $\Sigma A_o/A$.

Note : the perforated duct length measured 7.3 m and in all cases, 12 pairs of outlets were used at a spacing of 610 mm.

The duct's average air velocity was measured using the grid method over the cross sectional area of the duct. Static air pressure inside the duct was measured using a piezometric tap. For the same fan air flow, the type of opening was changed randomly. The fan was operated at three speeds set respectively at 1600 rpm, N1, at 1100 rpm, N2, and at 500 rpm, N3.

The value of the discharge coefficient for the frontal opening, C_{df}, was verified according to equation (9) while comparing the air flow performance of both types of openings, frontal and lateral:

$$C_{df} = V*A/(V_f*A_f) = V/\sqrt{(V^2/2 + P/\rho)*r} \quad \ldots\ldots\ldots \quad (9)$$

where:

V: measured average duct air velocity, m s^{-1}

A: duct cross-section area, m^2

A_f: frontal outlet area, m^2

$V_f = \sqrt{(V^2/2 + P/\rho)}$: potential outlet velocity, m s^{-1}

$r = A_f/A$: aperture ratio, dimensionless

Once the value of C_{df} was measured for all three frontal openings, their effective area was corrected.

To test the hypothesis, a regression analysis was carried out to relate the duct's static air pressure and average air velocity to the effective aperture ratio of both the frontal and lateral outlets, for the same fan operating speed. The R^2 value of the regression analysis was used to test wether or not the hypothesis was true.

6.5 Results and discussion

6.5.1 Validation of the design method

The measured duct average air velocity and the outlet air jet discharge angle were used to test the accuracy of the model (Figure 6.2 and 6.3). For the duct average air velocity, the error between the measured and predicted value

was less than 1%. The maximum cumulative error is at the closed end of the duct, since the duct's average air velocity was determined from a series of calculation starting at the fan end and finishing at the closed end of the duct (X= 7 m).

The maximum error between the measured and predicted outlet air jet discharge angle occurred at the closed end of the duct and was equal to 1, 6 and 4 percent for an aperture ratio of 0.5, 1 and 1.5 respectively. The standard deviation for the discharge angle measured at each outlet increased for higher air flows and, accordingly, with aperture ratio. However, the error level was 50% smaller than the standard deviation measured by repeatedly measuring the discharge angle at each outlet. For both the duct average air flow and outlet air jet discharge angle, the level of error between the measured and the predicted values were well within the experimental error associated with the measurement of the parameters. Thus, the model developed by El Moueddeb et al.[1] proved to accurately predict the air flow performance of the three wooden perforated ventilation ducts.

6.5.2 Air flow distribution from the Outlets

The uniformity of the air flow distribution from the outlet varied with aperture ratio (Figure 6.4). For the aperture ratio of 0.5, the air flow distribution was rather uniform over the full length of the duct. As the aperture ratio increased from 0.5 to 1.5, more air was distributed at the closed end of the duct. This unbalanced air flow distribution resulted from higher static air pressures developing at the closed end as a result of the regain effect of a relatively larger air flow discharge from the outlets.

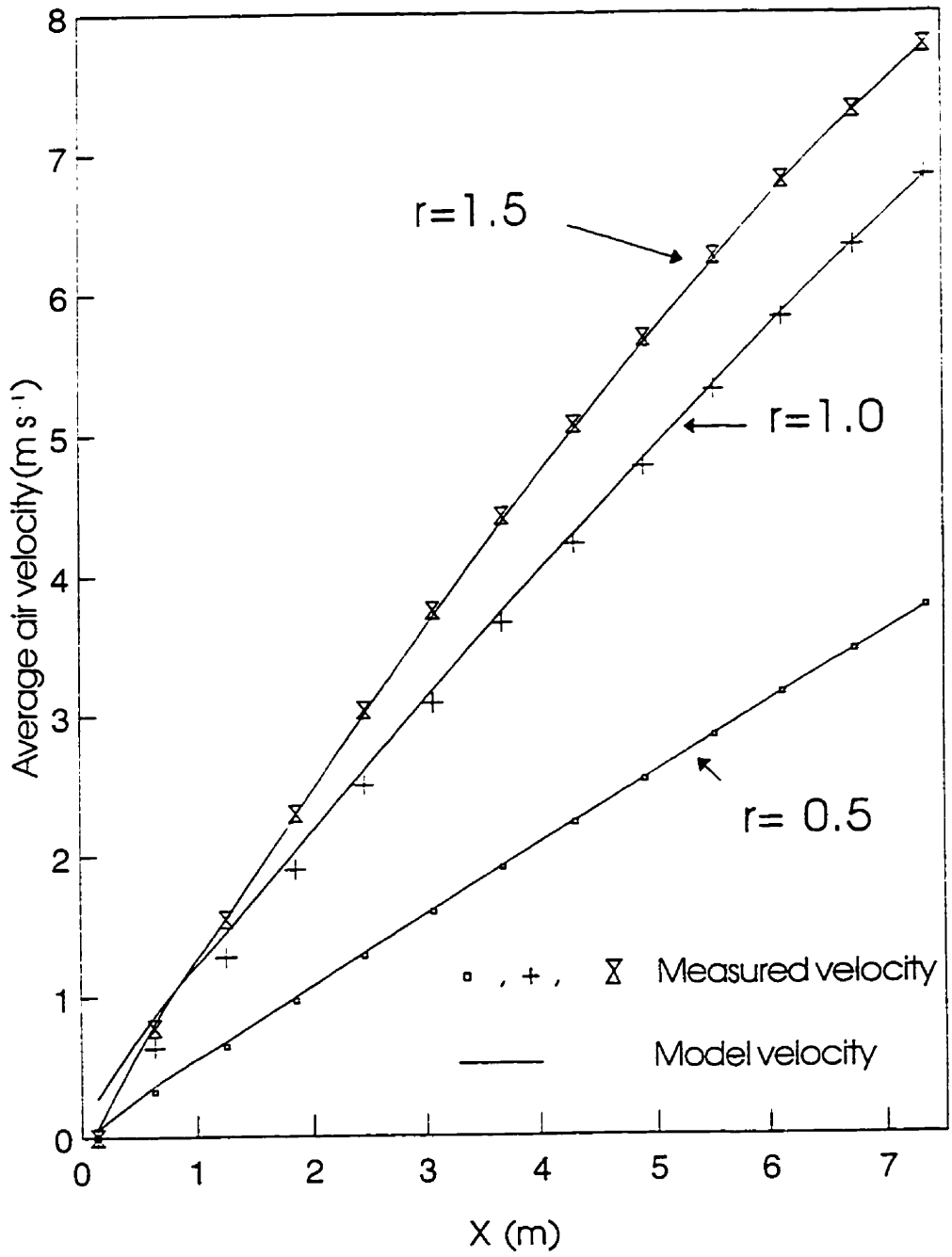

Figure 6.2 Duct average air velocity as a function of lateral distance along the length of the duct, where X is measured from the closed end of the duct.

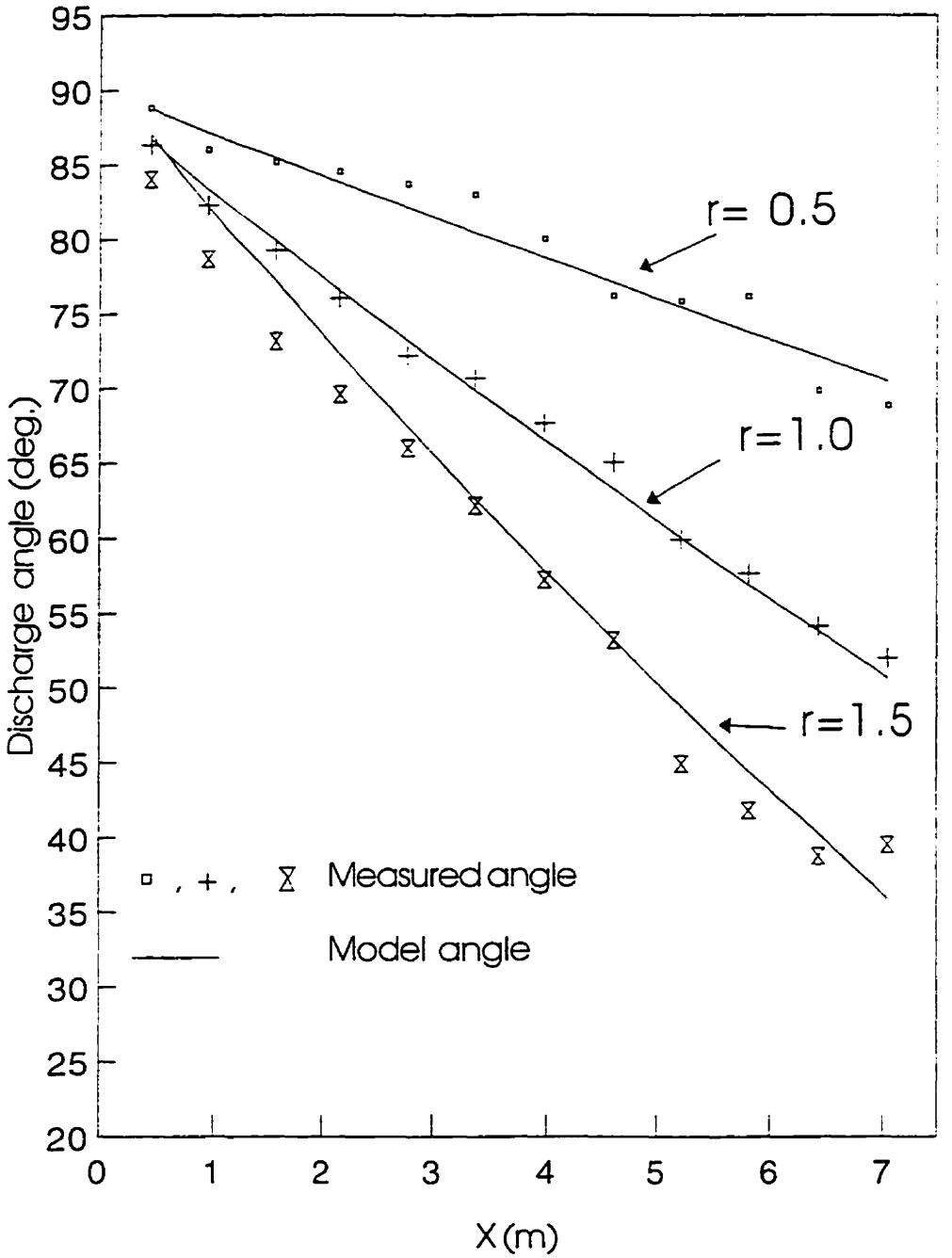

Figure 6.3 Outlet discharge angle as function of lateral distance along the length of the duct, where X is measured from the closed end of the duct.

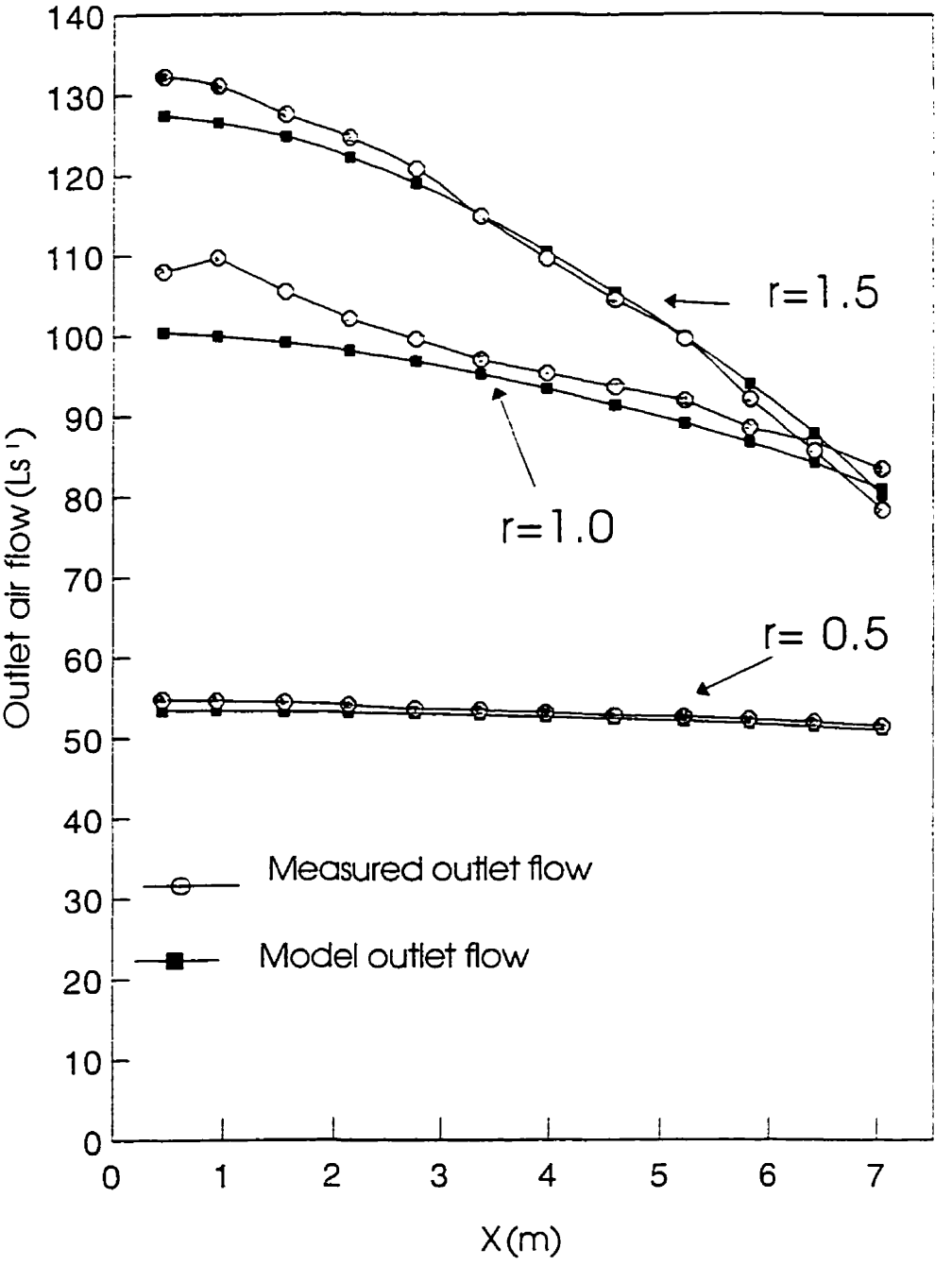

Figure 6.4 Outlet air flow as function of lateral distance along the length of the duct, where x is measured from the closed end of the duct.

The model accurately predicted the air flow distribution over the full length of the duct. Since the measurement of the outlet air flow is derived from the duct air average velocity, a higher error between the measured and the predicted values is recorded at the duct closed end. The higher error is due to the lower accuracy of the Alnor anemometer at low speed (less than 1 $m.s^{-1}$). Nevertheless, the outlet air flow was predicted with a maximum error of 9% and this error is less than the combined experimental error associated with the measurement of the duct average air velocity and physical characteristics of the duct.

A balance air flow distribution with the aperture ratio of 1.5, could be obtained according to equations (6) to (8) by decreasing the outlet area from 75 mm x 152 mm to 75 mm x 96.8 mm, from the fan to the closed end of the duct.

6.5.3 Operating balance point

Before testing the hypothesis, the discharge coefficients of the frontal outlets was calculated (Figure 6.5) and used to correct the value of their effective area. For each size of frontal outlet, the discharge coefficient was found to be equal and independent of the fan operating speed. Thus, the frontal outlet areas of 0.0544, 0.0833 and 0.1105 m^2 were corrected using a discharge coefficient of 0.74, 0.81 and 0.90 to give an effective opening area of 0.0403, 0.0675 and 0.0995 m^2 and an effective aperture ratio of 0.24, 0.40 and 0.59.

The hypothesis equating the effective outlet opening to the fan's delivery area was tested by comparing the duct's static air pressure and average air velocity developed by all three sizes and types of openings for the same fan operating speed (Figure 6.6 and 6.7). For each fan operating speed, an exponential regression was found to give the best fit between the duct's static air pressure and the effective opening for all six sizes and types (Figure 6.6). R^2 value of 0.83, 0.96

and 0.95 respectively was obtained for the fan's speeds N1, N2 and N3 for these regression lines. This indicated that both the frontal and lateral outlets gave the same duct static air pressure for the same effective opening. Using the value for both the frontal and lateral outlets, the logarithmic regressions between the effective outlet area and the duct air flow also gave an R^2 value of 0.94. 0.91 and 0.97 respectively for the fan's speeds of N1, N2 and N3.

The high regression coefficient between the effective outlet area and the duct's static air pressure and air flow demonstrated that the test hypothesis was true. For unexplained reasons, the effect of the lateral outlet discharge angle was negligible. Thus, the effective outlet area can be equated to the fan effective delivery area to solve the balance operating point between the fan and the duct, except that the effect of the lateral outlet discharge angle requires further investigation. Furthermore, the air flow performance of fans designed for perforated ventilation ducts should be characterized in term of their effective delivery area and their static air pressure differential.

6.6 Conclusion

The model developed by El Moueddeb et al.[1] proved to accurately predict the air flow distribution of three wooden ducts. This model also demonstrated that the approach to the design of perforated ventilation ducts can be simplified by assuming a regain coefficient of 1.0 and an outlet discharge coefficient of 0.65, along the full length of the perforated section. The model requires further validation by testing it for centrifugal fans and metal as well as polyethylene ducts.

The fan characteristics can be incorporated in the model for the design of perforated ventilation duct if its air flow performance is described as a function of its static air pressure differential and its effective delivery area.

Presently, fan manufacturers only characterize fans from their air flow performance as a function of static air pressure differential. Nevertheless, the effect of the discharge angle of lateral outlets requires further investigation.

6.7 Acknowledgement

The project was carried out with the financial contribution of the Government of Tunisia, the Natural Sciences and Engineering Research Council of Canada and of le Ministère de l'Agriculture, des Pêcheries et de l'Alimentation du Québec.

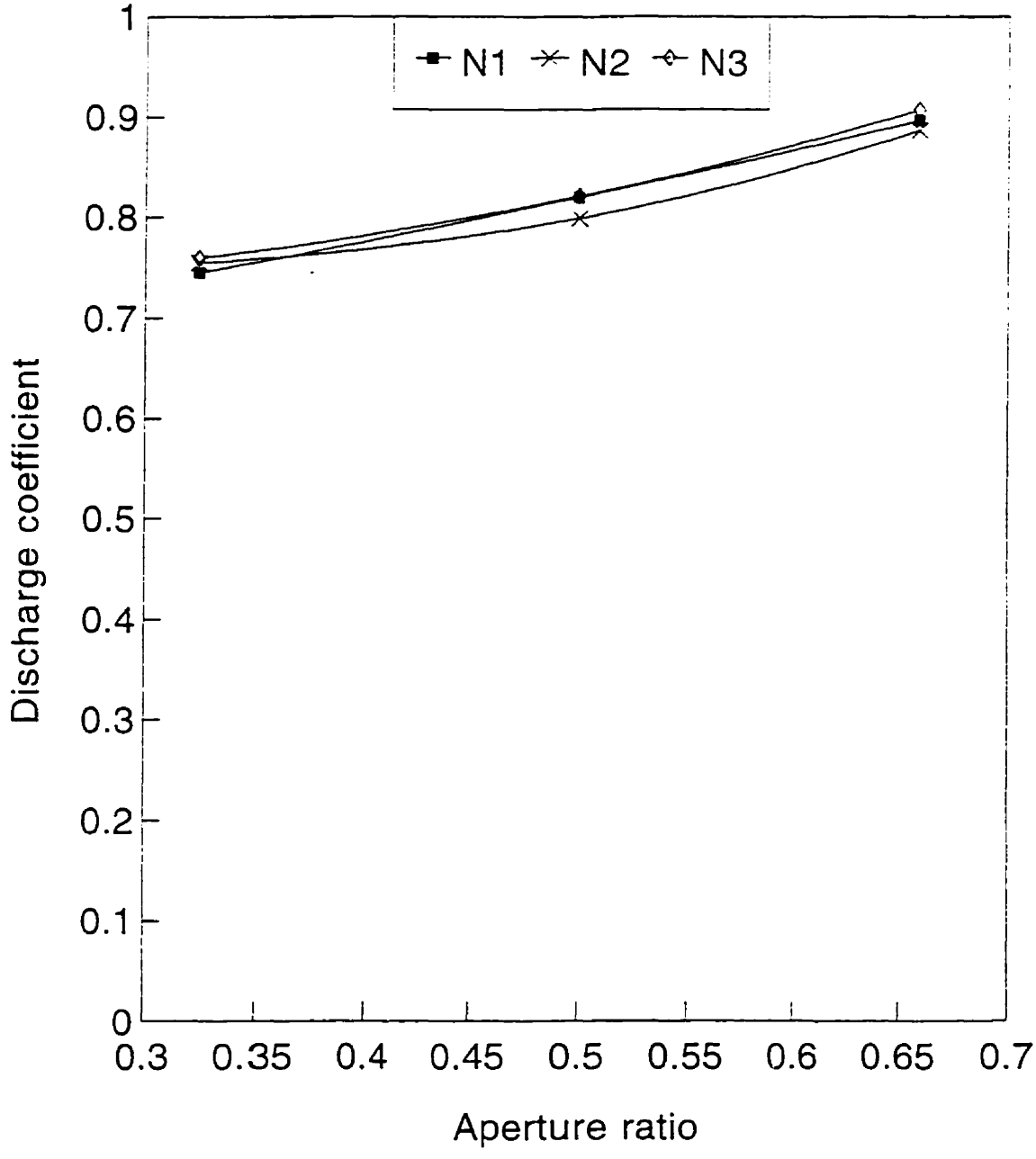

Figure 6.5 Discharge coefficient for the frontal outlets, for the three fan operating speeds.

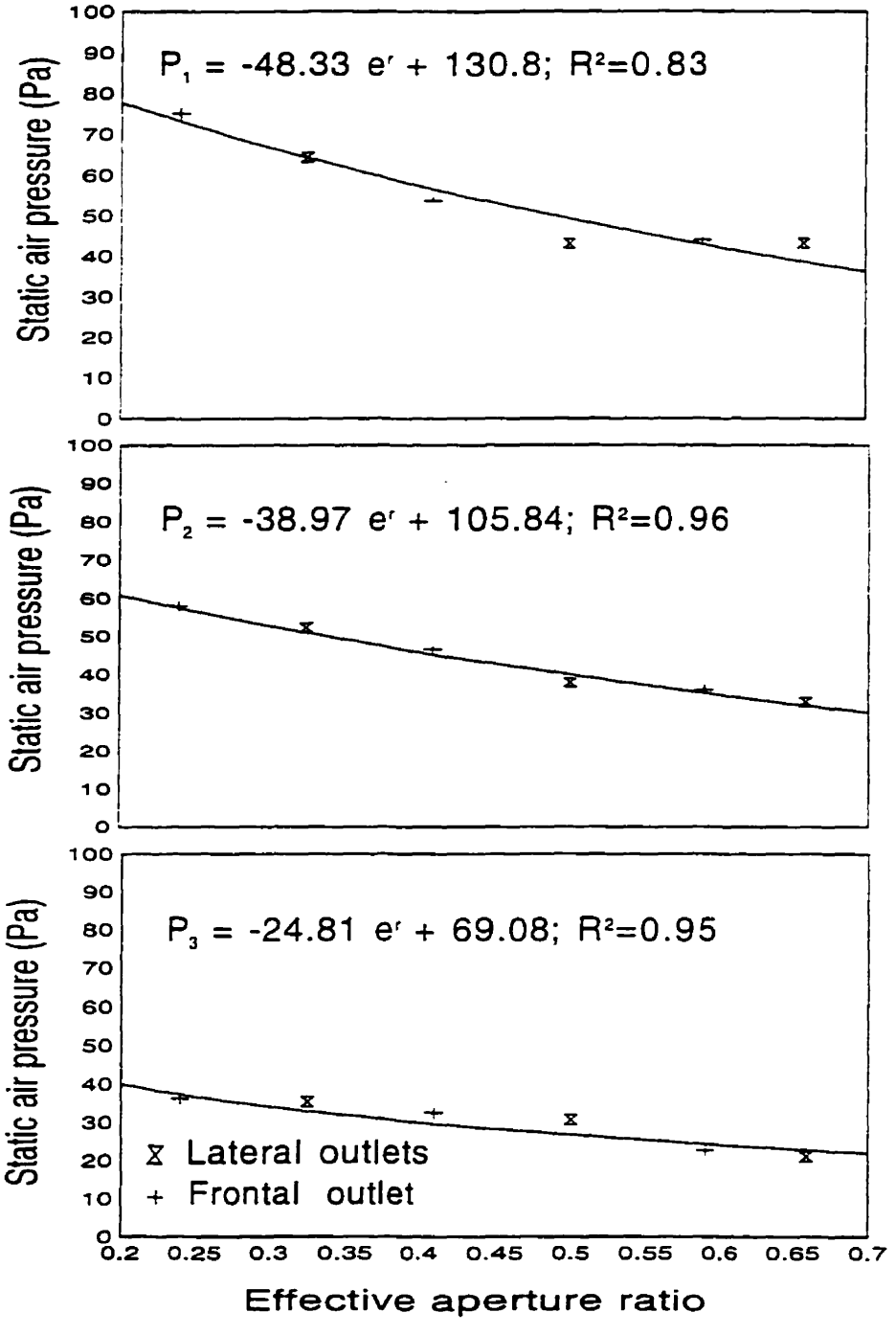

Figure 6.6 Duct static air pressure as a function of outlet size for the three fan operating speeds and two outlet types.

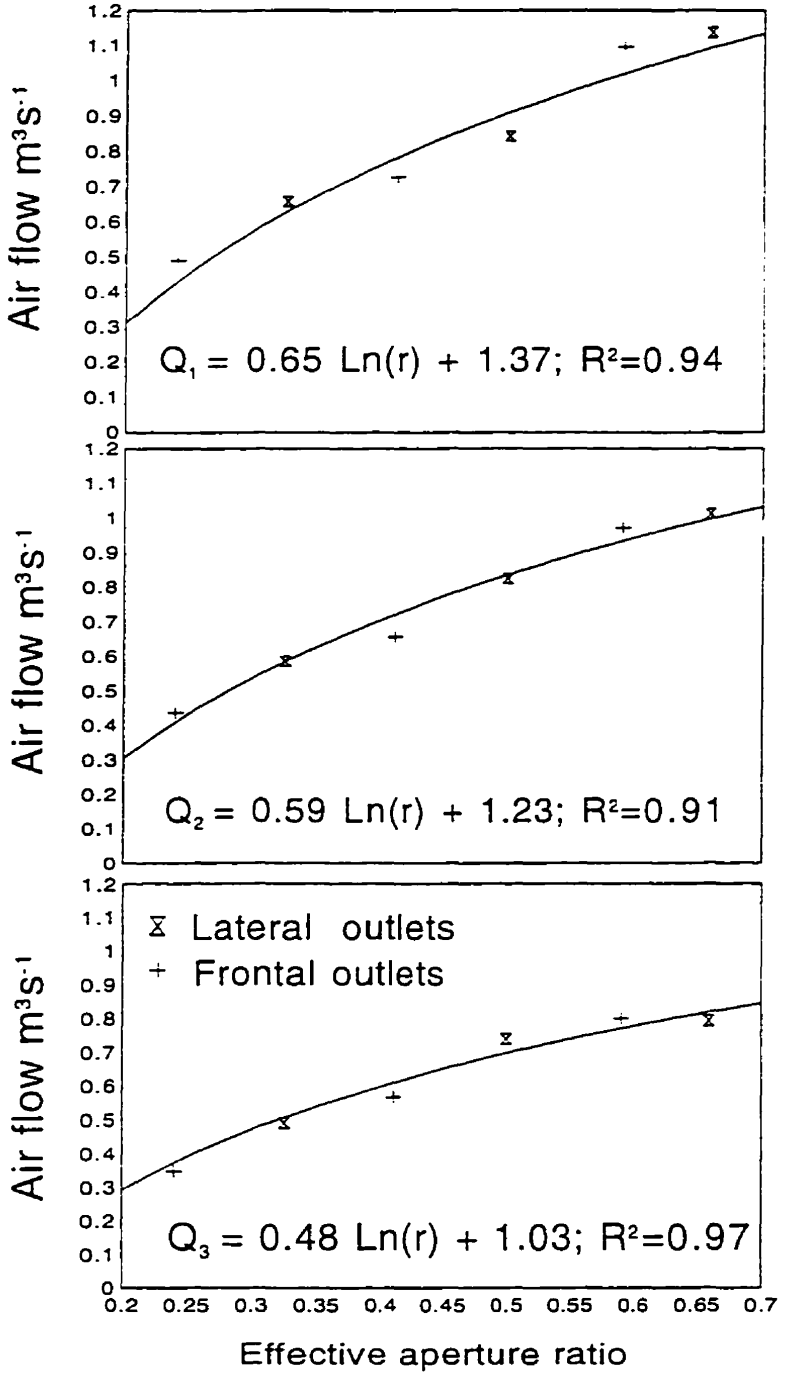

Figure 6.7 Duct air flow as a function of outlets size, for the three fan operating speeds and for the two outlet types.

Table 6.2 Notation

---

a : outlet air flow distribution parameter, m^2

A_o: single outlet area, m^2

A_x: single outlet area at lateral distance X, m^2

A: duct cross-section, m^2

A_f: fan delivery area, m^2

C_d: discharge coefficient at the outlet, dimensionless number

C_{df}: discharge coefficient of the fan discharge area, dimensionless number

D: duct hydraulic diameter, m

e: measure of pipe roughness, mm

f: friction coefficient, dimensionless number

P_i: static air pressure, Pa

Q : total duct air flow, $m^3\ s^{-1}$

q_o: air flow from a specific outlet, $m^3\ s^{-1}$

qo_x: outlet air flow at lateral distance x, $m^3\ s^{-1}$

q_x: outlet air flow, $m^3\ s^{-1}$

R_{ey}: Reynolds number, dimensionless number

V_0 potential air outlet velocity, $m\ s^{-1}$

V_i duct average air velocity, $m\ s^{-1}$

V_x: axial air discharge velocity, $m\ s^{-1}$

V_y: normal air discharge velocity, $m\ s^{-1}$

α: discharge angle, degree

ρ: air density, $kg\ m^{-3}$

r: aperture ratio: $\Sigma A_o/A$ dimensionless number

x: abscise coordinate along the length of the duct, x=0 at the closed end of the duct, m

i: =0, 1, 2

0: outlet

1: upstream from the outlet

2: downstream from the outlet

6.8 References

[1] **El Moueddeb K; Barrington S F; Barthakur N N** Perforated ventilation ducts. Part I and Part II. Journal of Agricultural Engineering Research. In Press.

[2] **Howland W E** Design of perforated pipe for uniformity of discharge. Proc. 3rd Midwestern Conference on Fluid Mechanics 1953, 687-701.

[3] **Carpenter G A** The design of permeable ducts and their application to the ventilation of livestock building. Journal of Agricultural Engineering Research 1972, 17: 219-230.

[4] **Ogilvie J R; Barber E M; Randall J M** Floor air speeds and inlet design in swine ventilation systems. Transactions of the ASAE 1990, 33:(1) 255-259.

[5] **Bailey B J** Fluid flow in perforated pipes. Journal of Mechanical Engineering Science 1975, 17: 338-347.

[6] **Davis D C; Romberger J S; Pettibone C A; Andales S C; Yeh H J** Mathematical model for air flow from perforated circular ducts with annular corrugations. Transactions of the ASAE 1980, 19(4): 661-666.

[7] **Saunders D D; Albright L D** Airflow from perforated polyethylene tubes. Transactions of the ASAE 1984, 23(6): 1144-1149.

[8] **Swamee P K; Jain A K** Explicit equations for pipe-flow problems. Journal of Hydraulic Division Proceeding of the ASCE 1976, 657-664.

[9] **Burgess W A; Ellenbecker M J; Treitman R D** Ventilation for control of the work environment 1989. A Wiley-Interscience publication

[10] **El Moueddeb K; Barrington S F; Newman B G** Evaluation of methods to measure the performance of ventilation ducts. Canadian Agricultural Engineering 1996, 38(3):207-213.

[11] **ACMA** Fans and systems 1985, publication 201

7 GENERAL CONCLUSION

The air flow performance of perforated ventilation ducts requires the use of accurate measurement methods. The present work compared various methods and arrived at the following conclusions:

1) To measure static air pressure inside perforated ventilation ducts, both static tube and piezometric taps can be used as they give similar readings. But, air swirling inside the perforated duct, close to the fan end, must be eliminated by inserting, between the fan and the perforated section, a non perforated section of length equal to 10 times the duct's hydraulic diameter. The static tube is better suited to polyethylene perforated ducts because of the flexible lining while the piezometric taps are preferred for the wooden perforated ducts.

2) To measure outlet air flow, its air jet discharge angle must be accurately measured at its exterior surface. A three-tube-pitot instrument was used for this purpose and it proved sensitive enough to accurately measure the air jet angle within an error of 2.5°. The air jet angle was found to vary over the length of the perforated duct.

3) To accurately obtain the outlet air flow, the duct's cross sectional air flow should be measured upstream and downstream from each outlet using the grid method over the duct's cross-sectional area. The effective discharge area of the outlet is difficult to measure because of the air jet contraction. Thus, outlet air flow cannot be measured accurately from its cross sectional velocity profile. The three-tube-pitot (built of three 3mm tubes) was found to be too large to measure the air jet contraction area as it lead to errors of 3 % to 28 % for aperture ratios of 0.5 to 2.0, respectively. The larger error obtained with the larger aperture ratio or outlet area could have been reduced by increasing the number of grid subsections.

A model was developed to predict the air flow distribution of perforated ventilation ducts using both the energy and momentum equations, instead of just the momentum equation as done in the past. The model determines the flow parameters of perforated ventilation ducts without the need to evaluate the friction losses. Expressions for the friction losses were derived independently from energy and momentum equations and their equivalence was verified experimentally. A discharge angle was included for the calculation of outlet air flow, which implied a constant discharge coefficient over the length of the duct. The regain coefficient was estimated from both the energy and the momentum equations with the conclusion that it is equal to or slightly greater than the energy correction factor which is basically equal to one specifically for turbulent flow. Thus $C_r \approx 1$, for Re 4.5×10^3 to 1.5×10^6.

The experimental validation of the mathematical model was done by measuring the flow performance in four experimental ducts with a respective aperture ratio of 0.5, 1.0, 1.5 and 2.0. The main hypotheses used to develop the model were upheld and the skin friction losses calculated from the momentum equation were found to be the same as that of the energy equation. Thus, the energy equation was found to give the regain coefficient without considering friction losses. The value of the regain coefficient and the energy correction factor was found to be very close to one for turbulent flow. The discharge coefficient remained constant and approximately equal to 0.65, over the full length of the perforated duct. The frictional losses occurred along the length of the duct but had no significant effect at the outlet on the discharge angle. The discharge angle was found to be a function of the duct's average air velocity and the potential outlet air jet velocity, V_o.

The validation of the mathematical model defined design criteria for perforated ventilation ducts with a uniform

outlet area along their length. However, it uses as main input, the static and dynamic air pressure at the inlet of the perforated section which are related to the fan's effective delivery area. The effective fan delivery area was found to be equal to the effective area of the lateral outlets of perforated ducts. Accordingly, the characteristics of the fan can be introduced in the perforated ventilation duct design model if its air flow performance are described in terms of its effective delivery area and static air pressure differential. Thus, a common fan and duct balance operating point can be predicted by matching the physical dimension of the duct and the fan characteristics. Currently, fan manufacturers provide data relating solely pressures and air flow. For perforated ventilation ducts, they need to provide additional data relating air flow to effective delivery area.

Based on the present research results, future research should be carried out to validate the model using :

1) longer ducts built of different materials;
2) different shapes and sizes of outlets;
3) distributions of outlets along the length of the duct;
4) centrifuge fans rather than axial fans;
5) fans characterized based on their effective delivery area.

The effect of the discharge angle of lateral outlets on the fan effective delivery area requires further investigation.

8 CONTRIBUTION TO KNOWLEDGE

Since the 1950's, ventilation duct models have been designed based on a variety of equations and hypotheses (Carpenter, 1972). Several hypotheses have been used and often, the hypotheses used are poorly stated and have not been demonstrated. The principal objective of the research conducted for this thesis was therefore to establish the design criteria and tools for the conception of perforated ventilation ducts. The specific original contributions to knowledge are the following:

8.1 The Definition of a correct methodology for the study of ventilation ducts:

- Demonstrated that the pitot tube and the piezometric opening methods are equivalent for the detection of the air static pressure along a perforated duct;
- Demonstrated that the most accurate method of measuring outlet air flow is the difference between the outlet upstream and downstream air flow;
- Derived a fluid mechanic model from the energy and momentum equations applied to a perforated ventilation duct;

8.2 The establishment of basic air energy phenomena occurring inside the duct to:

- Derive expressions for the friction losses independently from energy and momentum equations and verify their equivalence experimentally. This eliminates the difficult task of measuring or estimating friction losses and improves the accuracy of the derived model;
- For turbulent flow inside the ventilation duct, find a value of one for the regain coefficient and the energy correction factor;
- Demonstrate that air friction losses are significant inside

the perforated duct;

- Demonstrate that friction losses have no effect on the discharge angle of the outlet air jet.
- Define the discharge angle of the outlet air jet in terms of the duct's average air velocity and the potential outlet air jet velocity calculated from Bernouilli's equation;
- Demonstrate that the discharge coefficient at the outlets is constant and approximately equal to 0.65, along the full length of the perforated duct when the discharge angle is used to define outlet air flow.

8.3 The development of a methodology to predict duct air distribution or design:

Presently duct design parameters are not well defined and engineers find the fan and duct balance point by trial and error, on the site. This work demonstrated that the effective fan delivery area induces the resistance to flow and consequently defines the static and dynamic pressure at the entrance of the perforated duct. This fan effective delivery area has been found equal to the summation of the areas of duct lateral outlets multiplied by the discharge coefficient (0.65). The static and dynamic pressures corresponding to that delivery area define the fan-duct balance operating point

A design method is also presented for ventilation duct to provide a specific air distribution pattern along its perforated section. As initial input, a value is assumed for the dynamic and static air pressures for the outlet at the fan end. By iteration, the ventilation parameters are calculated. The iteration is continued by adjusting the discharge angles and the outlet flow for all the outlets, until the calculated air flow at the duct's closed end is close to zero. Then, the corresponding air distribution performance of the perforated duct had been predicted.

9 REFERENCES

ACMA Fans and systems 1985, publication 201

ANSI/ASME Measurement of uncertainty. ANSI/ASME PTC 19.1-1985 Part 1 1986. The American Society of Mechanical Engineers, 345 East 47th Street New York, N.Y. 10017.

Allen D Air flow distribution from tapered ducts. paper 74-6514. ASAE 1974, St. Joseph, Michigan, USA.

Ashley C M; Gilman S F; Church R A and Syracuse N Y Branch fitting performance at high velocity. Transactions of the ASHRAE 1956, 56: 279-294

ASHRAE 1993. Equipment Handbook, 1993 Chapter 18. Atlanta, Georgia.

Bailey G J Fluid flow in perforated pipes. Journal of Mechanical Engineering Science. 1975, 17:(6) 338-347.

Bajura R A A model for flow distribution in manifolds. ASME Journal of Engineering for Power 1971, 93: 7-12.

Bajura R A; Jones E H Flow distribution manifolds. Transactions of the ASME 1976, 98: 654-665.

Barrington S F and MacKinnon I R Air distribution from rectangular wooden ventilation ducts. Transactions of the ASAE 1990, 33(3):944-948.

Brundrett E and Vermes P T Evaluation of tube diameter and fan induced swirl in polyethylene ventilation tubes. Transaction of the ASAE 1987, 30(4): 1131-1138.

Burgess W A; Ellenbecker M J and Treitman R D Ventilation for control of the work environment 1989. A Wiley-Interscience publication.

Carpenter G A The design of permeable ducts and their application to the ventilation of livestock building. Journal of Agricultural Engineering Research. 1972, 17:219-230.

Colebrook C F Turbulent flow in pipes with particular reference to the transition region between smooth and rough pipe laws. Journal of the Institution of Civil Engineers 1938, 4: 133-156.

Davis D C; Romberger J S; Andales S C; Yeh H J Mathematical model for air flow from perforated ducts with annular corrugations. Transactions of the ASAE 1980, 23(3): 661-666

El Moueddeb K; Barrington S F; Barthakur N N Perforated ventilation ducts. Part I. A model for flow distribution. Journal of Agricultural Engineering Research. In press

El Moueddeb K; Barrington S F and Barthakur N N Perforated ventilation ducts. Part II: Validation of an air distribution model. Journal of Agricultural Engineering Research. In Press.

El Moueddeb K; Barrington S F; Newman B.G Evaluation of methods to measure the performance of ventilation ducts. Canadian Agricultural Engineering. 38(3): 207-213.

Esmay, M L and Dixon J E Environmental control for agricultural buildings. The AVI Publishing Company, Inc., 1986, Westport, Connecticut, U.S.A. 84-88

Haerter A A Flow distribution and pressure change along slotted or branched ducts. Transactions of the ASHRAE 1963,

69: 124-137.

Horlock J H An Investigation of the flow of manifolds with open and closed ends. Journal of the Royal Aeronautical Society 1956, 60: 749-753.

Howland W E Design of perforated pipe for uniformity of discharge. Proc. 3rd Midwestern Conference on Fluid Mechanics 1953, 687-701.

Jackson K R Branched losses in high velocity duct systems. Journal Institution Heating and Ventilating Engineers 1969, 4: 208-214.

Kline S J The purposes of uncertainty analysis. Journal of Fluids Engineering 1985, 107: 153-160

Koestel A and Tuve G L The discharge of air from a long slot. Transactions of the ASHVE 1948, 54: 87-100.

Koestel A and Young C The control of air stream from a long slot. Transactions of the ASHVE 1951, 12: 407-418.

Leonard J J; McQuitty J B Archimedes number criteria for the control of cold ventilation air jets. Canadian Agricultural Engineering 1986, 28(2): 117-123.

McNown J S Mechanics of manifold flow. Transactions ASCE 1954, 119: 1103-1142.

McNown J S; Hsu E Y Application of conformal mapping to divided flow. Proceeding Mid-western Conference on Fluid Dynamics 1951, 143-155.

McQuiston F C; Parker J D Heating, ventilating and air conditioning analysis and design 1988. Third edition. Jhon Wiley and Sons, 344-347.

Newman B G A hodographic solution for flow leaving a manifold through a slit. Canadian Aeronautics and Space Journal 1989, 35: 205-210.

Ogilvie J R; Barber M E and Randall J M Floor air speeds and inlet design in swine ventilation systems. Transactions of the ASAE 1990, 33(1): 255-259.

Pastula R; Feddes J J R and Leonard J J Discharge coefficients for openings in metal or plywood walls of recirculation ducts. Canadian Agricultural Engineering 1992, 34(4):359-363

Randall J M; V A Battams Stability criteria for airflow patterns in livestock buildings. Journal of Agricultural Engineering Research 1979, 24: 361-374.

Saunders D D and Albright L D Airflow from perforated polyethylene tubes. Transactions of the ASAE 1984, 23(6): 1144-1149.

Shove G C and Hukill W V Predicting pressure gradients in perforated grain ventilation ducts. Transactions of the ASAE 1963, 6(2): 115-116,122

Soucek E; Zelnick E W Lock manifold experiments. Transactions of the ASCE 1945, 1357-1400.

Steel R D and Torrie J H Principles and procedures of statistics 1980. A biometrical approach. Second edition. McGraw-Hill Book Company.

Streeter V L The kinetic energy and momentum correction factors for pipes and open channels of great width. Civil Engineering 1942, 12(04): 212-213.

Streeter V L; Benjamin E W Fluid mechanics. First SI metric edition 1981. MacGraw-Hill Ryerson limited, 342-344.

Streeter V L and Wylie E B Fluid mechanics. First SI metric edition 1981. McGraw-Hill Ryerson Limited.

Swamee P K and Jain A K Explicit equations for pipe-flow problems. Journal of Hydraulic Division Proceeding of the ASCE 1976, 657-664.

IMAGE EVALUATION
TEST TARGET (QA-3)

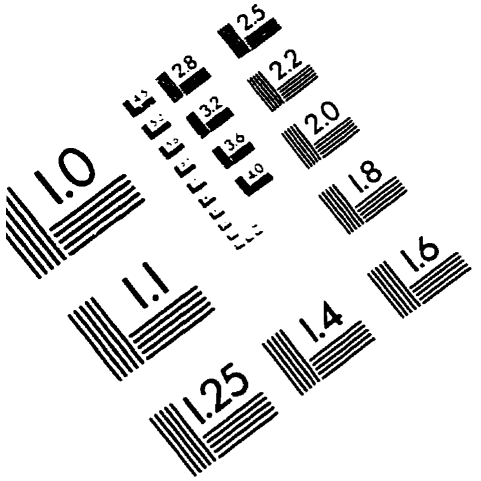

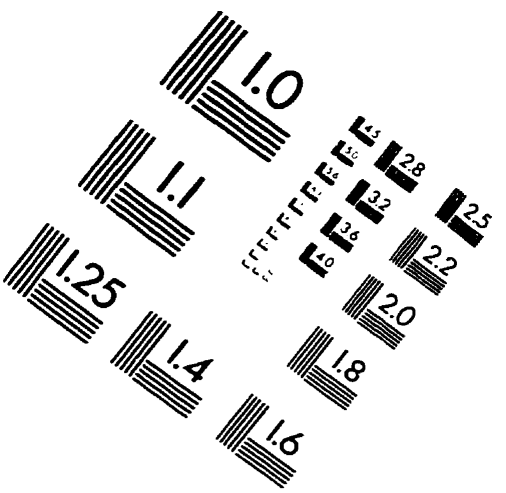

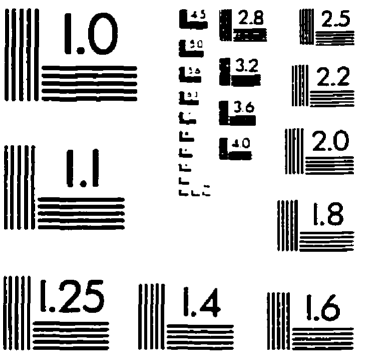

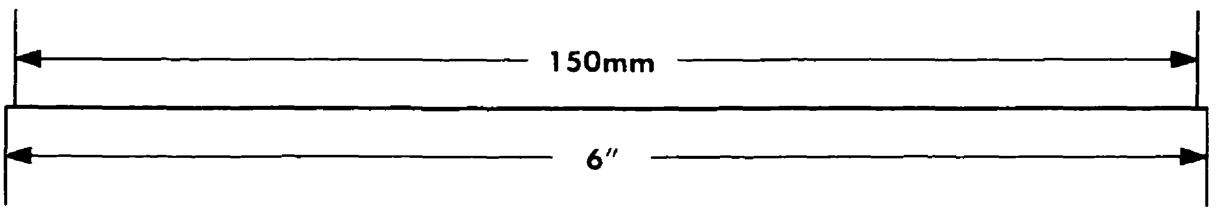

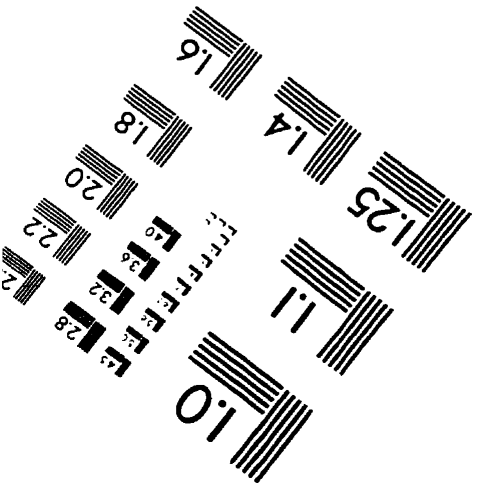

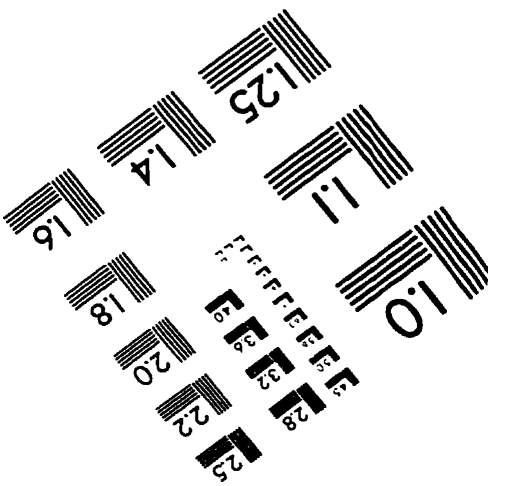

APPLIED IMAGE, Inc
1653 East Main Street
Rochester, NY 14609 USA
Phone: 716/482-0300
Fax: 716/288-5989

© 1993, Applied Image, Inc., All Rights Reserved